

STATUS OF THESIS

Title of thesis

Condition Monitoring of Induction Motors via Instantaneous Power Analysis

I MUHAMMAD IRFAN

hereby allow my thesis to be placed at the Information Resource Center (IRC) of Universiti Teknologi PETRONAS (UTP) with the following conditions:

1. The thesis becomes the property of UTP
2. The IRC of UTP may make copies of the thesis for academic purposes only.
3. This thesis is classified as

☐ Confidential

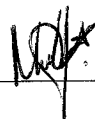
☒ Non-confidential

If this thesis is confidential, please state the reason:

The contents of the thesis will remain confidential for _____ years.

Remarks on disclosure:

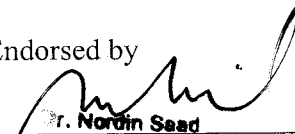
Signature of Author



Permanent address: Chah Gath Wala
Moza Sanda, P/O Tibba Sultan Pur
Tehsile Malisi District Vehari, State
Punjab, Pakistan

Date : 10-06-2013

Endorsed by



r. Nordin Saad
Signature of Supervisor
Technical & Electronics Engineering Programme
Universiti Teknologi PETRONAS
17500 Supervisor
Perak Darul Ridzuan, MALAYSIA
AP. Dr. Nordin Saad

Date : 10/6/2013

UNIVERSITI TEKNOLOGI PETRONAS

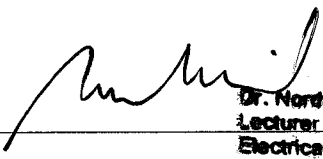
CONDITION MONITORING OF INDUCTION MOTORS VIA INSTANTANEOUS
POWER ANALYSIS

by

MUHAMMAD IRFAN

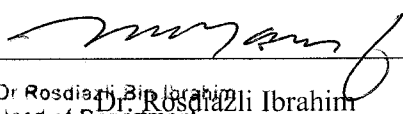
The undersigned certify that they have read, and recommend to the Postgraduate
Studies Programme for acceptance this thesis for the fulfillment of the requirements
for the degree stated.

Signature:


Dr. Nordin Saad
Lecturer
Electrical & Electronics Engineering Programme
Universiti Teknologi PETRONAS
31750 Tronoh,
Perak Darul Ridzuan, MALAYSIA

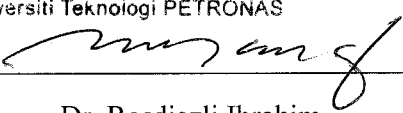
Main Supervisor:

Signature:


Dr. Rosdiazli Bin Ibrahim
Head of Department
Electrical & Electronic Engineering Department
Universiti Teknologi PETRONAS

Co-Supervisor:

Signature:


Dr. Rosdiazli Bin Ibrahim

Head of Department:

Date:

Dr Rosdiazli Bin Ibrahim
Head of Department 16-06-2013
Electrical & Electronic Engineering Department
Universiti Teknologi PETRONAS

CONDITION MONITORING OF INDUCTION MOTORS VIA INSTANTANEOUS
POWER ANALYSIS

by

MUHAMMAD IRFAN

A Thesis

Submitted to the Postgraduate Studies Programme

as a Requirement for the Degree of

MASTER OF SCIENCE

ELECTRICAL AND ELECTRONICS ENGINEERING

UNIVERSITI TEKNOLOGI PETRONAS

BANDAR SERI ISKANDAR

PERAK

JUNE 2013


DECLARATION OF THESIS

Title of thesis Condition Monitoring of Induction Motors via Instantaneous Power Analysis

I MUHAMMAD IRFAN

hereby declare that the thesis is based on my original work except for quotations and citations which have been duly acknowledged. I also declare that it has not been previously or concurrently submitted for any other degree at UTP or other institutions.

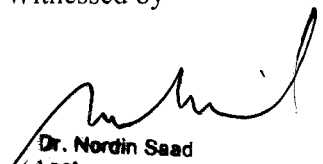
Witnessed by



Signature of Author

Permanent address: Chah Gath Wala
Moza Sanda, P/O Tibba Sultan Pur
Tehsile Malisi District Vehari, State
Punjab, Pakistan

Date : 10-06-2013



Dr. Nordin Saad
Lecturer
Electrical & Electronic Engineering Programme
Universiti Teknologi PETRONAS
31750 Tronoh,
Perak Darul Ridzuan, MALAYSIA
Name of Supervisor
Dr. Nordin Saad

Date : 10-06-2013

DEDICATION

To my beloved parents

ACKNOWLEDGEMENTS

At the end of this journey of dissertation, I realize the importance of acknowledging. First of all, I would like to say Alhamdulillah, praise Allah The Most Gracious and The Most Merciful, for munificence in bestowing me with so many of His favours throughout my life particularly in enhancing my courage for the completion of this work successfully.

I would like to express my gratitude to my respected supervisor, AP Dr. Nordin Saad for his consistent support, guidance and well rounded experience, which I will treasure in my career. He has always been soft but fair in his criticism of my work and I have great appreciation for his management in maintaining such a difficult balance. I also want to acknowledge AP Dr. Rosdiazli Ibrahim for his significant contribution for this achievement as a co-advisor. I cannot forget our long discussions we have had over my work during that he sat and listened, no matter how tight his schedule was.

Further I want to extend my gratitude to AP Dr. Vijanth Asirvadam, who provided me with extremely useful technical input and directions. Without their encouragement and helping hands, it was not easy to achieve this goal.

I definitely cannot miss this opportunity to thank Asjid Ali, Javed Akbar Khan Niazi, Mauwia, Hung, Nouman Haider and senior lab technician Mr. Azhar for all those valuable discussions at certain times even at my doorstep when I was stuck up with my work. To all my distinguished friends and colleagues, Tariq Ali, Muhammad Awais, Imran Baig, Mutee-ur-Rahman, Ihtasham, Zaheer Fazal, Faisal Naveed Khan Niazi who supported me along the whole this journey, your good will shall not be forgotten.

There certainly exist no words that could possibly express the extent of gratitude I owe my family being there as ever lasting source of support and encouragement. I am deeply grateful to my respected father Allah Ditta and brother Rizwan Ahmad for the uncountable sacrifices they made for my studies throughout the years. I strongly believe that, if I were here today then its all due to an answer to my mother's and

grand mother's prayers. My beloved mother, grand mother and sister, whose hands always rise for praying for my success. My love and respect to them are endless and immense.

The author wants to extend his gratefulness to the many anonymous reviewers as their thoughtful and unselfish comments greatly improved the quality of my research articles from which this thesis has been partly extracted.

Last but not least, I appreciate the efforts and cooperation of management of Universiti Teknologi PETRONAS and ministry of higher education (MOHE) Malaysia for the award of ERGS grant, as without their support, this project would not have been possible.

ABSTRACT

Many techniques have been developed which support the construction of condition monitoring and fault diagnosis for induction motors. However, most of these techniques use sensors as their integral components which usually expensive and need to be properly installed on the machines for accurate results. Furthermore, sensors have some life period after which they may fail and in certain cases earlier than the bearings life period, which make these techniques unreliable.

The idea for proposing instantaneous power analysis monitoring technique in this thesis comes from the usual practices in industries to have current and voltage transformers installed for the measurement of the current and voltage for control and display purposes.

This research aims to provide a new non-invasive and sensorless method for the detection of bearing faults under un-loaded and loaded conditions of the induction motors via instantaneous power analysis.

Detail experiments and evaluations of several bearing localized and distributed defects are presented. The results indicate the viability and effectiveness of the proposed instantaneous power analysis over its predecessor i.e. the stator current analysis. An intelligent diagnostic condition monitoring system which compromises of industrial firmwares and hardwares is developed. The findings demonstrate the ability of the approach as a reliable condition monitoring and fault diagnosis for induction motors.

ABSTRAK

Banyak teknik telah dibangunkan yang menyokong pembinaan pemantauan keadaan dan diagnosis kerosakan untuk motor aruhan. Walau bagaimanapun, kebanyakan teknik-teknik ini menggunakan sensor sebagai komponen penting yang biasanya mahal dan perlu dipasang dengan kemas pada mesin untuk keputusan yang tepat. Tambahan pula, sensor mempunyai tempoh hayat tertentu yang mana selepas itu mereka mungkin gagal dan dalam kes-kes tertentu lebih awal daripada tempoh hayat bearing, yang membuat teknik-teknik ini tidak mempunyai kepercayaan yang memuaskan. Idea untuk mencadangkan teknik pemantuan analisis kuasa sertamerta dalam tesis ini alalah dari kebiasaan dan amalan dalam industri yang menggunakan pengubah arus dan voltan untuk mengukur of arus dan voltan untuk mengawal dan untuk tujuan paparan. Kajian ini bertujuan untuk menyediakan satu kaedah baru bukan invasif dan tanpa sensor untuk mengesan kesalahan di bawah keadaan undimuatkan dan dengan beban dalam motor aruhan melalui analisis kuasa serta-merta. Eksperimen yang terperinci dan penilaian beberapa kecacatan bearing setempat dan kecacatan tertabur dibentangkan. Keputusan menunjukkan daya maju dan keberkesanan cadangan analisis kuasa serta-merta ini ke atas analisis semasa pemegun. Satu keadaan diagnostik sistem pemantauan pintar yang terdiri daripada firmware industri dan perkakasan telah dibangunkan. Hasil kajian menunjukkan keupayaan pendekatan ini sebagai pemantauan keadaan yang boleh dipercayai untuk diagnosis kerosakan motor aruhan.

In compliance with the terms of the Copyright Act 1987 and the IP Policy of the university, the copyright of this thesis has been reassigned by the author to the legal entity of the university,

Institute of Technology PETRONAS Sdn Bhd.

Due acknowledgement shall always be made of the use of any material contained in, or derived from, this thesis.

© MUHAMMAD IRFAN, 2013

Institute of Technology PETRONAS Sdn Bhd

All rights reserved.

TABLE OF CONTENTS

DECLARATION OF THESIS.....	iv
DEDICATION.....	v
ACKNOWLEDGMENT.....	vi
ABSTRACT.....	viii
ABSTRAK	ix
LIST OF FIGURES	xiv
LIST OF TABLES	xx
CHAPTER 1 INTRODUCTION	1
1.1 Background.....	1
1.2 Motivation	3
1.3 The Shortcomings of Previous Research Work on Condition Monitoring	4
1.4 Objectives and Contribution of the Research.....	5
1.5 Outlines of the Thesis.....	6
CHAPTER 2 LITERATURE REVIEW.....	8
2.1 Introduction	8
2.2 Overview of the Induction Motors	8
2.3 Faults in Induction Motor	10
2.3.1 Mechanical Defects	11
2.3.1.1 Bearing Defects	11
2.3.1.2 Airgap Eccentricity Defects.....	12
2.3.1.3 Load Defects.....	12
2.3.2 Electrical Defects.....	13
2.3.2.1 Stator Winding Defects.....	13
2.3.2.2 Rotor Defects	14
2.4 Requirements for Condition Monitoring.....	15
2.5 Condition Monitoring Techniques	16
2.5.1 VibrationMonitoring	17
2.5.2 Acoustic Emission.....	18
2.5.3 Thermal Monitoring.....	19
2.5.4 Sound Monitoring	20
2.5.5 Chemical Analysis	21

2.5.6 Electrical Monitoring	21
2.6 Important Observations	32
2.7 Summary.....	33
CHAPTER 3 EXPERIMENTAL SET-UP.....	35
3.1 Introduction	35
3.2 Condition Monitoring System	36
3.2.1 Mechanical Parts.....	37
3.2.1.1 Motor Connections	37
3.2.1.2 Bearing Load Calculation	38
3.2.1.3 Bearing Assembly.....	40
3.2.2 Data Acquisition and Processing	42
3.2.2.1 Configuration of the Measurement Automation Explorer.....	43
3.2.2.2 Fault Analysis Software.....	45
3.3 Summary.....	47
CHAPTER 4 RESULTS AND DISCUSSIONS	48
4.1 Introduction	48
4.2 Various Bearing Faults Analysis.....	48
4.2.1 Bearing Outer Race Defects.....	50
4.2.1.1 Outer Race Defects Analysis at Various Hole Sizes under no Load condition of the motor	51
4.2.1.2 Outer Race Defects Analysis at Various Hole Sizes under Full Load condition of the motor.....	56
4.2.1.3 Comparison of the Instantaneous Power Analysis with the Stator Current Analysis.....	63
4.2.2 Bearing Inner Race Defects	64
4.2.2.1 Inner Race Defects Analysis at Various Hole Sizes under no Load condition of the motor	65
4.2.2.2 Inner Race Defects Analysis at Various Hole Sizes under Full Load condition of the motor.....	70
4.2.2.3 Comparison of the Instantaneous Power Analysis with Current Analysis for Bearing Inner race Defects	77
4.2.3 Bearing Ball Defects	78
4.2.3.1 Bearing Ball Defects under no Load condition of the motor...	79

4.2.3.2 Bearing Ball defects under full Load Conditions of the Motor	82
4.2.3.3 Comparison of the Instantaneous Power Analysis with Current Analysis for Bearing Ball Defects under Full Load Condition of the Motor	85
4.2.4 Bearing Cage Defects.....	86
4.2.4.1 Bearing Cage Defects Analysis under no Load conditions of the Motor	86
4.2.4.2 Bearing Cage Defects Analysis under Full Load conditions of the Motor	88
4.2.5 Bearing Distributed Defects.....	90
4.2.5.1 Distributed Defect in Outer Race of Bearing	90
4.2.5.2 Distributed Defect in Inner Race of Bearing	93
4.3 A Complete Intelligent Diagnostic CM System.....	95
4.4 Summary.....	97
CHAPTER 5 CONCLUSIONS AND FUTURE DIRECTIONS	98
5.1 Conclusions	98
5.2 Contributions	100
5.3 Directions for Future Work	101
REFERENCES	102
LIST OF PUBLICATIONS.....	111

LIST OF FIGURES

Figure 3.1: Design flow of experimental test rig	35
Figure 3.2: The schematic diagram of the test rig	36
Figure 3.3: The induction motor used in test rig	37
Figure 3.4: The connection scheme of the motor	37
Figure 3.5: (a) The VFD and (b) Tachometer used in test rig	38
Figure 3.6: Structure of steel plates used as radial load in test rig	39
Figure 3.7: Geometry of bearing used for this work	40
Figure 3.8: Bearing with various health conditions used for this work.....	41
Figure 3.9: Data acquisition card NI 6281.....	42
Figure 3.10: AC current sensor ACT-013-005	42
Figure 3.11: AC voltage sensor	43
Figure 3.12: Relation between DAQ and MAX	44
Figure 3.13: The flow chart of configuration of DAQ input channel with MAX	44
Figure 3.14: Flow chart of the LabVIEW program developed for spectrum analysis	46
Figure 4.1: Defects induced in outer race of motor bearing	51
Figure 4.2: Instantaneous power spectrum of the healthy and defected motor under no load condition at 1mm outer race defect at 29.875 Hz	52
Figure 4.3: Instantaneous power spectrum of the healthy and defected motor under no load condition at 1mm outer race defect at 129.875Hz	52
Figure 4.4: Instantaneous power spectrum of the healthy and defected motor under no load condition at 2mm outer race defect at 29.875 Hz	53
Figure 4.5: Instantaneous power spectrum of the healthy and defected motor under no load condition at 2mm outer race defect at 129.875Hz	53
Figure 4.6: Instantaneous power spectrum of the healthy and defected motor under no load condition at 3mm outer race defect at 29.875 Hz	53
Figure 4.7: Instantaneous power spectrum of the healthy and defected motor under no load condition at 3mm outer race defect at 129.875Hz	54
Figure 4.8: Instantaneous power spectrum of the healthy and defected motor under no load condition at 4mm outer race defect at 29.875 Hz	54

Figure 4.9: Instantaneous power spectrum of the healthy and defected motor under no load condition at 4mm outer race defect at 129.875Hz	54
Figure 4.10: Instantaneous power spectrum of the healthy and defected motor under no load condition at 5mm outer race defect at 29.875 Hz	55
Figure 4.11: Instantaneous power spectrum of the healthy and defected motor under no load condition at 5mm outer race defect at 129.875Hz	55
Figure 4.12: Instantaneous power spectrum of the healthy and defected motor under full load condition at 1mm outer race defect at 24.375 Hz, showing that at the specific defect frequencies the amplitude starts to appear.....	57
Figure 4.13: Instantaneous power spectrum of the healthy and defected motor under full load condition at 1mm outer race defect at 124.375 Hz, showing that at the specific defect frequencies the amplitude starts to appear.....	57
Figure 4.14: Instantaneous power spectrum of the healthy and defected motor under full load condition at 2mm outer race defect at 24.375 Hz and, showing that at the specific defect frequencies the amplitude value increases.....	58
Figure 4.15: Instantaneous power spectrum of the healthy and defected motor under full load condition at 2mm outer race defect at 124.375 Hz and, showing that at the specific defect frequencies the amplitude value increases.....	58
Figure 4.16: Instantaneous power spectrum of the healthy and defected motor under full load condition at 3mm outer race defect at 24.375 Hz, indicating significant increase in amplitude values	59
Figure 4.17: Instantaneous power spectrum of the healthy and defected motor under full load condition at 3mm outer race defect at 124.375 Hz, indicating significant increase in amplitude values	59
Figure 4.18: Instantaneous power spectrum of the healthy and defected motor under full load condition at 4mm outer race defect at 24.375 Hz, showing that at the specific defect frequencies the amplitude value increases still further	60
Figure 4.19: Instantaneous power spectrum of the healthy and defected motor under full load condition at 4mm outer race defect at 124.375 Hz, showing that at the specific defect frequencies the amplitude value increases still further	60
Figure 4.20: Instantaneous power spectrum of the healthy and defected motor under full load condition at 5mm outer race defect at 24.375 Hz, showing that	

at the specific defect frequencies the amplitude value increases to much larger values.....	61
Figure 4.21: Instantaneous power spectrum of the healthy and defected motor under full load condition at 5mm outer race defect at 124.375 Hz, showing that at the specific defect frequencies the amplitude value increases to much larger values.....	61
Figure 4.22: Comparison of amplitude values for various outer race defect sizes at no load and full load conditions of the motor.....	63
Figure 4.23: Comparison of the instantaneous power analysis with stator current analysis	64
Figure 4.24: Defect induced in inner race of motor bearing.....	65
Figure 4.25: Instantaneous power spectrum of the healthy and defected motor under no load condition at 1mm inner race defect at 69.75 Hz	66
Figure 4.26: Instantaneous power spectrum of the healthy and defected motor under no load condition at 1mm inner race defect at 169.75 Hz	66
Figure 4.27: Instantaneous power spectrum of the healthy and defected motor under no load condition at 2mm inner race defect at 69.75 Hz	67
Figure 4.28: Instantaneous power spectrum of the healthy and defected motor under no load condition at 2mm inner race defect at 169.75 Hz	67
Figure 4.29: Instantaneous power spectrum of the healthy and defected motor under no load condition at 3mm inner race defect at 69.75 Hz	67
Figure 4.30: Instantaneous power spectrum of the healthy and defected motor under no load condition at 3mm inner race defect at 169.75 Hz	68
Figure 4.31: Instantaneous power spectrum of the healthy and defected motor under no load condition at 4mm inner race defect at 69.75 Hz	68
Figure 4.32: Instantaneous power spectrum of the healthy and defected motor under no load condition at 4mm inner race defect at 169.75 Hz	68
Figure 4.33: Instantaneous power spectrum of the healthy and defected motor under no load condition at 5mm inner race defect at 69.75 Hz	69
Figure 4.34: Instantaneous power spectrum of the healthy and defected motor under no load condition at 5mm inner race defect at 169.75 Hz	69
Figure 4.35: Instantaneous power spectrum of the healthy and defected motor under full load condition at 1mm inner race defect at 64 Hz, showing that at the specific defect frequencies the amplitude starts to appear.....	71

Figure 4.36: Instantaneous power spectrum of the healthy and defected motor under full load condition at 1mm inner race defect at 164 Hz, showing that at the specific defect frequencies the amplitude starts to appear.....	71
Figure 4.37: Instantaneous power spectrum of the healthy and defected motor under full load condition at 2mm inner race defect at 64 Hz, showing that at the specific defect frequencies the amplitude value increases	72
Figure 4.38: Instantaneous power spectrum of the healthy and defected motor under full load condition at 2mm inner race defect at 164 Hz, showing that at the specific defect frequencies the amplitude value increases.....	72
Figure 4.39: Instantaneous power spectrum of the healthy and defected motor under full load condition at 3mm inner race defect at 64 Hz, indicating that at the specific defect frequencies, the amplitude value continue to increase	73
Figure 4.40: Instantaneous power spectrum of the healthy and defected motor under full load condition at 3mm inner race defect at 164 Hz, indicating that at the specific defect frequencies, the amplitude value continue to increase	73
Figure 4.41: Instantaneous power spectrum of the healthy and defected motor under full load condition at 4mm inner race defect at 64 Hz, showing that at the specific defect frequencies the amplitude value increases still further...	74
Figure 4.42: Instantaneous power spectrum of the healthy and defected motor under full load condition at 4mm inner race defect at 164 Hz, showing that at the specific defect frequencies the amplitude value increases still further	74
Figure 4.43: Instantaneous power spectrum of the healthy and defected motor under full load condition at 5mm inner race defect at 64 Hz, showing that at the specific defect frequencies the amplitude value increases to much larger values	75
Figure 4.44: Instantaneous power spectrum of the healthy and defected motor under full load condition at 5mm inner race defect at 164 Hz, showing that at the specific defect frequencies the amplitude value increases to much larger values.....	75
Figure 4.45: Comparison of amplitude values for various inner race defect sizes at no load and full load conditions of the motor.....	77

Figure 4.46: Comparison of the instantaneous power analysis with stator current analysis for bearing inner race defects.....	78
Figure 4.47: Ball defects induced in bearing of motor	79
Figure 4.48: Instantaneous power spectrum of the healthy and defected motor under no load condition and at one ball damaged at charecteristic ball defect frequency of 145.875 Hz and 147.875 Hz	80
Figure 4.49: Instantaneous power spectrum of the healthy and defected motor under no load condition and at two balls damaged at charecteristic ball defect frequency of 145.875 Hz and 147.875 Hz	81
Figure 4.50: Instantaneous power spectrum of the healthy and defected motor under no load condition and at three balls damaged at charecteristic ball defect frequency of 145.875 Hz and 147.875 Hz	81
Figure 4.51: Instantaneous power spectrum of the healthy and defected motor under full load condition at one ball damage, showing that at charecteristic ball defect frequencies of 136.5 Hz and 143.25 Hz the amplitude value starts to appear.....	82
Figure 4.52: Instantaneous power spectrum of the healthy and defected motor under full load condition at two balls damage, showing that at charecteristic ball defect frequencies of 136.5 Hz and 143.25 Hz the amplitude value increases.....	83
Figure 4.53: Instantaneous power spectrum of the healthy and defected motor under full load condition at thee balls damage, showing that at charecteristic ball defect frequencies of 136.5 Hz and 143.25 Hz the amplitude value increase to much larger value	83
Figure 4.54: Comparison of amplitude values for various ball defect sizes at no load and full load conditions of the motor.....	84
Figure 4.55: Comparison of the instantaneous power analysis with stator current analysis for bearing ball defects	85
Figure 4.56: Cage defect induced in bearing of motor	86
Figure 4.57: Instantaneous power spectrum of healthy and defected motor at no load condition, indicating that presence of cage defect in motor appear as rise in amplitude values at 31 Hz and 40.5 Hz	87

Figure 4.58: Instantaneous power spectrum of healthy and defected motor at no load condition, indicating that presence of cage defect in motor appear as rise in amplitude values at 59.5 Hz and 69 Hz	87
Figure 4.59: Instantaneous power spectrum of healthy and defected motor at full load condition, indicating that presence of cage defect in motor appear as much increase in amplitude values at 32.375 Hz and 41.25 Hz	89
Figure 4.60: Instantaneous power spectrum of healthy and defected motor at full load condition, indicating that presence of cage defect in motor appear as much increase in amplitude values at 58.875 Hz and 67.75 Hz	89
Figure 4.61: Distributed defect in outer surface of bearing	91
Figure 4.62: Instantaneous power spectrum of the distributed defect in outer race of bearing indicating no change in amplitude at 24.375 Hz	91
Figure 4.63: Instantaneous power spectrum of the distributed defect in outer race of bearing indicating no change in amplitude value at 124.375 Hz.....	92
Figure 4.64: Instantaneous power spectrum of the distributed defect in outer race of bearing indicating rise in amplitude value at 25.625 Hz	92
Figure 4.65: Instantaneous power spectrum of the distributed defect in outer race of bearing indicating rise in amplitude value at 100.375 Hz	92
Figure 4.66: Distributed defect in inner race of bearing.....	93
Figure 4.67: Instantaneous power spectrum of the distributed defect in inner race of bearing indicating no change in amplitude at 164 Hz	93
Figure 4.68: Instantaneous power spectrum of the distributed defect in inner race of bearing indicating no change in amplitude value at 178 Hz.....	94
Figure 4.69: Instantaneous power spectrum of the distributed defect in inner race of bearing indicating rise in amplitude value at 14 Hz	94
Figure 4.70: Instantaneous power spectrum of the distributed defect in inner race of bearing indicating rise in amplitude value at 153.875 Hz	94
Figure 4.71: LabVIEW front panel.....	95
Figure 4.72: LabVIEW block diagram	96
Figure 4.73: Block diagram of the intelligent diagnostic CM system	96
Figure 4.74: Developed experimental test rig.....	97

LIST OF TABLES

Table 2.1: Various motor faults and their detection methods.....	15
Table 2.2: Comparison of the various motor faults detection methods.....	33
Table 3.1: Specifications of the test motor	38
Table 3.2: Specifications of DAQ card NI PCI 6281	43
Table 3.3: NI DAQ parameters.....	45
Table 4.1: Experiment details for CM system.....	50
Table 4.2: Expected outer race defect frequencies at various loading conditions.....	51
Table 4.3: Amplitude values at outer race defect frequencies at various defect levels and under no load conditions	56
Table 4.4: Amplitude values at outer race defect frequencies at various defect levels and under full load conditions	62
Table 4.5: Comparison of the instantaneous power analysis with stator current analysis	64
Table 4.6: Expected inner race defect frequencies under various loading conditions.	65
Table 4.7: Amplitude values at inner race defect frequencies at various defect levels and under no load conditions	70
Table 4.8: Amplitude values at inner race defect frequencies at various defect levels and under full load conditions	76
Table 4.9: Comparison of the instantaneous power analysis with stator current analysis for bearing inner race defects.....	78
Table 4.10: Expected ball defect frequencies under various loading conditions	79
Table 4.11: Amplitude values at bearing ball defect frequencies at various defect levels and under no load conditions.....	81
Table 4.12: Amplitude values at bearing ball defect frequencies at various defect levels and under full load conditions	84
Table 4.13: Comparison of the instantaneous power analysis with stator current analysis for bearing ball defects.....	85
Table 4.14: Expected cage defect frequencies under full load on motor.....	86

Table 4.15: Amplitude values at bearing cage defect frequencies under no load conditions	88
Table 4.16: Amplitude values at bearing cage defect frequencies under full load conditions	90

LIST OF ABBREVIATIONS

AC	Alternating Current
AI	Analog Input
AO	Analog Output
AE	Acoustic Emission
ASD	Adjustable Speed Drive
CBM	Condition Based Maintenance
CM	Condition Monitoring
DC	Direct Current
DSP	Digital Signal Processing
DAQ	Data Acquisition
EPRI	Electric Power Research Institute
FFT	Fast Fourier Transform
FEA	Finite Element Analysis
FL	Full Load
IES	Industry Application Society
LSB	Lower Side Band
MCSA	Motor Current Signature Analysis
MAX	Measurement Automation Explorer
NN	Neural Network
NI	National Instrument
NL	No Load
PM	Predictive Maintenance
PLC	Programmable Logic Controller
PDT	Power Decomposition Technique
RPM	Revolution Per Minute
TBM	Time Based Maintenance
USB	Upper Side Band

UMP	Unballanced Magnetic Pull
VFD	Variable Frequency Drive
VI	Virtual Instrumetation

NOMENCLATURE

V	Supply voltages
I	Stator current
f_e	Electric Supply Frequency
f_{of}	Bearing Outer Race Characteristic Defect Frequency
f_{if}	Bearing Inner Race Characteristic Defect Frequency
f_{bd}	Bearing Ball Characteristic Defect Frequency
f_{cd}	Bearing Cage Characteristic Defect Frequency
N_b	Number of Balls inside the Bearing
f_r	Rotor Frequency in Hz
d	Ball Diameter
D	Pitch Diameter of Bearing
α	Ball Contact Angle
ρ	Density of Material
h	Height of Plate
D_o^2	Outer Diameter of Steel Plate used as Radial Load
D_i^2	Inner Diameter of Steel Plate used as Radial Load
g	Acceleration due to Gravity

CHAPTER 1

INTRODUCTION

1.1 Background

The type of motors most often utilized in industries worldwide are the induction motors. These motors make up 95% of the prime movers and they utilize up to 40 to 50% of all the electric energy generated [1]. They have been applied in various applications, such as, the petroleum industry, chemical processing plants, nuclear power plants, paper mills, cooling water systems and the mining industry. Induction motors have also been used in more general situations such as with compressors, pumps, crushers, fans, lifts, air conditioners, machine tools, tractions, robotics and etc.

Although induction motors are very dependable with low failure rate and require only basic maintenance, still as with other kinds of motors, they will break down and fail after some time [2]. The unexpected breakdowns of the motors cause a great deal of unacceptable production loss. This is quite unacceptable in applications that are vital for the industry.

Consequently, detecting initial failures and replacing damaged parts according to schedule will prevent the problems of unexpected breakdowns on the machines [3]. The prevention of unscheduled downtime for electrical drive systems has been the goal of every industry for a long time as this would help in reducing the costs associated with maintenance.

It has been found most commonly that more than 50% of operating cost of manufacturing and processing plants is related to maintenance [87]. Consequently, this is a major area of concern in industries.

The researchers are constantly looking for new techniques that can lower the cost of maintenance and to reduce the possibility of unexpected breakdowns.

In general, three methods for the machine maintenance used in industrial areas are classified as scheduled replacement, scheduled maintenance and condition based maintenance.

In the scheduled replacement, replacement of machine parts is conducted on a regular basis. It is very simple and easy method but proves to be very expensive. On the other hand, in the scheduled maintenance, the checking and/or overhauling of the equipment has to be done on a regular basis. It is the method typically used in industries as it is less expensive than the schedule replacement technique. In condition based maintenance, the condition of a machine is determined by taking measurements using a sensor. By this method, the time periods between maintenance can be increased and machines can be monitored continuously so that maintenance can be scheduled on needed basis. Condition monitoring (CM) is a technique that serves the condition based maintenance (CBM). It is an effective type of predictive maintenance (PM).

Normally, the condition monitoring maintenance process would be monitoring the specific parameters like vibration, overheating, over current of equipment for early sign of coming failure and to forecast the need of maintenance before rigorous failure and/or to estimate the machines health. It could be achieved by visual inspection or through sophisticated intelligent diagnosis system. It embraces the life mechanism of the machine parts, the different data acquisition methods and exploitation of the data to forecast the trends. Condition monitoring is mainly appropriate for continuous process plants where breakdowns can be very costly. Before CM, time based maintenance (TBM) was the technique served for preventive maintenance. In TBM method, maintenance was performed on predefined running hours of equipment, without the information of current conditions of machine so most of the times it causes wastage of manpower, time and money. As maintenance was performed offline so it causes many unnecessary shutdowns. However unpredicted breakdowns may still occur in the intervals.

The methods of condition monitoring are categorized into two primary classifications, namely the off-line tests and the on-line tests.

The off-line tests are performed by isolating the machine from main AC power supply. Although this is comprehensive approach, sometimes causes unnecessary shut-downs on machines.

Alternatively, the sensors which are installed on the machine are used to detect faults for on-line condition monitoring and fault diagnosis in an induction motor during the operation of the machine. The on-line tests cause fewer disturbances than off-line tests but the results produced from on-line testing are more complicated and their interpretation is difficult than off-line tests. However for this study only the on-line testing of the induction motors during operation was considered.

Over the past two decades, there has been an abundance of research work done in the condition monitoring field and techniques for diagnosing problems in induction motors. For the detection of the various faults usually affecting machines, several different techniques have been not only proposed but also used successfully [4, 5, 6]. However, a good understanding of the mechanical and electrical properties of the machine in healthy condition and in faulty condition dramatically influences the accuracy and reliability of the on-line condition monitoring methods.

On-line condition monitoring techniques can be classified into two categories: firstly the classical method and secondly the digital method [7]. In classical method, electromechanical devices are used to protect the motor. The electromechanical devices are expensive, less efficient, having very slow response and not reliable as some of the devices have even shorter life than the motor itself. The digital method is the latest method for the condition monitoring and it involves integrated circuits, micro controllers, micro processors and programmable logic controllers.

1.2 Motivation

In recent years, the use of novel analysis methods along with the aid of systems of progressive computerized data processing and acquisition has brought forth new areas in the research field of condition monitoring for induction motors. One of the leading

research topics for energy and electrical industries today is the development of novel condition monitoring (CM) system for the induction motors. The lifetime of electrical machinery is prolonged by condition monitoring and this has minimized the possibility of disastrous machine failure. Computer and transducer technologies along with advanced signal processing methods have resulted in the ability to apply condition monitoring systems in a more effective manner [8,9]. As a result, condition monitoring can be made to be more reliable with lower maintenance cost. Another important issue is that, during the maintenance period, the data regarding the status of the machinery should be obtained by on-line condition monitoring and hence the disastrous machinery failure can be reduced more effectively. As related to this study, a baseline study of faulty and healthy motors should be conducted and will be utilized to analyze localized as well as distributed faults. Many methods have been developed which support the development of condition monitoring system, however these have been using specialized and expensive sensors [36-50]. The need to explore on a more effective and less costly method on monitoring and analyzing the faults by utilizing the stator current signal has been overlooked. Condition based maintenance provides the current status of machines and indicates clearly where and what type of maintenance is required with the aims of achieving optimal use of machine parts and guarantees that the breakdowns will not occur unexpectedly. CBM will be the most favorable maintenance under the help of intelligent diagnostic condition monitoring system to present the exact and valuable information about the condition of the machine. In this work the information about the conditions of the motors will be based on analysis of the instantaneous power FFT spectrum analysis.

1.3 The Shortcomings of Previous Research Work on Condition Monitoring

The reliability of the methods for the signal-processing is dependent upon an adequate understanding of the mechanical and electrical properties of the motor in both the healthy and faulty states under various conditions of loading. The following limitations have been identified based on the data discussed in the review of the literature related to condition monitoring of the induction motors.

- Most of the studies focused on localized defects due to outer and inner races of the bearing. However, only limited research has been carried

out on investigation of localized defects related to rolling elements (balls) and cage of the bearings [63,70,79,84-86].

- Some of the researchers have deliberately discussed the distributed defects in the bearings but no one has explained it experimentally [72,91].
- Most of the research work has only taken the stator current FFT spectrum analysis into consideration as a diagnostic medium for the detection of the various faults in induction motors [51-86]. Some of the researchers have used the instantaneous power analysis method for detection of stator defects, eccentricity defects and broken rotor bars [87]. Using instantaneous power FFT spectrum analysis for the detection of bearing faults in the motors has not been reported in earlier research work.
- Most of the researchers focused on the development of intelligent diagnosis condition monitoring system using the sensors i.e vibration analysis method, temperature analysis method and acoustic emission method [38,39,52,67,85,88,89]. All of these methods require expensive sensors and also have installation limitations.

1.4 Objectives and Contribution of the Research

One of the important observations on the fault diagnosis of the induction motor has been that any one of the sensor based or sensor-less technique can determine the presence or absence of the faults. A comparison of the different kinds of condition monitoring methods must be performed and an appropriate method must be chosen to determine the specific faults.

The research presents an approach to:

- Diagnose motor bearing localized and distributed faults at incipient stages experimentally via instantaneous power FFT spectrum analysis method. The observation has been made that the majority of the work found in literature

today has been based on the Matlab programming; this may cause problems with on-line condition monitoring which is practical and highly sought after in industry. In this study, the LabVIEW environment will be employed for determining the faults with online condition monitoring. To interface directly with the system, LabVIEW software could possibly be the best choice.

- Investigates the effectiveness of the fault frequency signals of the motor instantaneous power to detect motor bearing faults. Therefore, it is significant to evaluate how the existence of various bearing faults affects on the different fault frequencies under loaded and unloaded conditions of the motor.
- Builds an intelligent diagnostic condition monitoring system for continuous real time tracking of motor bearing localized and distributed faults, to estimate the severity of various faults, also to switch-off the motor automatically if fault exceeds preset values and to show the motor status on computer screen.

1.5 Outlines of the Thesis

The best way to begin the thesis would be by giving the fundamental knowledge of the principles and construction of the induction motors. A description of various kinds of the motor faults followed by the various condition monitoring techniques is presented. A simple outline overview of the various phases of the process for condition monitoring will be explained and a survey of the subject is also provided.

This thesis presents the research work in five chapters. An overview of the condition monitoring, research objectives and organization of the thesis is presented in Chapter 1.

Chapter 2 handles the comprehensive literature survey and a review of earlier work related to induction motor condition monitoring. The chapter also provides the motivation that has led to the work on different kinds faults in the bearings of the motor.

Chapter 3 deals with development of experimental rig for intelligent diagnosis of various faults related to the bearings of the motor. A generalization of the experimental condition monitoring system software and hardware modules employed

in this work is presented in this chapter. The test rig built for this research work been designed for operation at different motor speeds, under various loads and with bearings at different states of health. The data acquisition and processing system used in this work consists of the National Instruments data acquisition card NI 6281, an AC current and voltage transformer and LabVIEW version 8.2. The details of the LabVIEW programme, which has been created so that the characteristic fault frequencies could be identified, will also be explained.

The ultimate objective of the machine condition monitoring is to gain reliable and accurate data about the status of induction motors so that timely decisions can be made. A satisfactory understanding of how fault severity and the conditions of loading affect the amplitudes of the characteristic fault frequency elements is required to achieve this objective. An extensive series of laboratory tests will be presented to support the viability of the proposed technique. Chapter 4 deals with results, analysis and discussions about the various defects of the motor. Also intelligent fault diagnosis system for condition monitoring of the motor is discussed in this chapter.

Chapter 5 consists of the conclusions of the research. Also future work related to motor condition monitoring is proposed in this chapter.

The references and list of publications are presented at the end of the thesis.

CHAPTER 2

LITERATURE REVIEW

2.1 Introduction

This chapter presents a review on the research work related to electric motor fault diagnosis and condition monitoring. It encompasses several vital topics, such as induction motor defects, vibration analysis, acoustic emission method, thermal monitoring, noise monitoring, chemical analysis, electric current monitoring and etc. Furthermore, the developments in condition monitoring methods from the earlier studies until the most current are also covered.

2.2 Overview of the Induction Motors

Induction motors are comprehensively used in almost all types of industries. Induction motor is an asynchronous machine made up of a magnetic circuit that is joined to two electrical circuits; these circuits rotate with respect to each other. Electromagnetic induction is used to pass power from one circuit to the other. These electric motors are used to convert electrical energy into mechanical energy [10]. The conversion of energy is dependent upon the natural presence of the phenomena connecting magnetic and electrical fields in one side while motion and mechanical force are connected into other side. On the basis of types of rotor winding, induction motors can be placed into two categories. They are the wound-rotor induction motors and squirrel-cage motors [11].

The induction motor of the squirrel cage type is made up of conducting bars that are placed in slots of the rotor body. These conducting bars are short circuited through end rings. Magnesium, copper, aluminum or alloy is the materials usually used in

manufacturing of the rotor bars. There is no insulation in the rotor of the squirrel cage motors because large currents are conducted by the bars at low voltages.

Another kind of rotor is known as a form-wound rotor since it possesses a winding that is poly phase much like that of the winding of the stator. There are three slip rings which are joined to the winding of the rotor shaft. In a rotor that is form-wound, the slip rings are joined to a variable resistance and it can restrict the current as well as the heating of the rotor [11].

The induction motor of the squirrel-cage type is quite basic, more economical, and more robust than the induction motor of the wound-rotor type. At constant supply voltages and frequency, induction motor of the squirrel-cage type runs at a constant speed. In this motor if there is an increase in the load torque, the speed will decrease slightly. Therefore, it is appropriate to be used in drive systems that run at a constant speed [10,11]. However, a variety of applications used in industrial areas need adjustable speeds drives. Traditionally, it is a DC motor that is utilized in a drive system that is adjustable. However, DC motors are expensive, and they possess brushes and commutators that must be frequently maintained. As squirrel cage induction motors have no brushes so they are cheap and are preferred for high speed applications. Furthermore, due to the availability of solid state controllers, mostly high speed drive systems use induction motors of squirrel cage type. This type of induction motor is extensively utilized in drive applications of both low and high performance, this is because of its versatility and ruggedness.

Induction motors are often exposed to operating environments that may not be ideal and in some cases are even harsh. These situations could be insufficient cooling, inadequate lubrication, overload, frequent motor starts and stops etc. In such situations, induction motors are put under detrimental stresses which lead to failure of the motor [12]. Because of the significant role that motors play in various applications, improvement in the reliability of motors is required.

AC induction motors are suitable for almost all commercial and industrial applications due to their construction being so simple and they have only a few parts, which reduce the cost of the maintenance. Applications in both adjustable speed-drive (ASD) and constant-speed drive are the main use of induction motors [13].

2.3 Faults in Induction Motor

As induction motor is most often symmetrical so faults in the motor normally disturb the symmetry of the motor. Reduced efficiency, unbalanced air gap voltages and line currents, increased space harmonics, decreased shaft torque, increased torque pulsation and increased losses are the usual symptoms related to the disturbed symmetry. There are several factors which contribute to burning of motors and some of them are thermal overloading, overloading due to undesirable stresses, air gap eccentricity, speed oscillations, stator winding failure, broken rotor bars, bearing failure and unbalanced voltages. The most common defects of the motors are shown in Table 2.1 [14,15,16]. A concise discussion is made regarding these defects based on how important they are in regards to the condition monitoring of induction motors.

According to a survey conducted in 2005 by the Electric Power Research Institute more than 40% burning of AC motors are due failure of bearings. The survey report is shown in Figure 2.1 [17].

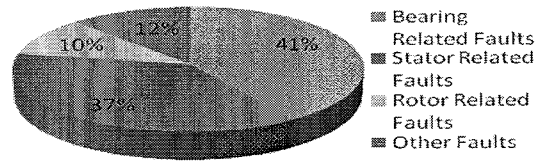


Figure 2.1: EPRI survey report 2005 [17]

The defects of the motor are categorized into two groups [18,19].

- Mechanical defects
- Electrical defects

Air gap eccentricity, bearing defects, shaft misalignment and defects due to the load are included in the list of mechanical defects. Broken rotor bar and stator winding defects are included in the list of electrical defects. The detail of these defects is discussed in following subsections:

2.3.1 Mechanical Defects

The typical examples of mechanical defects that usually occur in an induction motor are presented as below:

2.3.1.1 Bearing Defects

Bearings are typical components found in the motors that are used to allow for the shaft rotation. Majority of motor failure is due to the bearing malfunctions. Bearings are made up of an inner and an outer race. Several rolling elements (balls) are placed in between these two races. Cage is used to keep the balls moving at equal distance from each other. Stresses developed in the motor causes fatigue in the bearing races. This fatigue causes localized defects (single point defects like flaking or spalling or holes) and distributed defects (multiple holes, surface roughness) in the bearings of the motor. Vibration and noise is generated in the motor due to these defects. Some other factors that contribute to bearing malfunctions are improper lubrication, contamination, improper installation, corrosion and brinelling [20]. The failure of bearings can also occur due to high bearing temperature. The temperature of the bearings should not increase beyond specific degrees at rated conditions. An example of this would be in the petroleum and chemical industries where the IEEE 841 standard specifies that the rise in temperature of the bearings under a rated load should not go above 45 degrees. Rise in the winding temperature, improper lubrication, the distribution of the temperature within the motor and the operating speed of the motor are the main factors for the rise of the bearing temperature. Consequently, the bearing temperature measurements can give helpful data to estimate the health of the bearings as well as health of the motor [21,22]. The defect in the bearing element produces the vibration at the characteristic defect frequencies. These frequencies can be calculated using the running speed of the motor and bearing dimensions.

2.3.1.2 Air gap Eccentricity Defects

Air gap eccentricity is a typical defect found in the rotor of the motor. Noise and vibration in the motor structure are usually produced due to eccentricity. For the healthy motors the center of the rotor and stator bore is perfectly aligned moreover, the center of rotation for the rotor is the same as the stator bore center. If the rotor is not aligned centrally, radial forces or magnetic pull will develop which causes the rotor-stator rub resulting in the damage of rotor and stator [23,24]. Air gap eccentricities are of three kinds [18,19,23]:

- Dynamic eccentricity
- Static eccentricity
- Mixed eccentricity

A dynamic eccentricity results in a unbalanced magnetic pull (UMP) that acts on the rotor. The rotation of the UMP is same as rotation of the motor. This UMP can be easily monitored via current or vibration analysis.

On the other hand, eccentricity that is static possesses a constant pull in only one direction which also causes a UMP. However, it is not easy to detect this UMP [23,25].

Sometimes, dynamic and static eccentricities often exist together. Moreover, one can never assume that ideal centric conditions exist. Therefore, a certain amount of eccentricity is always expected in any real motor. This combination of eccentricities such as dynamic and static is known as mixed eccentricity.

2.3.1.3 Load Defects

Detecting load faults has been a vital area of study in mechanical engineering for quite a long time. Mechanical loads and gears are frequently connected to motors and a variety of faults such as defected gearing system and coupling misalignment are possible in these mechanical arrangements. In some applications like air craft's, the condition monitoring of gears couples with drive system is very much important to enhance the reliability of the gear [26].

2.3.2 Electrical Defects

Presented below are some of the typical examples of electrical defects in the induction motors.

2.3.2.1 Stator Winding Defects

The general belief is that damage of the insulation of the winding turns contributes majority of the defects related to stator. This kind of defect is known as a “stator turn defect” [27]. In a symmetrical induction motor, a stator turn fault produces a huge amount of current to flow through turns which creates too much heat in the shorted turns. The motor will burn if this heat, which is in direct proportion to the square of the current, is more than the threshold value [28]. In induction motors, the insulation used in stator winding is subjected to degradation due to contamination, transient voltage stresses on the insulating material, mechanical stresses and thermal overloading. Out of all, thermal stresses are the primary cause for the deterioration of the insulation in the winding of the stator. Insulation even of the best quality could experience a rapid failure if the motor is run at a temperature greater than its threshold value. Generally, the life time of the insulation is decreased by 50 % for every 10 degrees centigrade increase over the threshold value of the temperature of stator winding [29]. Therefore, monitoring of the temperature of the winding of the stator is vital so that the motor will not run at a level greater than its thermal capacity. To accomplish this, lot of methods have been introduced. However, these methods could not identify the exact heating point at earliest stage [30,31].

Some factors that speed up the deterioration of the insulation include the defected bearings, broken rotor bars, vibrations of the rotor, movement of a coil, misalignment of the rotor and air gap eccentricity [32]. Consequently, these mechanical failures should be identified before they cause the failure of the insulation in the stator winding [33,34]. Another problem for the insulation is foreign materials such as dust and bearing grease which can cause contaminations over the insulation of the stator. This contamination could possibly cause the reduction in dissipation of heat from the stator winding [35]. Due to this reason it is recommended that all motors should kept clean and dry.

2.3.2.2 Rotor Defects

Most often, the rotor bars in lower rated motors are produced by methods of die casting. However, the rotor bars of high rating motors are manufactured using copper. Producing rotor bars using methods of die casting has been found to cause a variety of technological problems. Asymmetries in the rotor of the induction motors have been found which were caused by either technological problems, or because of the melting of end rings or bars. On the other hand, there is abundance of other factors causing the failure of rotors. Some of these are listed below [17,18]:

- Metallurgical stresses that are non-uniform could possibly be created in the assembly of the cage during manufacturing process and these stresses could result in a failure while the motor is operating later on.
- When thermal stresses are put on the rotor bar at the start-up of the motor; the rotor might not be capable of moving longitudinally in its slot.
- Some stresses could develop on the rotor bars due to heavy end rings.

The reasons mentioned above could cause damage to the bars of the rotor and at the same time cause the rotor to become unbalanced. Furthermore, asymmetrical rotor currents are produced due to asymmetry of the cage of the rotor. Because of this, damage to just one rotor bar could result in damage to the surrounding bars. This damage could then spread, resulting in fractures in several rotor bars. Cracks in bars causes overheating of the bar due to which bar may break. Consequently, the bars in the surrounding area will begin to carry higher currents subjecting them to even greater mechanical and thermal stresses. These stresses can start cracking in rotor bars and rotor lamination will be damaged as well [18]. The distribution of the temperature throughout the lamination of the rotor is also altered because of the asymmetry of the rotor. Bar fractures can take place at different areas on the rotor. During frequent starts of the motor, the chances of fracture in the rotor end rings increase [32].

Table 2.1: Various motor faults and their detection methods

Type of Motor Defects	Causes	Defect Detection Methods
Rotor Defects	<ul style="list-style-type: none"> • Dynamic torques • Thermal Stresses • Frequent starts • Mechanical stresses • Corrosions 	<ul style="list-style-type: none"> • Vibration analysis • Temperature analysis • Acoustic Emission method • Current analysis • Noise Monitoring
Bearing Defects	<ul style="list-style-type: none"> • Improper lubrication • Improper installation • Contamination • End of life 	<ul style="list-style-type: none"> • Vibration analysis • Temperature analysis • Acoustic Emission method • Current analysis • Chemical Analysis • Noise Monitoring
Stator Defects	<ul style="list-style-type: none"> • Over-current • Mechanical stresses • Loose lamination • Contamination of insulation • Over-heating of winding 	<ul style="list-style-type: none"> • Vibration analysis • Temperature analysis • Acoustic Emission method • Current analysis
Eccentricity Defects	<ul style="list-style-type: none"> • Misalignment • Bearing damage • Bent rotor 	<ul style="list-style-type: none"> • Vibration analysis • Temperature analysis • Acoustic Emission method • Current analysis

2.4 Requirements for Condition Monitoring

Continuously evaluating the health status of an industrial plant and its machinery throughout the entirety of its service is known as condition monitoring. Incipient

failure detection is a vital process by which detection of defects in the early stages of their development is possible [18]. Fault diagnosis of the induction motor with some comprehensive condition monitoring system is becoming even more vital day by day. An early alert about forthcoming failure is possible through the use of condition monitoring system. Furthermore, scheduling of preventive maintenance of the machines is also possible. Optimal preventive maintenance schedules are a result of this and it also leads to the least amount of down time on the machines [19]. Moreover, condition monitoring system gives indication to maintenance staff to arrange the required spare parts before serious breakdown occur on machine, thus it reduces overall down time. Consequently, to improve productivity, reliability and safety of electric machines, a suitable condition monitoring system is essential.

2.5 Condition Monitoring Techniques

The fault diagnosis and condition monitoring of the bearings of the induction motor has been the focus of this research. A tremendous significance has been put on by condition monitoring system in the environment of business because of several reasons that are listed below [18,19]:

- To decrease the maintenance cost.
- To determine the failure of machinery.
- To enhance the reliability of both the machines and their parts.
- Optimal use of manpower and machine spare parts
- To maximize the performance of the machinery.
- To enhance the failure prediction accuracy.

The usage of condition monitoring for both mechanical and electrical machinery is not new. While there have been a variety of techniques developed and improved over time, thermal monitoring, chemical monitoring, acoustic emission, vibration monitoring, electrical monitoring and noise monitoring are considered as the most prominent methods.

2.5.1 Vibration Monitoring

Noise and vibrations are produced by all motors. Health of the motor can be estimated by analyzing these noises and vibrations. A high level of noise can be generated by just tiny amplitude of vibration in the frame of a machine. Magnetic and/or mechanical forces are the cause of noise and vibrations in motors [36]. The radial forces resulting from the air gap field are the greatest sources of vibrations in the motors. The resultant magneto motive force wave and total permeance wave generate the air gap flux density distribution. The resultant magneto motive force possesses the effect of potential stator or rotor asymmetries and the permeance wave is dependent upon the differences of the air gap. Therefore, detecting the different kinds of defects and asymmetries is possible when the vibration signal of the motors is analyzed [37]. The best situations for performing diagnostics based on vibrations involve rotor eccentricities, unbalanced rotors, bearing and gear faults. The motors vibration monitoring is carried out by using the analysis, either narrow-band or broad-band of the measured vibration energy signal. Condition monitoring method based on vibration analysis is the best fault diagnosis technique; however, costly vibration sensors and their associated wiring are required. As a result, use of vibration analysis is restricted in a variety of applications. This is particularly so with applications using small sized motors as cost has an important role to play when making the decision as to which technique of condition monitoring is to be used.

For the diagnoses of the bearing defects, [38] performed vibration analysis. An artificial neural network was utilized to perform the diagnoses. This study was carried out using real measurements and using a simulated vibration. In both situations, the results showed that neural network can effectively diagnose the motor bearing defects by measuring the vibration signature. In this work, Fast Fourier transform (FFT) was used to extract the vibration features from time domain of the signal. The construction of five vibration signatures was carried out using power spectrum of the vibration signal. Data regarding the time domain, such as the Kurtosis factor of the vibration waveform, and the mean and maximum values of the waveform were also taken into consideration. As a result, there were six input measurements in the complete neural network. Researchers have shown how the neural network can be utilized in an effective way to diagnose bearing defects by measuring the vibration signals of the

bearings of a motor. Better results have been found with an approach by [39]. In their approach, genetic algorithm is used to train the artificial neural network. Statistics of the signal's vibration were considered as features for input in this study. The study examined how the genetic algorithm was used to choose the input features of the most importance in the context of motor condition monitoring. [38] and [39] have critically focused on the detection of mechanical faults of the motor. Furthermore, that technique could also be applied for detection of electrical defects inside the motor.

On the other hand, high cost is the major disadvantage of this technique. For example, vibration sensors (accelerometers, velocity transducers) which are integral part of this technique are too much expensive. Another disadvantage of this technique is that sensors need to be installed on machine so it needs access to machine which is not possible in every application. Sensor needs to be mounted on machine rightly for accurate results. As sensors also have some life period after which they fail and in this aspect bearings life are more significant than sensor life [23,24,40].

2.5.2 Acoustic Emission

There are few challenges related to the vibration analysis method in an atmosphere which is full of noise. This happens as a result of the small frequencies created by the small deteriorations in the bearings which add a small energy spectrum into the atmosphere as compared to other noises in the surroundings. Therefore, vibrations analysis as a bearing defect detection system is not suitable for some applications, such as with liquid rocket engines, gas turbines, nuclear plants and aircraft transmissions, as it does not provide satisfactory results. However, the stress wave emissions in high-frequency regions (above 100 kHz), can still present comprehensible data regarding defects in the machinery in noisy environments and thus give an early and more reliable sign of defects in the bearings. Transient elastic waves are generated due to the quick release of strain energy as a result of changes in the structure of the solid materials. Acoustic emission (AE) is the name of this phenomenon. AE in metals is caused by the creation and propagation of cracks. The AE transducers have the ability to sense acoustic emission waves. The parameters that AE focuses on are the amplitude, events of the signal and the number of counts. The benefit received from using the AE method is that it gives a higher signal-to-noise

ratio in a noisy environment through detection of growth of cracks in the subsurface. However, this method also has some disadvantages; the first is that it is expensive as it needs sensors that are costly to take the measurements. Another disadvantage is that specialized expertise is necessary to measure the acoustic emission [41,42].

2.5.3 Thermal Monitoring

The thermal monitoring of the induction motor is carried out in either of two ways. The first way is to take a measurement of the bulk temperature or the local temperature of the motor; the second way is to perform an estimation of the parameter. Excessive amount of heat is produced in the motor stator due to fault in the motor and this heat indicates how severe the fault is until it gets to a destructive point. Consequently, thermal models of the electrical motors have been developed by some researchers. Basically, there are two categories for the classification of the various thermal models of the motor [43]:

- The finite element Analysis based models (FEA).
- The lumped parameter thermal models.

Although finite element analysis based models function more accurately but they are computationally intensive. On the other hand, lumped parameter thermal models are the same as a thermal network which consists of thermal capacitances and resistances as well as their associated power losses. A model's accuracy usually depends on how many thermally homogenous bodies the model consists of [43,44]. There are two methods that are most commonly used for determining the parameters of a lumped parameter thermal model. One method is to use an intensive knowledge about the motors, materials used to build them and their physical dimensions. The other method is through the identification of the parameters from the measurements of the temperature that have been taken extensively at various parts of the motor. While the motors are made up of a variety of materials having various properties, each motor is believed to be composed of several lumped bodies that are thermally homogenous. On the basis of these beliefs, a more basic version of an induction model and a PMSM made up of two lumped thermal bodies were proposed in [45,46]. Similarly, a thermal model of an electrical machine was developed by [47]. Their thermal model was

utilized to make estimation of the motor's temperature and for the identification of any defects present. Basically, thermal monitoring can be used as an indirect manner for detecting some types of faults in the stator and in the bearings of the motor. For stator defects, the temperature rises in the area of the defect. However, incipient fault detection is not possible as temperature changes are being occurred too slowly. In a situation for the detection of bearing faults, the increased wear in bearings causes increase of friction which leads to rise in temperature at that point. Thermal monitoring can be used to detect this temperature increase present in the motor.

Temperature sensor and embedded system is required for temperature measurement of the bearing which is major disadvantage of this technique. Even if the bearing temperature increase is acknowledged further analysis will be required to find the reason of the temperature rise. Consequently temperature monitoring is a conventional way for bearing condition monitoring but not very well-liked today.

2.5.4 Sound Monitoring

When defect occurs in bearings it produces some noise so bearing condition can be monitored through measurement of sound pressure. Microphones can be used for recording of bearing noise also sound from defected bearings can be heard by human ears. Sound measurement proves to be less interfering than other techniques. However, in this technique unwanted noise and background sound must be separated. Without doing this result obtained from sound analysis will not give correct information about the condition of bearings. However, there is no practicality in applying noise measurements in an industrial plant as the other machinery running in the vicinity make the background too noisy. Therefore, the accuracy of the fault detection would be reduced due to background noise. However, air gap eccentricity was detected by [48] using this technique. They conduct their test in an anechoic chamber to verify the static eccentricity faults in the motor.

2.5.5 Chemical Analysis

As result of degradation of lubricants by heat, a large number of chemical products are produced in solid, liquid and gaseous states. Similarly bearing degradation produces debris. Therefore, greases and oil lubricants posses not only their own degradation materials but also they carry debris of bearings [49] [50].So chemical analysis of these greases and oil lubricants can be used as fault diagnosis and condition monitoring tool for the bearings. Though the analysis of these greases can provide useful information regarding bearing health but this could only be done if these oil lubricants and greases are available. So this analysis is applicable to only large machines which use oil lubricants. For small and medium size machines, greases are usually encapsulated inside bearings so chemical analysis methods are not practical for these small machines.

2.5.6 Electrical Monitoring

The electric monitoring also known as motor current signature analysis (MCSA) is utilized for detection of the motor and inverter defects using information from the stator current. In the majority of the applications, the stator current of an induction motor is easily obtainable because it is utilized in the protection of the motors from over-currents, ground currents. So, current monitoring is a method of detection that is sensor-less and needs no extra hardware for its implementation.

Current signature analysis for the condition monitoring of the motors finds its application majorly in nuclear power plants and defense industry where access to the motor is not possible. In the majority of the applications, the stator current was monitored for the detection of various induction motor defects. [51] use the current signature analysis scheme for the detection of the motor rotor and bearing defects. Their research investigated the effectiveness of current monitoring to detect the faults in bearings and rotor by comparing the relationship between the current and the vibration frequencies. This study shows the different bearing and rotor defects and the characteristic fault frequencies associated with these defects. An explanation of how the spectrum of the stator current was affected due to the rotor and bearing faults was given and determination of the related frequencies was made. The vibration spectrum

and current spectrum of bearing and rotor defects obtained through experiments were utilized for the verification of the relationship between the current and vibration frequencies. It was clearly illustrated by the test results, that the motor current signature analysis could be utilized for the diagnosis of the rotor and bearings defects.

[52] Describes a technique which provides on-line detection of motor defects. This technique requires no human involvement for the interpretation of the motor current signature. A selective frequency filter learned the motor characteristic frequencies at normal operating conditions. The physical construction of the motor was used to set the rules for the expert system and to generate the frequency table. The inputs of the NN clustering algorithm were formed by this list of frequencies. These inputs were compared to the characteristics found during operation of the initial motor performance. To accomplish this, the only requirement was that the motor should be in good operating condition while the system was being trained. A fault will continuously degrade the signature of the current and the system will look for those alterations in the spectra and shows the condition of the motor. An alarm would sound when the changes in spectra moved enough away from the normal condition. Combining a neural network (NN) and a rule-based (expert system) frequency filter maximized the ability of the system to detect the small spectral alterations created by initial fault formation. Implementation of the developed algorithm for the detection of failures was performed and tested. Simulation of a failure in the motor was carried out with the introduction of a rotating mechanical eccentricity into the motor being tested. After the NN was trained, the system was capable of readily detecting the alterations in the current spectrum caused by the presence of the defect.

A technique for the removal of the effects of the load torque from the motor current spectrum was presented by [53]. The authors determined that approaches introduced earlier for condition monitoring based on the motor current do not take into consideration the effect of the load. As a result, a technique is required to separate the effect of presence of load torque and effect of defects to estimate the health of machine. Making a comparison of a model reference value which included the load effects with the real stator current would accomplish this. The variance between these two signals would give a filtered quantity which would not be dependent on the variances in the load and would provide on-line condition

monitoring to be carried out continuously without the need to consider the condition of the load. The results of the simulation indicated the effectiveness of this approach and experimental results demonstrated the feasibility of this method. It was shown that the characteristic spectral elements exist in the current and it was possible to remove the load effects effectively from the spectrum.

[54] Suggested a technique for monitoring faults such as the cracked rotor bars, shorted stator winding and air gap eccentricity in the motors. The air gap torque can be computed during the operation of the motor. This means that there would be no special down time needed when performing the measurement. Data regarding the air gap torque for a motor is collected time to time to be used for later comparisons. The potential and validity of this technique were demonstrated by experiments that were performed on a 3.7 kW motor.

[55] Created a new model for the motor to analyze the rotor static eccentricity. The model is based on the geometry of the motor and placement of windings in the motor. The model was able to provide a simulation of the effects of the static rotor eccentricity on the motor performance. Because the mechanical equation was included in the dynamic model of the motor, so any random time function of the load torque could be defined from which the resulting stator current could be computed. Simulation of a three-phase motor with a 50% rotor eccentricity was performed in order to demonstrate the utilization of this technique. Simulations have produce results that closely related with the experimental results found in earlier studies.

[56] Presented that condition monitoring of electric motors leads to estimation of electrical and/or mechanical defects before the breakdown occurs. Comprehensive research efforts have been done on the analysis of the current signature of the motor. This method makes use of the results of the stator current spectral analysis. Because distortions of the waveform of the current created by drive system abnormalities are most often tiny, so it is quite difficult to reliably interpret the spectra. Their research work have demonstrated that some asymmetrical motor defects have frequency signatures that are easily identifiable when the FFT is used. This leads to the good explanation of the spectra of the motor current. Experiments performed in the laboratory have shown that the defect detection of the motor via FFT base current signature analysis is more reliable.

[57] Studied the efficiency of the spectral analysis of the motor current on the detection of faults in the motors. The frequency signatures of the some defects such as broken bars, air gap eccentricity, bearing failures and rotor asymmetry were identified. The spectral analysis of the current was verified in this work in regards to its feasibility. The spectral analysis of the current was also implemented with other kinds of electrical machinery. For example, [58] apply the current spectrum analysis to diagnose the air gap eccentricity defects in the in a three-phase induction motor of a large size. Monitoring of the harmonic element of the current at rotating frequency for the detection of defects in the rotor of a permanent magnetic synchronous machine was performed by [59].

An appraisal of monitoring methods used for detection of air gap eccentricity the of induction motors was presented by [58]. They proposed stator current monitoring as a very applicable technique in an industrial environment. This research presented the current spectrum analyses of a variety of motors. The interpretation of the spectrum of the motor current indicates that this study successfully diagnosed the air gap eccentricity defects.

[60] Mentioned an adaptive time–frequency technique for the detection of bearing and broken bar faults. It demonstrated that the spectrum of time–frequency shows the characteristics relevant to the detection of faults better than the Fourier spectrum. The technique was created on the basis of a training method based on the healthy situations of the motor. This work suggested that there was a necessity to segment the information into modes of normal homogenous operation. The performance of the detection would deteriorate if this fact was not taken into consideration. The results of this work demonstrated that faulty motor signals were hundreds of standard deviations away from the modes of the normal operations. This gave an indication of usefulness of the proposed statistical method. In the end, the proposed technique was suggested to be mathematically general and could be applied for the detection of any defect that might occur in the motor.

[61] Presented a novel technique for the detection of rotor defects by analyzing the stator voltage. The technique was attractive because the detection would not be influenced by source non-idealities. Moreover, it was obvious from the nature of the test that it could be carried out even with a motor in un-loaded condition. Also the

harmonic elements that were predicted by the theoretical analysis completely agreed with the results of the simulation. However, because of the asymmetries that are inherent in the machinery, some of these elements could possibly be present even in healthy motor. It is also clear from both the experiments and the simulations, that while the number of broken bars has little influence over the magnitude of the harmonic elements, still it is easy to distinguish a healthy motor from one that is defective.

The impact of control on the behavior of defected motor was introduced by [62]. His study shows that the indexes most commonly utilized for diagnostics in open loop operations are not effective. Experimental as well as simulation results have indicated that the in field-oriented controlled motor, the field current component has the appropriate characteristics necessary to develop effective diagnostic system.

An analysis was made by [63] on motor current signature analysis (MCSA) as a medium for detection of motor defects. The study introduced precisely how the signature analysis of a motor could be used to detect and localize the abnormal conditions that may cause the burning of the induction motor. The MCSA makes use of the current spectral analysis to identify any bearing defect, air gap eccentricity, or broken rotor bars. Its basis is on how the current at the sideband related to the fault behaves. To accomplish this, a comprehensive knowledge of the construction of the motor is a must. It has been explained that the motor current will contain some spectral components due to the effect of the load torque variations with the position of the rotor. The oscillation of the torque creates current harmonics that can partially conceal those harmonics that are created by defects.

[64] Presented the effect of stator winding defects on the rotor of the motor. It was found that the winding defects could create spatial harmonics in the air gap field of the motor. However, the change in harmonics occurs at the single frequency which is supply frequency of the applied voltage. Currents in the rotor cage are created by the stator winding harmonics and due this field harmonics are developed in rotor. These newly generated field harmonics vary at specific frequencies. The harmonics of the air gap field generate electromotive forces in the winding of the stator and create stator currents harmonic at the same frequencies as rotor. These generated frequencies are similar to those produce by stator winding defect.

A method of pattern recognition was created by [65] based on the Bayes minimum error classifier for the identification of rotor defects of the motors. The algorithm that they proposed utilizes only the motor supply current information as input values. First, the speed of the rotor is determined from the motor supply current and then suitable characteristics are extracted. The proposed method could be used for on-line condition monitoring of the motor rotor. The feasibility and strength of the proposed technique were verified by theoretical model as well as experimental results obtained from three-phase induction motor. Moreover, the algorithm could be modified to diagnose other defects such as phase unbalance and eccentricity.

A non-invasive condition monitoring method was proposed by [66]. This method was used to identify defects in the stator winding of the motors by monitoring the negative sequence supply current. To determine the negative and positive sequence elements of the measured currents and voltages, a power decomposition technique (PDT) was utilized. These studies illustrated that the impedance of the negative sequence could have a variance of between 10% and 50% due to an inter-turn short circuit.

[67] Conducted experiments to detect turn-to-turn short circuit faults in the motor using negative voltage method. To learn and make an estimate of the negative-sequence voltage neural network algorithm was developed. The healthy motor data was collected and used to train NN. As reported by [67], the majority of the turn-to-turn short circuit-related signatures can be extracted from the supply voltage of the motor due to regulation of drive controllers. On the other hand, the impact of the mechanical load was not taken into consideration. In reality, the drive controllers, operating conditions and mechanical load all influence on the data related to defects. Accurately predicting the condition of a motor cannot be guaranteed by monitoring the voltage or the stator current only.

It has been recognized by [68] that MCSA is one of the extensively utilized techniques for diagnosis of the motor faults. The measurement of the sidebands present in the spectrum of the stator current was the basis on which this technique was developed. The sidebands are found near to the fundamental supply frequency. The inverters makes the supply frequency vary a bit in time and because of this more harmonics are generated in the current spectrum. Sometimes these harmonics are

misinterpreted as the sideband components resulting from the rotor defects. In their research, they compared the results of the experiments performed for the diagnosis of the defects using a normal supply and an inverter.

In the current spectrum analysis of the motor, running values are compared with baseline values. In real time applications, baseline values are dependent on the operating conditions. To tackle this issue, [69] proposed new method which keeps track of baseline data at various operating conditions of the motor. He uses different load conditions and for each one he compare the baseline values with running values to estimate the health condition of the motor. Along with the FFT method for the analysis of the spectrum, he use some advance signal processing and pattern recognition techniques for defect analysis of the motor.

A brief presentation of signal processing methods for detection of defects in the rotor of the induction motor was given by [70]. The primary benefits and implementation issues of the presented methods were also precisely presented. From the reports, it seems that, wavelet analysis is also proved to be a powerful tool for the defect detection of motor.

Some results were presented by [71] regarding the detection of rotor bars in the three-phase motors. He conducted five experiments on various defect situations of the motor. Their work provided results which indicated that when a rotor has even one broken bar, it will have a direct impact on the waveform of the stator currents and the voltages. Consequently, the analysis of the spectrum of the line current has been found to be one of the best techniques among those that are non-intrusive. The process for the diagnosis was carried out through the utilization of virtual instrumentation (VI). Various virtual instruments (VIs) were created in Labview. Controlling of the test measurements and the acquisition and processing of the data were carried out using these VIs. The experiments were performed on the healthy and defected motor under seven different loading conditions. The defects in the rotor were induced by drilling the holes in the rotor bars. The Fast Fourier Transformation (FFT) was used to process the measured current signals. A plot was created for the measured phase current power density. A comparison was made between the results of defected and healthy rotor. The main focus was on identification of sideband elements at specific frequencies. The significant presence of several sideband frequencies in the

harmonics spectrum of the line current show quite clearly the defects in the rotor of the induction motor.

[72] Proposed the idea of classifying the defects in rotor of the motor into two types. These were distributed and single-point defects. This idea was important as the defects would be sorted according to the kind of signatures generated by defects instead of where the defects were located physically. There are two advantages with this kind of classification. The first benefit is that it guarantees that distributed defects are not neglected. Most of the condition monitoring approaches concerning fault detection found in the literature has been mainly focused on identifying single-point defects. Indeed this class of defects is quite important; however, an approach that is comprehensive and robust must have the capability of detecting not only single-point defect but also distributed defects in the rotor. The second benefit is that by classifying defects according to the kind of signature gives good idea for development of suitable detection scheme.

A technique for identifying motor defects at earliest stages using the current of the stator was proposed by [73]. This technique starts off with the filtration of the stator current so that most of the significant frequency content not associated with the defects in the bearings can be removed. Following that, training of a signal model that is autoregressive is carried out using the stator current. First, healthy bearings are used to train the model so that a spectrum of baseline values can be created. The modeled spectrum moves away from the threshold values as the condition of the bearings deteriorates. This deviation of the amplitudes from threshold values is taken as fault indexed. This index has the ability to monitor any alterations in the vibrations of the machine caused by the bearing defects. Because of the filtering process at the beginning of the procedure, this technique is robust to a variety of influencing factors such as electromagnetic and environment noise. The results of experimentations with ten different bearings were used to provide the verification of the effectiveness of this technique.

There were two different techniques to analyze defects in the stator of the DTC driven induction motors. These techniques were proposed by [74]. It was verified through the qualitative analysis of the motor stator defects that the torque and flux hysteresis controllers usually generate a third harmonic element in the supply currents

of the induction motor. Therefore, the existence of a third harmonic element in the supply currents of the motor indicates that there is a defect in the stator. The results that were achieved with this method verified that it was effective for detection of the defect in the drive of a DTC induction motor.

The analytical as well as experimental validation of the equivalent internal circuit method implemented in an induction motor was presented by [75]. The model proposed in this research was the only one that provides the simulation of the state variables of the induction motor under healthy and defective conditions of the stator and rotor. The researchers matched the results from the simulation with the results of the analytical calculations. The small variances in the calculations of the frequencies were the result of the FFT resolution. The model that was proposed has ability to detect the influence of defects on the performance of the motor.

[76] Performed experimental investigation of broken rotor defects. The diagnosis of the defect in the motor was performed using the MCSA. A 0.5 kW induction motor was used in his experiments. The bar of the rotor was damaged by using a drill machine. Healthy and defective motor current spectrums were analyzed and compared. It was observed that due to the defects in rotor, sideband frequency components appear in the current spectrum of the defective motor. At the end of the study, the researchers came to the conclusion that the MCSA is a effective and reliable method for detection of rotor bar defects.

A system for the online diagnosis of induction motor faults using MCSA with advanced signal processing techniques was proposed by [77]. The system consisted of a digital signal processing (DSP) board to provide signal processing at high-speed and an advanced algorithm for processing of data. In order to apply MCSA in an efficient manner, the system was designed which consist of advance algorithms for the proper sample selection, the optimal-slip estimation and for the auto frequency searching. Bayesian estimation model was used to set the optimal-slip estimation algorithm. The proper-sample-selection algorithm defines the sampling rate required for MCSA. Finally, the frequency auto search algorithm finds the characteristic defect frequency components from the current signature of the motor. The laboratory tests were conducted on two motors of different ratings to verify the effectiveness and generality of the proposed algorithms. The system that was proposed had the ability to

distinguish between four different types of motor defects. The results of the experiments were able to effectively prove the functioning of the proposed algorithms and the diagnostic system.

A comparison of the various fault diagnosis techniques was performed by [78]. According to the results achieved by the experimentation, the rotor defects can be diagnosed through three techniques which are the three-phase current vector analysis, the outer magnetic field analysis and the instantaneous torque analysis. However, author suggested that MCSA is most favorable technique due to its simplicity.

A novel method for the use of the stator current and efficiency of the motors as pointer of rolling-bearing defects was proposed by [79]. This work describes the results of experiments performed on four kinds of faults found in bearings. These faults include hole in the outer race, crack in the outer race, corrosion and the deformation of the seal. Another new idea presented in the study was the analysis of the reduction in the efficiency of the motor due to defected bearings.

The load variation and the degree of eccentricity are two of the major elements influencing on the current spectrum of the eccentricity defects. The detection of the fault will not be accurate if the effect of the load variation is not taken into consideration. Consequently, [80] proposed a method for recognizing the dynamic and static eccentricities at various levels of load. He developed a systematic relation to describe the effect of load variations and severity of the eccentricity defects. The results of experiments performed on laboratory test rig validate the purposed method.

[81,82,83] present the review papers on the condition monitoring techniques for the induction motors. A comparison of various techniques was given which indicates that MCSA is the most suitable non-invasive and economical method for the detection of the motor defects.

[84] Uses the stator current analysis and vibration analysis techniques to detect the bearing defects. He also proposes the new model for the investigation of the effect of load torque variations on the stator current spectrum. The experimental results indicate that oscillations of the torque produce the varying frequency contents which can be observed in the stator current spectrum.

[85] Apply the FFT on the stator current signal to investigate the broken rotor bar, bearing defects and stator defects of the induction motor. The results indicate that the amplitude values at certain specific defect frequencies increase as the defect size increases. However, at incipient stages of the defect and under no load conditions of the motor, the rise in amplitude is small and difficult to recognize.

[86] Uses the motor stator current analysis scheme to identify the bearing localized defects. FFT spectrum of the motor stator current was obtained and analyzed. Experiments were conducted on the two defect levels (hole sizes 2mm and 4mm) in outer and inner race of the bearing at no load and full load conditions of the motor. The results obtained through the experiments indicate that at no load condition, the change in amplitude values at characteristic defect frequencies is very small (less than 5dB) however for full load conditions, the change in amplitude is detectable ($>5\text{dB}<8\text{dB}$).

[86] apply the wavelet analysis technique to investigate the broken rotor bar and stator defects of the motor. The result indicates that wavelet analysis is powerful tool for the condition monitoring of the motors in various loading conditions.

[87] Uses the motor current, voltage, flux and instantaneous power analysis methods to investigate the broken rotor bars and eccentricity defects of the motor. His study shows that although the rotor bars and eccentricity defect of the motor can be detected through current, voltage and flux analysis. However these techniques are not effective under no load conditions of the motor. On the other hand, the instantaneous power analysis scheme diagnosis the rotor and eccentricity defects effectively even under no load condition of the motor. This is due to the reason that the motor power is product of the supply voltage and current so it contains more information than the current and voltage only.

[88,89] presented an automated fault detection system for the induction motors based on programmable logic controllers. They use the speed sensor, temperature sensor and current sensor to measure the motor speed, motor temperature and running current. The system was developed to automatic turn off the motor if any one of the measured variable exceeds the preset values. However, proposed condition monitoring system proves to be very expensive due to involvement of the sensors.

2.6 Important Observations

The review of literature has shown that the sensor based methods like vibration analysis, acoustic emission, noise analysis, chemical analysis and temperature measurements were applied to protect motors from various faults. However sensors which are integral part of these techniques are too much expensive. Another disadvantage of these techniques is that sensors need to be installed on machine so it needs access to machine which is not possible in every application. Also it requires special expertise for the proper installation of sensors on the machine for accurate results. Furthermore, sensors also have some life period after which they fail and in most cases bearing life is more than sensor life. Therefore sensor based condition monitoring methods are not reliable. For condition monitoring of the electric motors, the stator current monitoring technique implementation is not so complex. In all industries current transformers are always installed for the measurement of current for control and display purpose. Current transformer and potential transformer are always part of electric protection system.

It has been found in the review of literature that the mechanical vibration has relation with the stator current components at some the specific characteristic frequencies. When the mechanical vibrations of the motor increases; the magnitude of the voltage at specific characteristic frequencies also increases. This is due to the modulation of the air gap by the mechanical vibration at the specific characteristic frequencies. The impact of this modulation appears in the inductance of the stator and finally in the motor stator current. Every type of the motor defect has its own unique characteristic defect frequencies. The MCSA is used to find out these frequency modulations from the spectrum of the motor current. So this technique is very useful and cost effective as it requires no special sensors for the measurements. It is a non invasive method and may implement distantly from the place where motor is installed. Therefore, this technique can provide considerable economic and implementation benefits. Not only the motor faults but over all motor efficiency, performance, speed and torque information can be extracted from the motor current. However, the change in amplitude values is very small and difficult to detect for the no load conditions of the motor.

The advantages and drawbacks of the existing condition monitoring and fault analysis methods are presented in Table 2.2.

Table 2.2: Comparison of the various motor faults detection methods

No	CM Technique	Advantages	Drawbacks
1	Vibration Analysis	Reliable and basic methodology	<ul style="list-style-type: none"> • Require expensive sensor • Intrusive • Subject to sensor failure
2	Acoustic Emission	<ul style="list-style-type: none"> • High signal to noise ratio • Detects fault at incipient stages 	<ul style="list-style-type: none"> • Require expensive sensor • Intrusive
3	Temperature Measurement	Standard available in industries	<ul style="list-style-type: none"> • Require expensive sensor • Intrusive
4	Sound Analysis	Simple method	<ul style="list-style-type: none"> • Require expensive sensor • Intrusive
5	Chemical Analysis	Detects fault at incipient stages	Applicable only to large size motors
6	Stator Current Analysis	<ul style="list-style-type: none"> • Inexpensive • Non Intrusive • Less complexity 	Unable to detect defects at incipient stages and at unloaded conditions of the motor

2.7 Summary

Most of the related work in the area of condition monitoring of induction motors shows that it is vital to determine the defects of a motor early so as to prevent unscheduled down time of machinery which can cause delays and drastic monetary losses. Notably, the review of the literature highlighted the challenges involved with the intelligent diagnostic condition monitoring system that includes the complexity in the analysis and the high cost of the sensors. Spurred by these factors, the goal of this research is to find answers to the defect analysis of the motors bearing faults utilizing

the commonly available stator current and voltage using methodology to be presented in Chapter 3.

CHAPTER 3

EXPERIMENTAL SET-UP

3.1 Introduction

An overview of the software and hardware module used in the development of experimental test rig for intelligent diagnostic condition monitoring system is presented in this chapter. The design flow of the experimental test rig is shown in Figure 3.1. The accuracy and reliability of the data acquired from the induction motor is vital in order to make timely decisions about the status of machine. This can be possible through the good awareness of effect of fault severity and loading conditions of machine on the amplitude values of the characteristic defect frequencies.

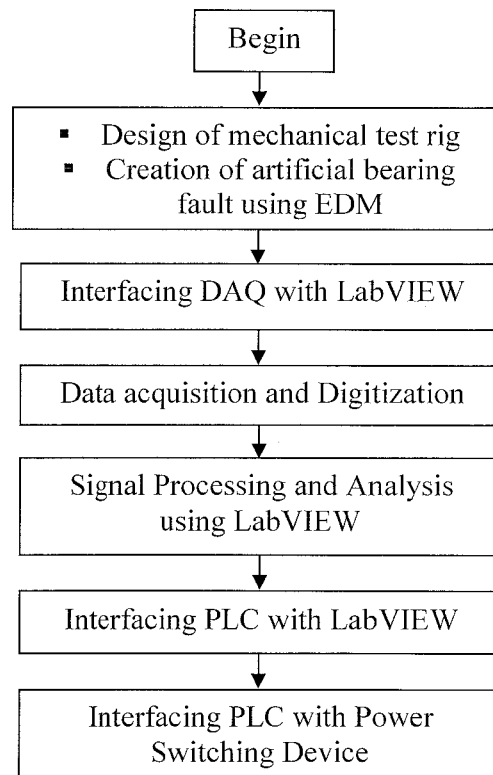


Figure 3.1: Design flow of experimental test rig

3.2 Condition Monitoring System

In this work an experimental test rig compromises of components used in industry was developed for the intelligent diagnosis of motor bearing faults. The schematic diagram of the developed experimental set-up is shown in Figure 3.2.

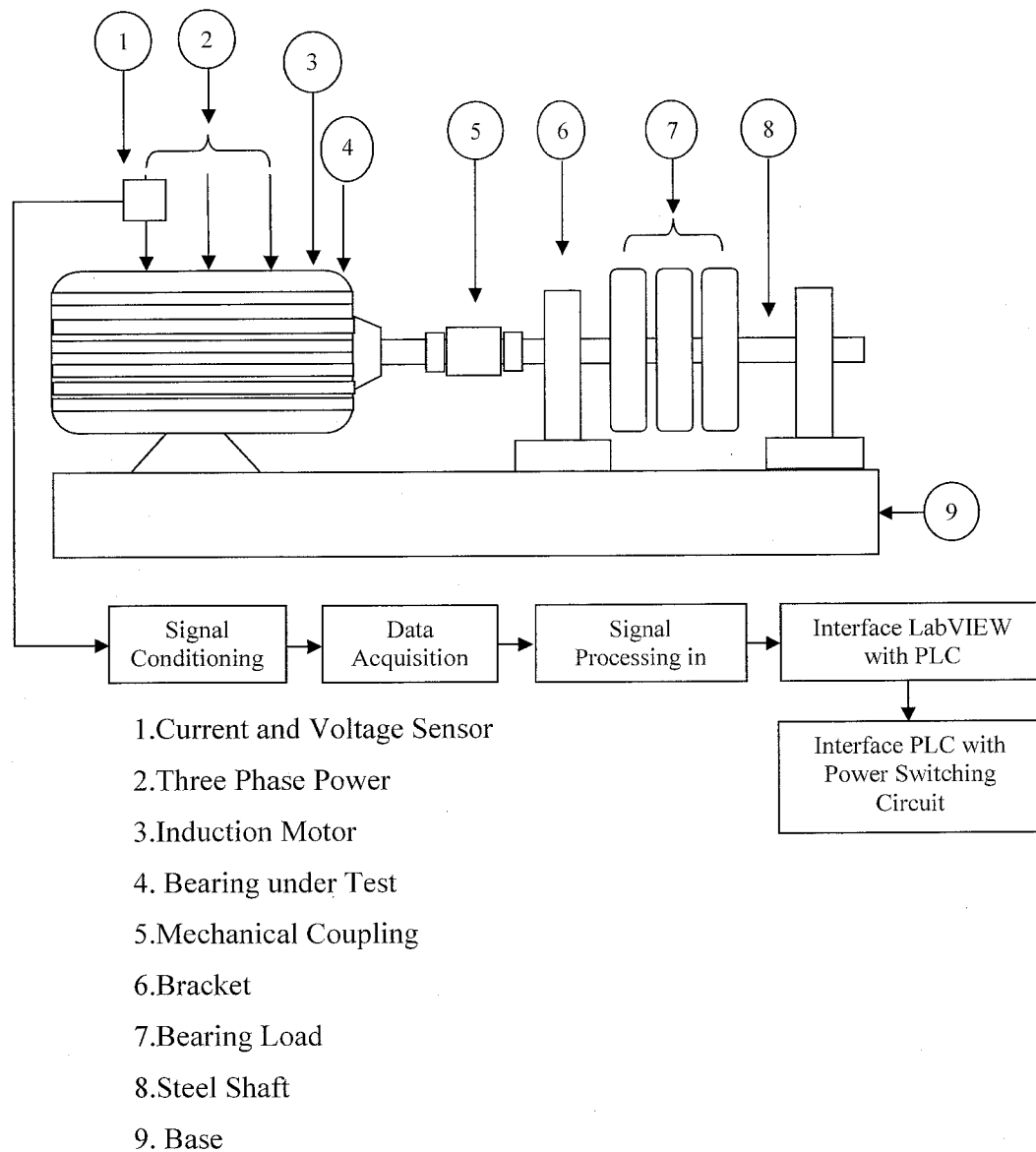


Figure 3.2: The schematic diagram of the test rig

3.2.1 Mechanical Parts

The mechanical parts of the test rig consist of a 3-phase induction motor and steel shaft coupled with motor shaft via flexible coupling. The coupling has rubber jaw to reduce the vibration occurring in the motor. The mechanical load is mounted on the steel shaft between two brackets.

3.2.1.1 Motor Connections

Two Motors of same specification are used during the experiments. One motor has healthy bearings while the other one has artificially defected bearings. Both motors used in laboratory test rig resemble the one shown in Figure 3.3. The specifications of the test motor are shown in Table 3.1. The connections of the motor are in star connected for 415VAC supply. The connection scheme is shown in Figure 3.4. An AC variable frequency drive (VFD) is used to run the motor at various speeds. The speed of the motor is measured by Prova digital tachometer. The tachometer and variable frequency drive pictures are shown in Figure 3.5.

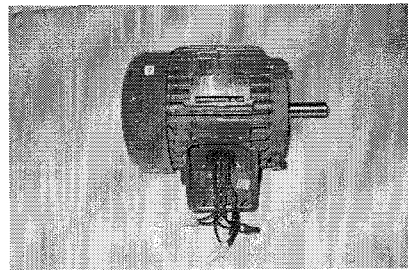


Figure 3.3: The induction motor used in test rig

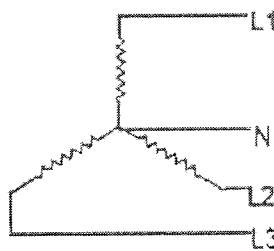
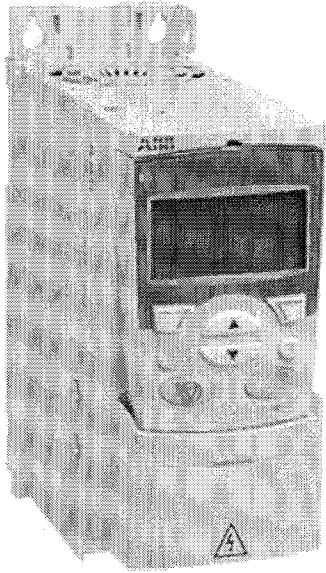
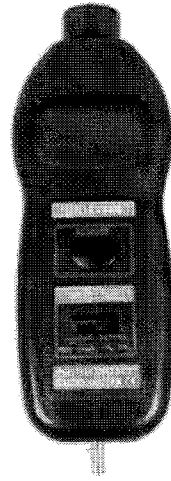


Figure 3.4: The connection scheme of the motor



(a)



(b)

Figure 3.5: (a) The VFD and (b) Tachometer used in test rig

Table 3.1: Specifications of the test motor

Parameters	Rating
Power (Hp)	0.5
No. of Phase	3
Rated Current (A)	1.05
No. of Poles	4
Frequency (Hz)	50
Rated Volts	400
Speed (RPM)	1500

3.2.1.2 Bearing Load Calculation

Loads are thought of as one of the most significant factors influencing the lifetime and characteristics of the bearings. In this work, tests were performed on un-loaded and loaded conditions of the motor. In the test rig used for the experiment as shown in Figure 3.2, three round steel plates were mounted on a steel shaft coupled with a

motor shaft to create the radial load. Aluminum coated steel comprised the round plates. The design of round plates is shown in Figure 3.6.

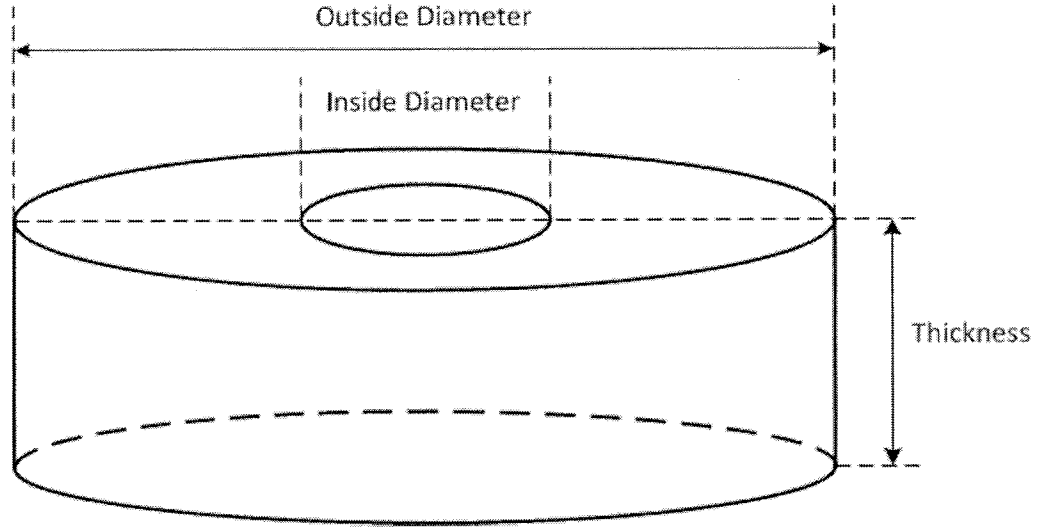


Figure 3.6: Structure of steel plates used as radial load in test rig

The mass of steel round plates in grams is calculated using Equation (3.1).

$$Mass = \frac{\pi \rho D^2 h}{4} \quad (3.1)$$

$$D^2 = D_o^2 - D_i^2 \quad (3.2)$$

$$Weight (N) = \frac{\pi g h D^2 \rho}{4} \quad (3.3)$$

where:

ρ , is the density of material and its value is 7.85 g/cm^3

h , is the height of plate

D_o^2 , is the outside diameter of steel plate used as radial load

D_i^2 , is the inside diameter of steel plate used as radial load

g , is the acceleration due to gravity

3.2.1.3 Bearing Assembly

Bearings installed in the test motors shaft end and fan end are the ball bearings 6202-2z. The outer diameter of the bearing is 35mm with inner diameter of 17mm. Each bearing contains 8 balls with diameter of 7.5mm. The contact angle of balls with race is assumed as zero degree. The SKF brand bearings were used for testing. The bearing consist of four parts namely, inner race, outer race, rolling elements (balls) and cage and is as shown in Figure 3.7. The cage is used to keep the balls at specific distance from each other during rotation of balls between inner and outer race. A number of experiments were conducted for normal (healthy) bearings and bearings with different defect in outer race, inner race, ball, cage and distributed defects. Figure 3.8 shows the healthy bearings and bearings with various types of localized and distributed faults. The electric discharge machine (EDM) is used to create defects of different types in the bearings.

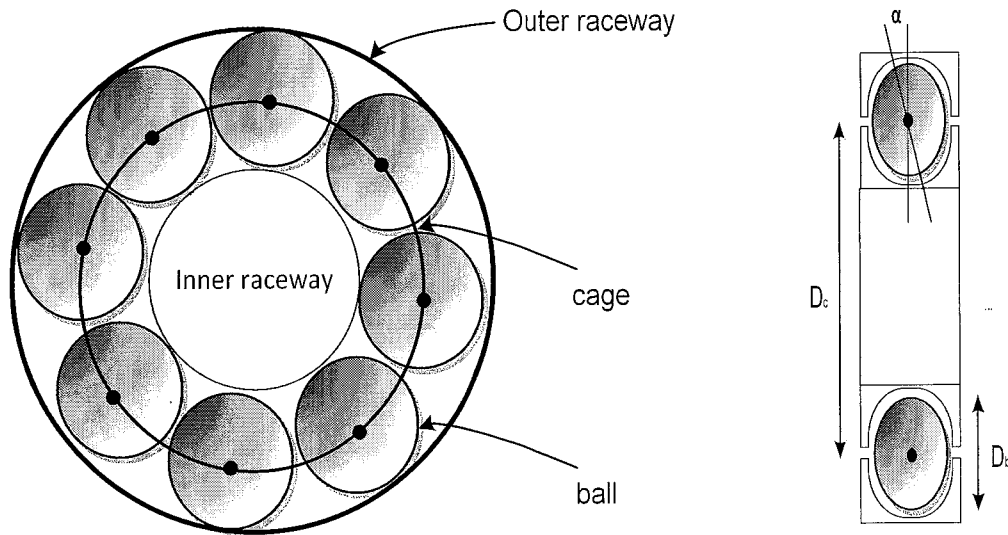
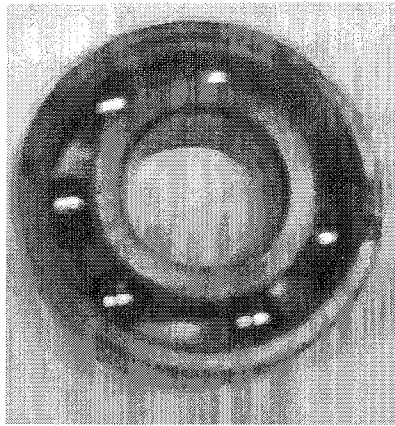
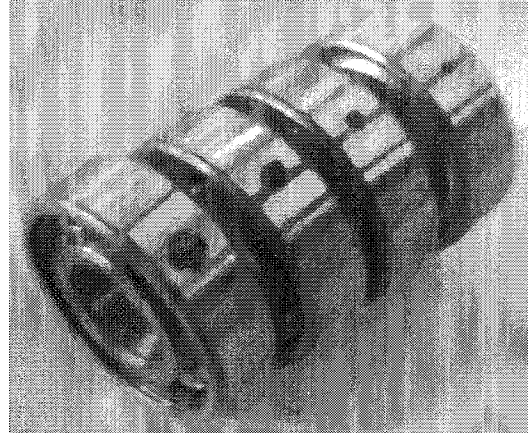


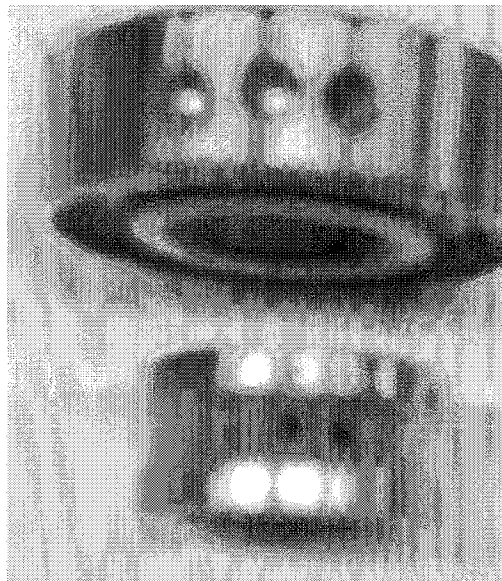
Figure 3.7: Geometry of bearing used for this work



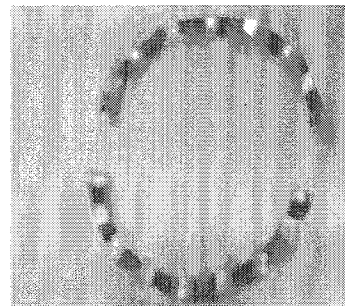
Bearing Ball Defect



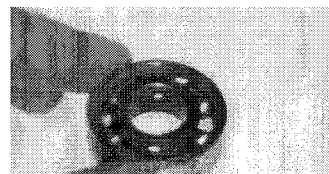
Bearing Outer Race Defect (Localized)



Distributed Defect in Outer and
Inner Race of Bearing



Bearing Broken Cage



Bearing Inner Race
Defect (Localized)

Figure 3.8: Bearing with various health conditions used for this work

3.2.2 Data Acquisition and Processing

The data acquisition and processing system used in this work consists of National Instruments data acquisition card NI 6281, an AC current and voltage transformer and LabVIEW 8.2. The data acquisition card NI 6281, current and voltage sensors are shown in Figure 3.9 to 3.11 respectively.

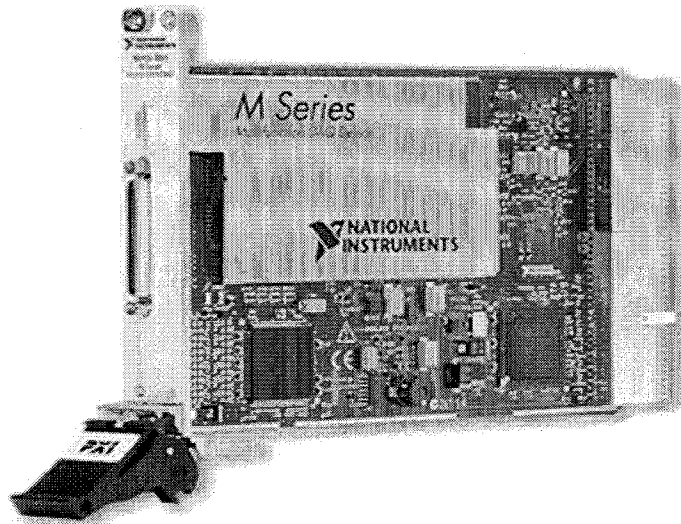


Figure 3.9: Data acquisition card NI 6281 used in this work

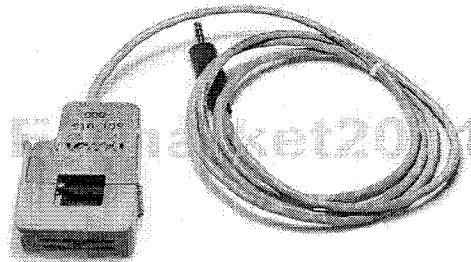


Figure 3.10: AC current sensor used in this work

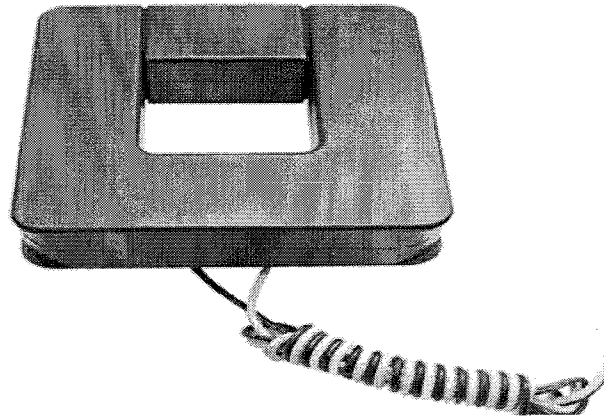


Figure 3.11: AC voltage sensor used in this work

The specifications of data acquisition card NI 6281 are shown in Table 3.2.

Table 3.2: Specifications of DAQ card NI PCI 6281

S.r No.	Specifications	
1	Analog Inputs	16
2	AI Range	± 10 Volts
3	Max. Scan Rate	625kS/s
4	AI Resolution	18bits
5	AO	2
6	AO Range	± 10 Volts
7	AO Resolution	16bits

3.2.2.1 Configuration of the Measurement Automation Explorer

LabVIEW has the configuration utility known as Measurement Automation Explorer (MAX) for the configuration and installation of all external data acquisition devices. MAX reads the information from device manager windows registry and assigns it specific device name from which the information is collected. The relation between the MAX and data acquisition device is shown in Figure 3.12 [90]. The flow chart for configuration of the analog input channel of DAQ NI 6281 device used to acquire data from AC current and voltage sensor is shown in Figure 3.13.

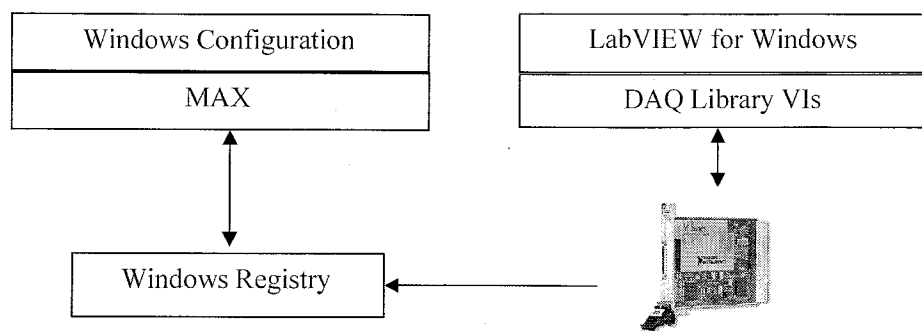


Figure 3.12: Relation between DAQ and MAX

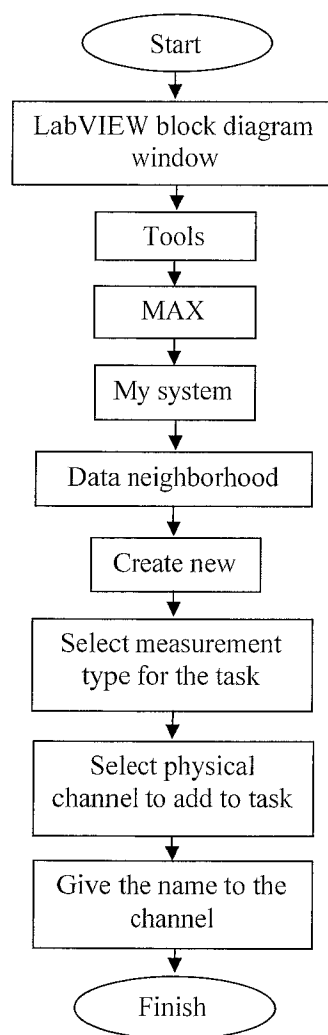


Figure 3.13: The flow chart of configuration of DAQ input channel with MAX

Data acquisition (DAQ) assistant was used in continuous mode to configure the LabVIEW window with the MAX. The DAQ assistant was placed inside the loop to acquire data continuously from the data acquisition device. During the measurements, the sampling of current and voltage signals was done simultaneously. The sampling parameters are shown in Table 3.3.

Table 3.3: NI DAQ parameters

Parameter	Set value
Total number of samples taken	50 KS/sec
Scan Rate	30 KHz
Scan Mode	Continuous
Terminal Configuration	Differential
Window	Hamming
Frequency Resolution	0.125 Hz
Nyquist Frequency	15 KHz

3.2.2.2 Fault Analysis Software

The instantaneous power FFT spectrum analysis was employed to recognize the specific defect frequencies of the motor and these defect frequencies utilized as the indices to indicate faulty or healthy conditions of the motor. In this work, a code was created in LabVIEW so that the fault frequencies from the instantaneous power FFT spectrum could be identified. The LabVIEW block diagram window was used to write the code that was used for the acquisition of real time data from the current transformer SCT-013-005 and voltage transformer. The main purpose for this software was to gather, display and save data for further analysis. The data coming from the current and voltage transformer was read by the LabVIEW programme, the instantaneous power of the motor was calculated by multiplication of both voltage and current signals and then the hanning window was applied on the specified data. Before being converting to decibel (dB), the spectrum was normalized with respect to the highest peak (fundamental element) and then it was plotted for future analysis.

The data logging was created by using the spreadsheet file so that the saved data could be plotted later by way of the MATLAB custom developed programme. The flow chart of the program used for analyzing the data is shown in Figure 3.14. The programme was initiated by reading the raw data coming from the motor by way of the DAQ device. The data was analyzed by performing a calculation of the Fourier transform of the instantaneous power signal.

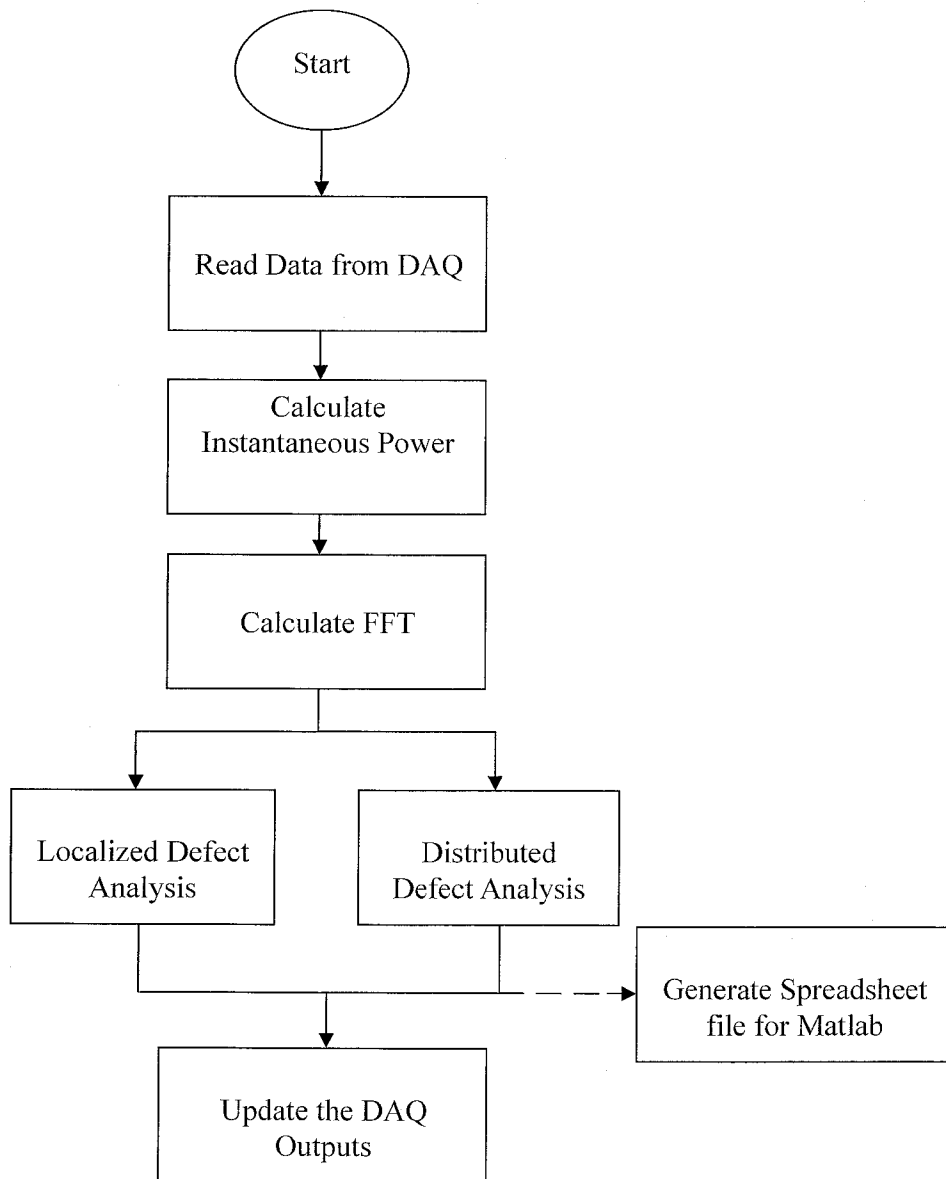


Figure 3.14: Flow chart of the LabVIEW program developed for spectrum analysis

3.3 Summary

The test set-up, measurement system and LabVIEW programme used for this research is described in this chapter. Also presented are the features of the test rig and the description of the particulars regarding the measurements of the software and the hardware. The fault analysis software was created in LabVIEW and was used for the identification of the fault frequencies of the induction motor. The experimental test rig developed in this chapter will be used for results and analysis of healthy and faulty motors.

CHAPTER 4

RESULTS AND DISCUSSIONS

4.1 Introduction

A reliable condition monitoring system is based on the knowledge of the magnetic, electrical and mechanical behavior of the machinery, not only in the healthy state but also in the faulty state. As an induction machine is highly symmetrical the existence of any kind of fault alters its symmetry and produces changes in magnetic flux distribution, or rather, in the magnitude of the specific fault frequencies. As has been explained in Chapter 2, faults in the induction motor generate characteristic fault frequencies which are observable by way of a spectrum analysis of one or more sensor elements, such as, voltage, current, axial leakage flux and vibration. Both the voltage and the current can be employed to calculate the instantaneous power.

The main objective in condition monitoring of the motor is the accuracy of the detection of the faults and provision of current status of machine to estimate the health of the motor and to take timely decision about preventive maintenance. Therefore, it is vital to know what magnitude of the characteristic fault frequency element signifies the severity of the various faults in the motors. The objective of this chapter is to explain the results of the experimentation from the healthy and faulty motors examining the various bearing faults at various severity levels. Experiments were done at load and unloaded conditions of the motor.

4.2 Various Bearing Faults Analysis

The bearing consists of mainly of outer race, inner race, balls and cages. The defects in these elements causes malfunction in bearing. The relationship between defect in bearing and its effect on the stator current and voltage spectrum can be determined by

remembering that any change in air gap between rotor and stator would cause magnetic flux variations. Since bearings are used to support the rotor during rotation, so any defect in bearing causes the radial movement of rotor during rotation. The radial movement of the rotor generates the stator current and voltages at certain specific frequencies. The instantaneous power of the motor and the characteristic defect frequencies are calculated using Equation (4.1) to (4.5) [6,81,83,84,87]. There are various types of faults in the bearings of motors, and in this work the focus of the study and experimentation are summarized in Table 4.1.

$$P_{ins} = VI \quad (4.1)$$

$$f_{es} = |f_e \pm M f_{of}| \quad (4.2)$$

$$f_{es} = |f_e \pm M f_{if}| \quad (4.3)$$

$$f_{es} = |f_e \pm M f_{bd}| \quad (4.4)$$

$$f_{es} = |f_e \pm M f_{cd}| \quad (4.5)$$

where:

V , is the supply voltages to the motor

I , is the stator current

f_e , is the electric supply frequency

f_{of} , is the bearing outer race characteristic defect frequency

f_{if} , is the bearing inner race characteristic defect frequency

f_{bd} , is the bearing ball characteristic defect frequency

f_{cd} , is the bearing cage characteristic defect frequency

$M = 1, 2, 3, 4, \dots$

Table 4.1: Experiment details for CM system

Case	Load Conditions	Severity of Bearing Defect
1	No Load	1 to 5mm outer race defect
2	Full Load	1 to 5mm outer race defect
3	No Load	1 to 5mm inner race defect
4	Full Load	1 to 5mm inner race defect
5	No Load	Ball defects
6	Full Load	Ball defects
7	No Load	Cage defects
8	Full Load	Cage defects
9	Full Load	Distributed defect in outer race
10	Full Load	Distributed defect in inner race

The following sections of the chapter describe the experiments conducted for the various faults of the bearing.

4.2.1 Bearing Outer Race Defects

The holes of various sizes are induced in the outer race of the bearing to create artificial defects using electric discharge machine (EDM). The defected bearing is shown in Figure 4.1. The bearing outer race characteristic frequencies are shown in Table 4.2 which are calculated using the Equations (4.1) and (4.6) [6,81,83,84].

$$f_{of} = 0.4N_b f_r \quad (4.6)$$

Where:

N_b , is the number of balls inside the bearing

f_r , is the rotor frequency in Hz

$$f_r = \frac{f_e}{p}(1 - s)$$

Table 4.2: Expected outer race defect frequencies at various loading conditions

Motor Speed (rpm)	Load Condition	m=1		m=2	
		LSB(Hz)	USB(Hz)	LSB(Hz)	USB(Hz)
1497	No Load	29.875	129.875	109.75	209.75
1395	Full Load	24.375	124.375	98.75	198.75

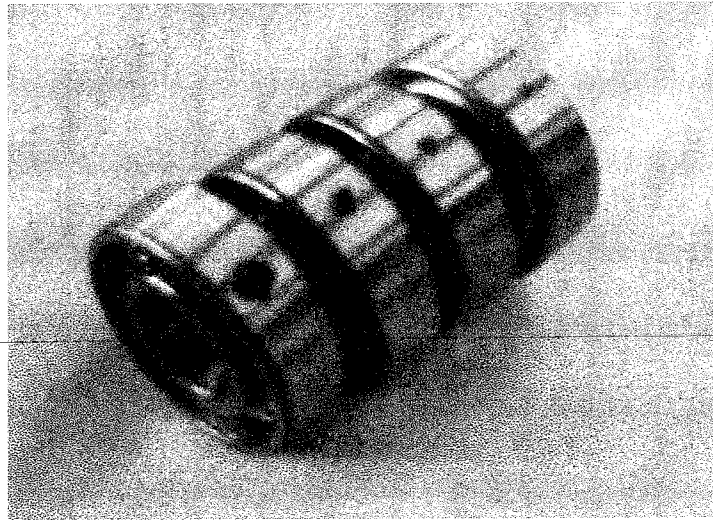


Figure 4.1: Defects (Localized) induced in outer race of motor bearing

4.2.1.1 Outer Race Defects Analysis at Various Hole Sizes under no Load condition of the motor

The defected bearing was installed on the drive end side of the motor under test at no load condition. The faults in bearing were induced by drilling holes of various sizes in the outer race of the bearing. For defected motor, five tests were conducted at different outer race hole sizes (1 to 5mm). The frequency spectrum of the healthy and defected motor instantaneous power is shown in Figures 4.2 to 4.11. The graphs represented in dotted line indicate the healthy motor spectrum and the solid line indicates the defected motor spectrum. It is observed from frequency spectrum that the amplitude values are -128.947 dB and -127.237 dB for healthy motor at specific characteristic defect frequencies of 29.875 Hz and 129.875 Hz respectively. For, defected motor, it is observed from the frequency spectrums that amplitude values at specific characteristic defect frequencies are not clearly visible (<10dB) due to the

fact that the change in slip frequency is very small. However as the hole size exceeds 4mm hole size, there is detectable change in amplitude values ($>10\text{dB}$) at specific characteristic defect frequencies. The analysis of the change in amplitude values at characteristic defect frequencies for no load condition is summarized in Table 4.3.

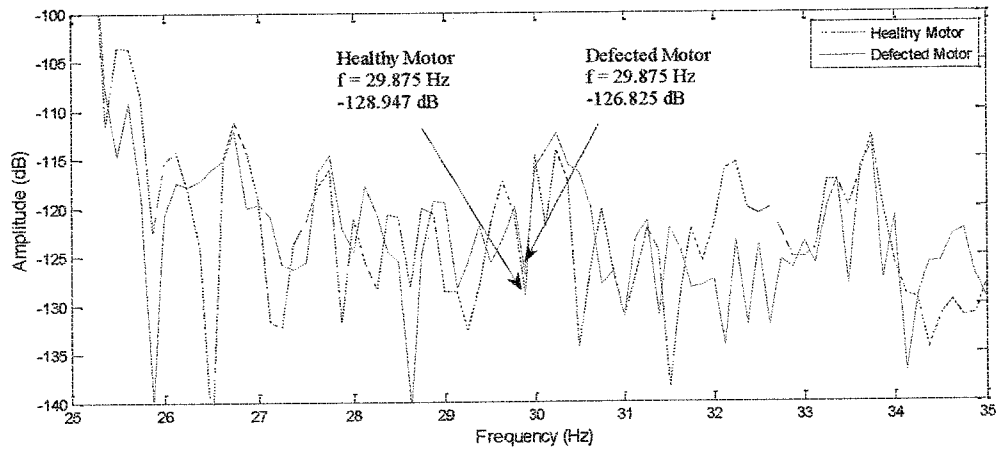


Figure 4.2: Instantaneous power spectrum of the healthy and defected motor under no load condition at 1mm outer race defect at 29.875 Hz

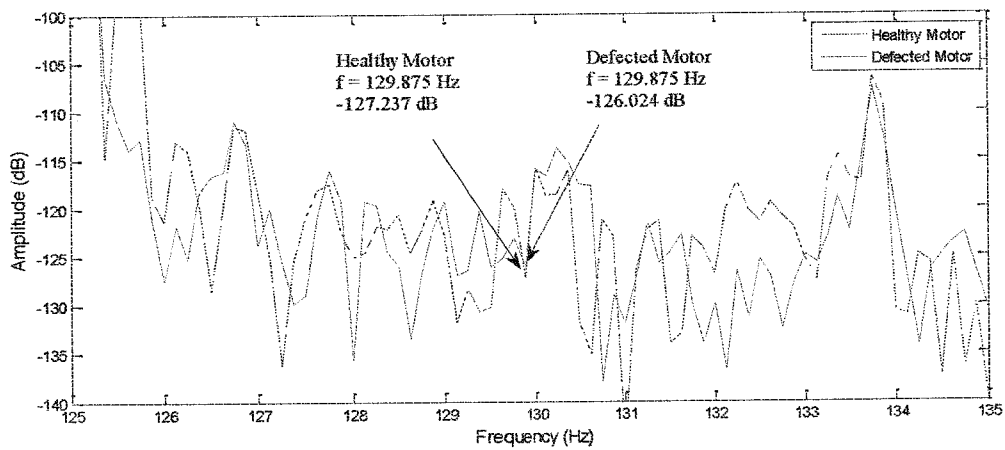


Figure 4.3: Instantaneous power spectrum of the healthy and defected motor under no load condition at 1mm outer race defect at 129.875Hz

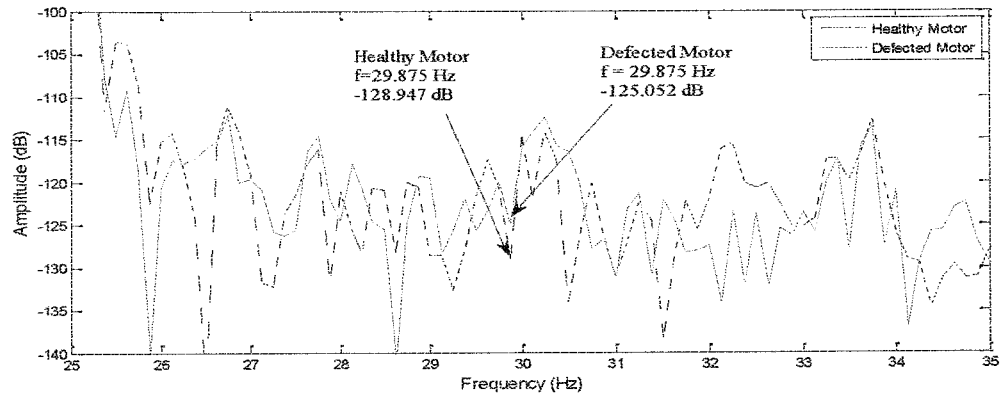


Figure 4.4: Instantaneous power spectrum of the healthy and defected motor under no load condition at 2mm outer race defect at 29.875 Hz

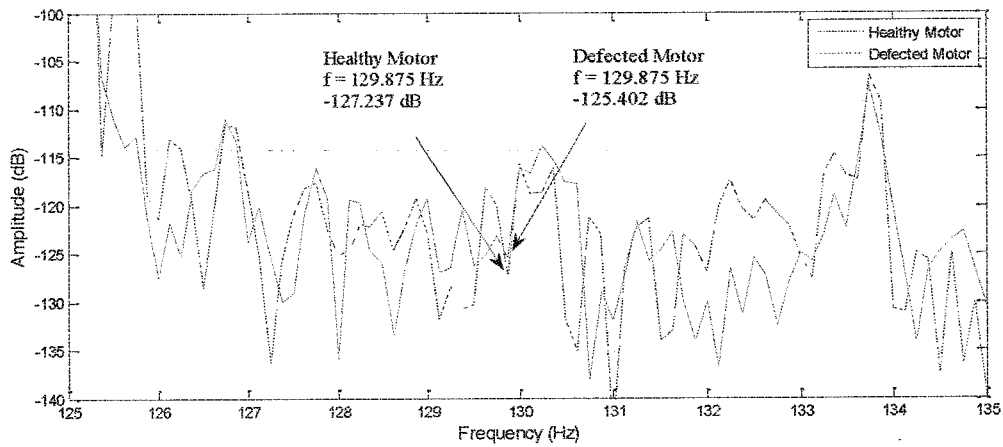


Figure 4.5: Instantaneous power spectrum of the healthy and defected motor under no load condition at 2mm outer race defect at 129.875Hz

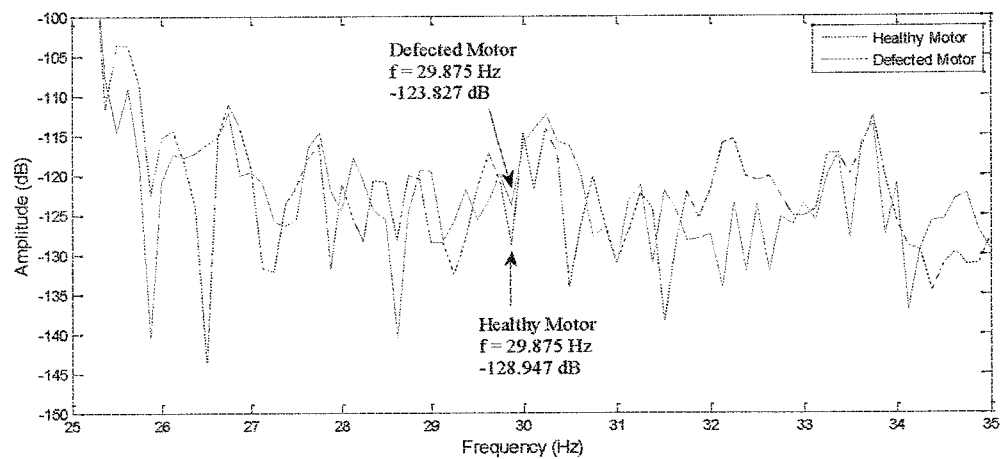


Figure 4.6: Instantaneous power spectrum of the healthy and defected motor under no load condition at 3mm outer race defect at 29.875 Hz

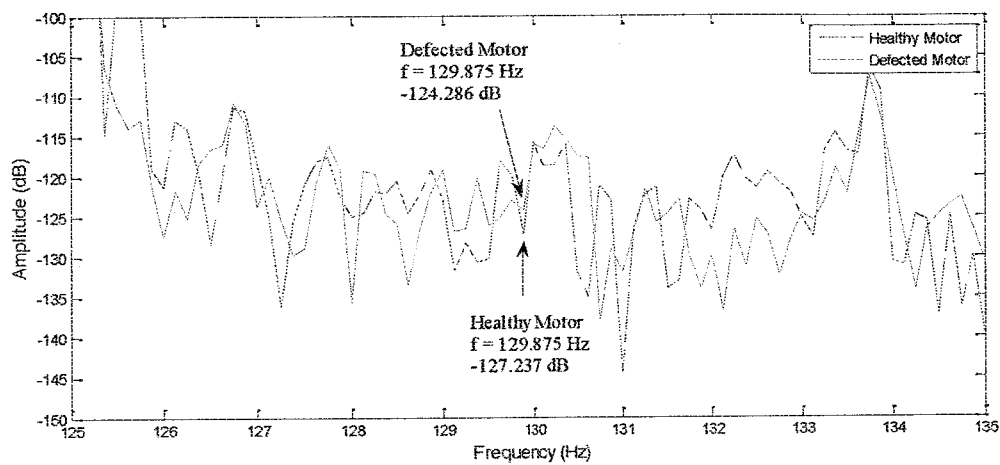


Figure 4.7: Instantaneous power spectrum of the healthy and defected motor under no load condition at 3mm outer race defect at 129.875Hz

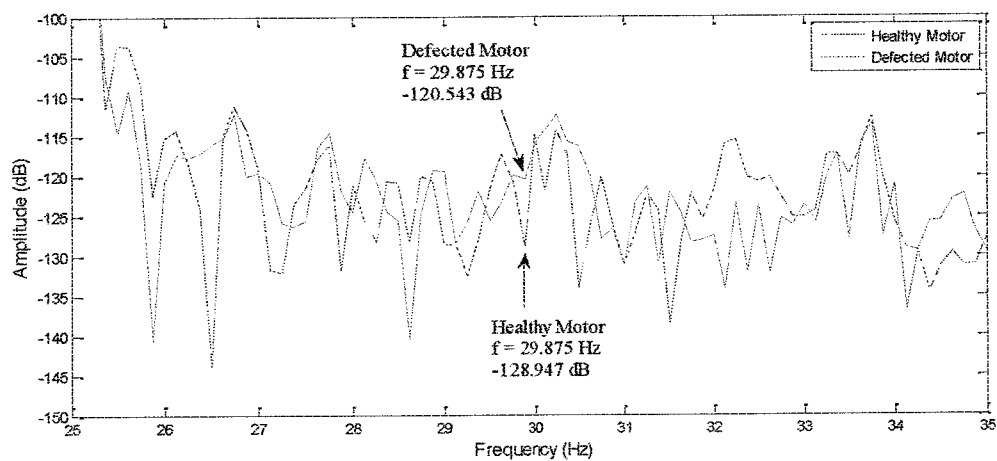


Figure 4.8: Instantaneous power spectrum of the healthy and defected motor under no load condition at 4mm outer race defect at 29.875 Hz

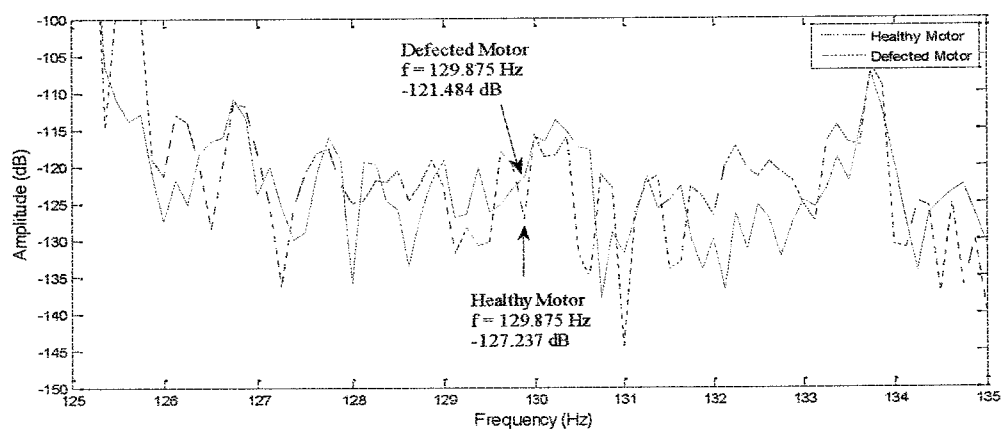


Figure 4.9: Instantaneous power spectrum of the healthy and defected motor under no load condition at 4mm outer race defect at 129.875Hz

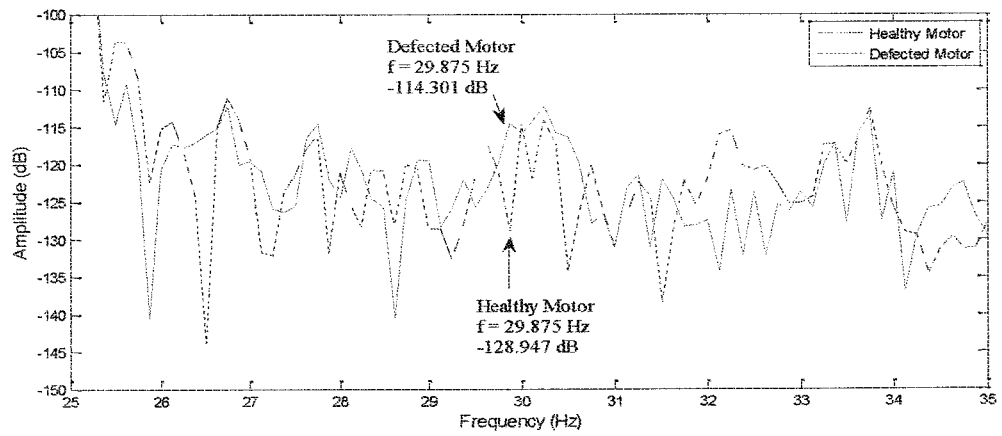


Figure 4.10: Instantaneous power spectrum of the healthy and defected motor under no load condition at 5mm outer race defect at 29.875 Hz

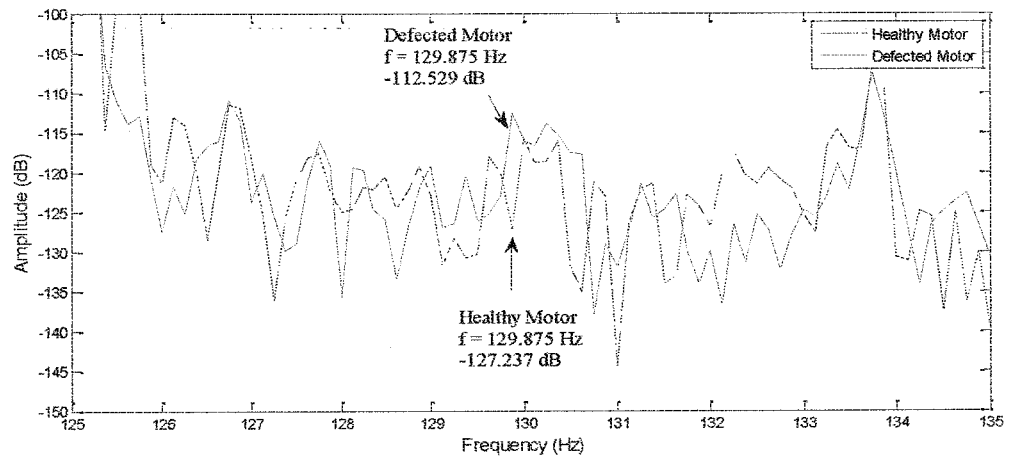


Figure 4.11: Instantaneous power spectrum of the healthy and defected motor under no load condition at 5mm outer race defect at 129.875Hz

Table 4.3: Amplitude values at outer race defect frequencies at various defect levels and under no load conditions

Outer Race Defect Size (mm)	Characteristic Outer Race Defect Frequency (Hz)		Amplitude Values(dB)		Reference Figure No.	Remarks
	LSB	USB	LSB	USB		
1	29.875	129.875	-126.82	-126.024	4.2,4.3	Defect frequencies difficult to identify
2	29.875	129.875	-125.05	-125.40	4.4,4.5	Defect frequencies difficult to identify
3	29.875	129.875	-123.82	-124.28	4.6,4.7	Defect frequencies difficult to identify
4	29.875	129.875	-120.54	-121.48	4.8,4.9	Defect frequencies difficult to identify
5	29.875	129.875	-114.54	-112.48	4.10,4.11	Defect frequencies visible

4.2.1.2 Outer Race Defects Analysis at Various Hole Sizes under Full Load condition of the motor

The frequency spectrum of the healthy and defected motor instantaneous power spectrum is shown in Figures 4.12 to 4.21. The dotted line in graphs indicates the healthy motor spectrum and solid line indicates the defected motor spectrum. It is observed from frequency spectrum that the amplitude values are -118.841 dB and -117.167 dB for healthy motor at specific characteristic defect frequencies of 24.375 Hz and 124.375 Hz respectively. From the analysis of healthy and defected instantaneous power spectrums, it is indicated that the presence of fault in outer race of motor bearings appears as increase in amplitude values at specific characteristic defect frequencies. It is observed that at full load condition of motor, there is

significant increase ($>10\text{dB}$) in amplitude value at 2mm defect size and the amplitude values increases with the increase of defect size in motor bearing. The analysis of frequency spectrum for various outer race defect sizes is summarized in Table 4.4.

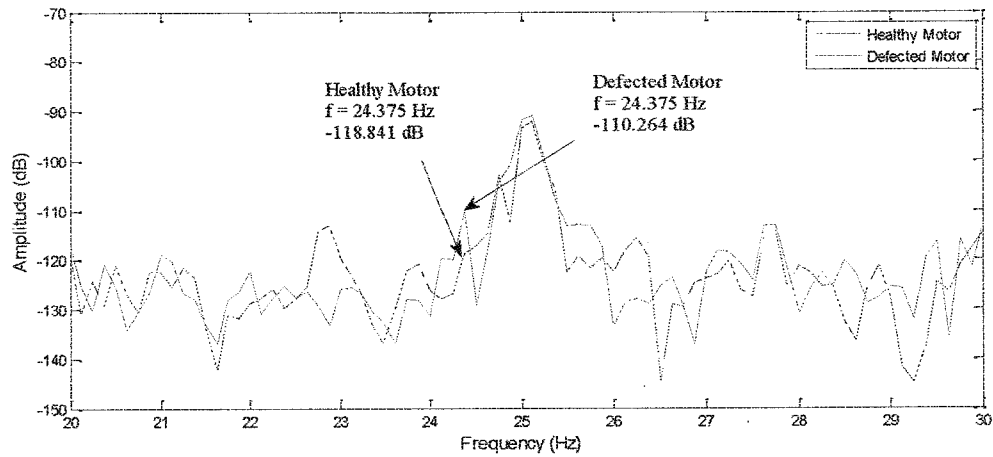


Figure 4.12: Instantaneous power spectrum of the healthy and defected motor under full load condition at 1mm outer race defect at 24.375 Hz, showing that at the specific defect frequencies the amplitude starts to appear

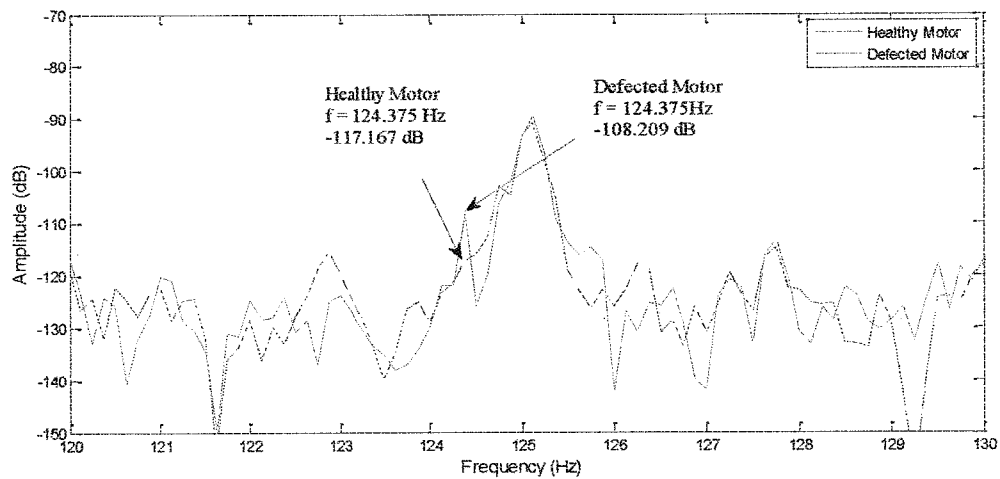


Figure 4.13: Instantaneous power spectrum of the healthy and defected motor under full load condition at 1mm outer race defect at 124.375 Hz, showing that at the specific defect frequencies the amplitude starts to appear

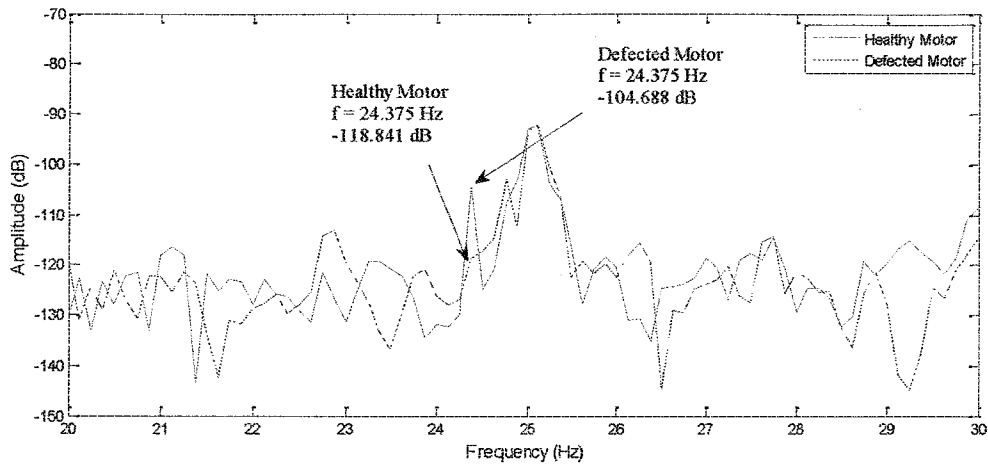


Figure 4.14: Instantaneous power spectrum of the healthy and defected motor under full load condition at 2mm outer race defect at 24.375 Hz and, showing that at the specific defect frequencies the amplitude value increases

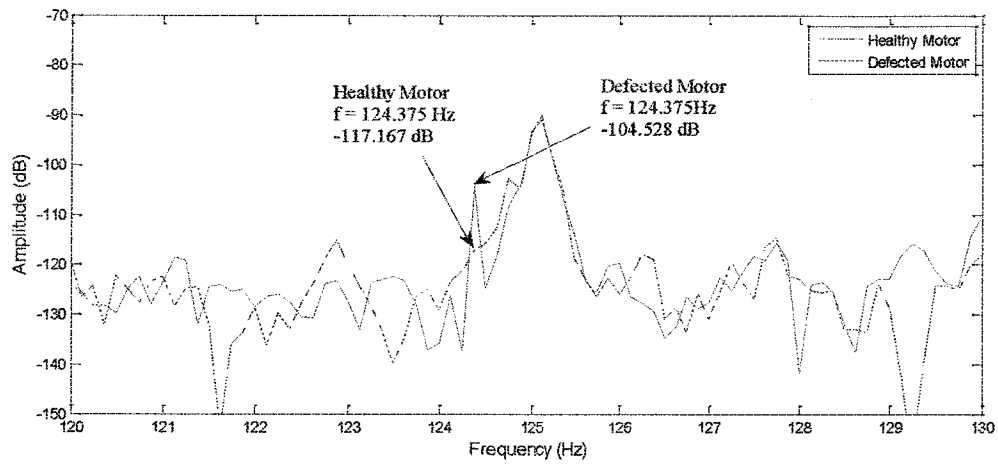


Figure 4.15: Instantaneous power spectrum of the healthy and defected motor under full load condition at 2mm outer race defect at 124.375 Hz and, showing that at the specific defect frequencies the amplitude value increases

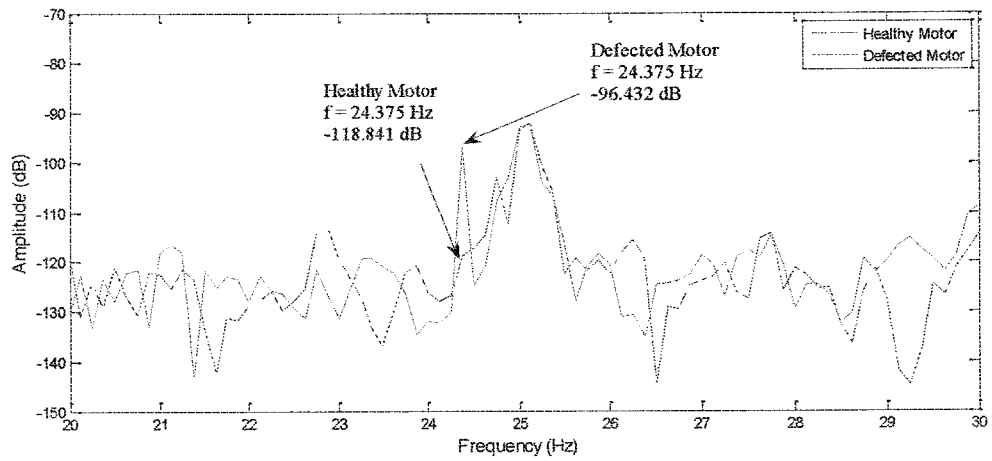


Figure 4.16: Instantaneous power spectrum of the healthy and defected motor under full load condition at 3mm outer race defect at 24.375 Hz, indicating significant increase in amplitude values

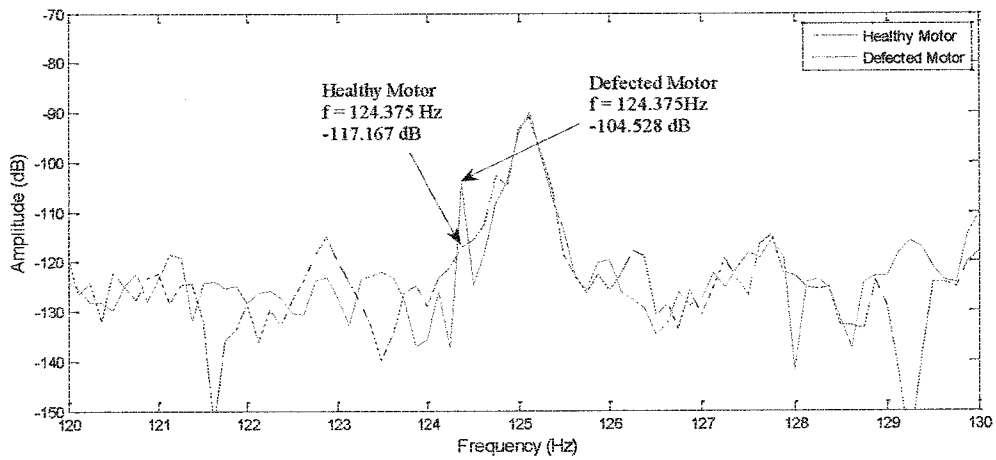


Figure 4.17: Instantaneous power spectrum of the healthy and defected motor under full load condition at 3mm outer race defect at 124.375 Hz, indicating significant increase in amplitude values

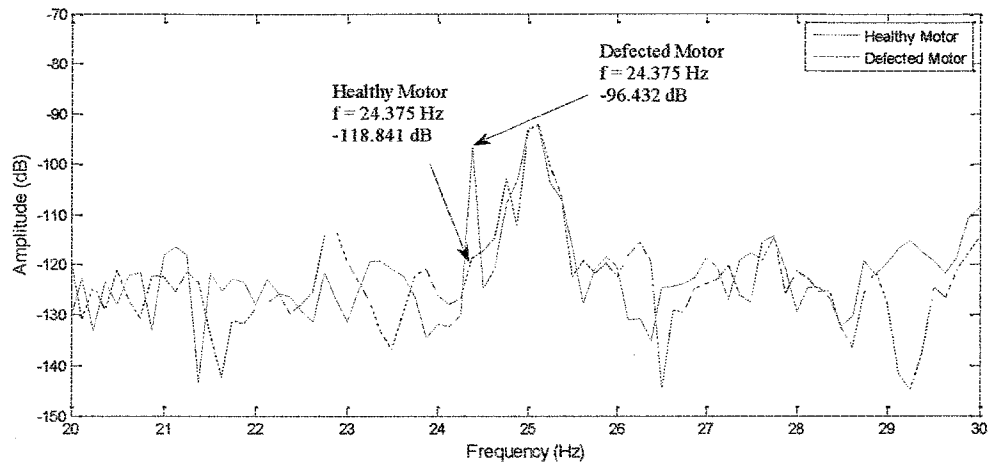


Figure 4.18: Instantaneous power spectrum of the healthy and defected motor under full load condition at 4mm outer race defect at 24.375 Hz, showing that at the specific defect frequencies the amplitude value increases still further

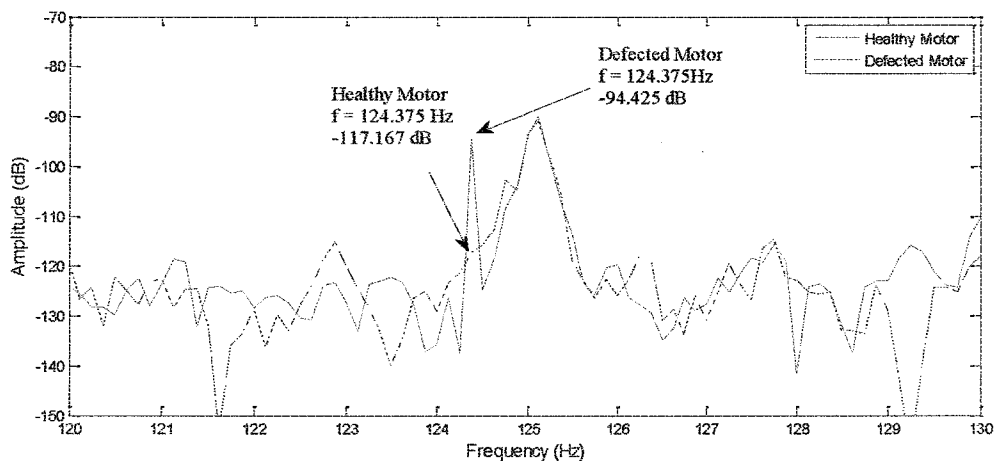


Figure 4.19: Instantaneous power spectrum of the healthy and defected motor under full load condition at 4mm outer race defect at 124.375 Hz, showing that at the specific defect frequencies the amplitude value increases still further

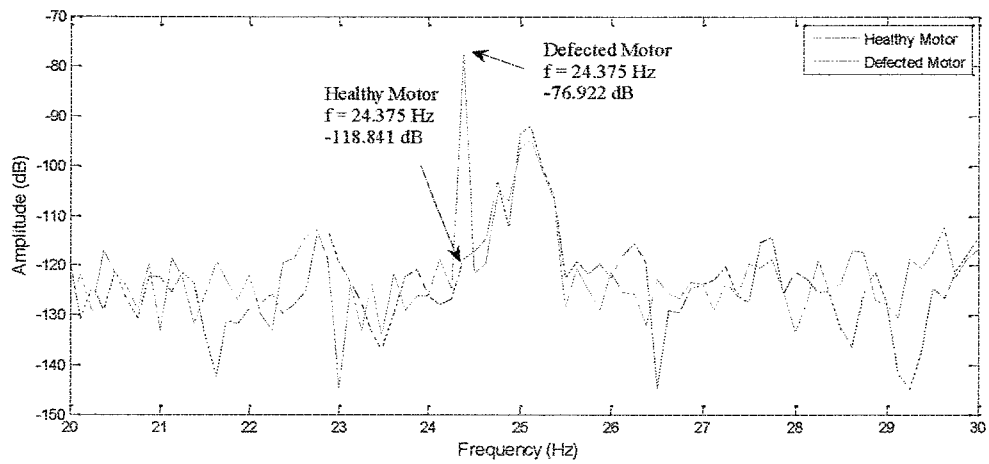


Figure 4.20: Instantaneous power spectrum of the healthy and defected motor under full load condition at 5mm outer race defect at 24.375 Hz, showing that at the specific defect frequencies the amplitude value increases to much larger values

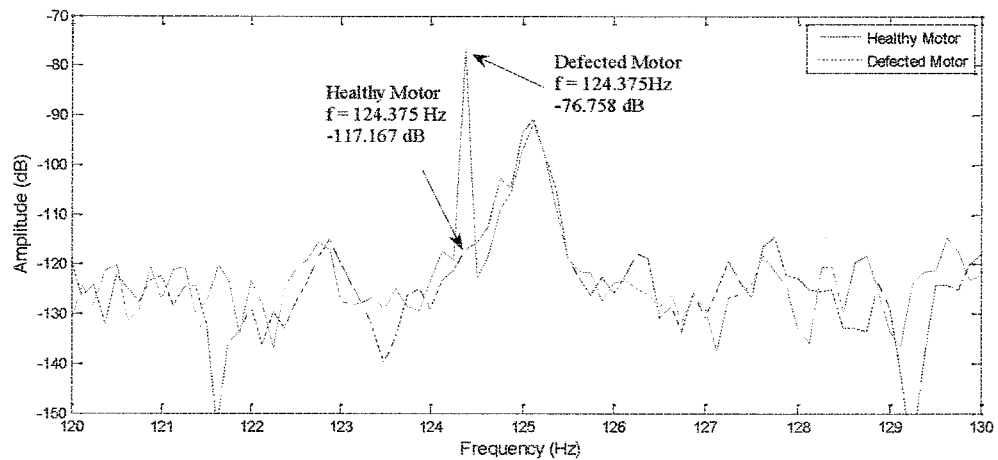


Figure 4.21: Instantaneous power spectrum of the healthy and defected motor under full load condition at 5mm outer race defect at 124.375 Hz, showing that at the specific defect frequencies the amplitude value increases to much larger values

Table 4.4: Amplitude values at outer race defect frequencies at various defect levels
and under full load conditions

Outer Race Defect Size (mm)	Characteristic Outer Race Defect Frequency (Hz)		Amplitude Values(dB)		Reference Figure No.	Remarks
	LSB	USB	LSB	USB		
1	24.375	124.375	-110.264	-108.209	4.12,4.13	Defect frequencies starts to appear
2	24.375	124.375	-104.688	-104.688	4.14,4.15	Defect frequencies increases
3	24.375	124.375	-96.688	-94.394	4.16,4.17	Defect frequencies easily identified
4	24.375	124.375	-87.272	-86.156	4.18,4.19	Defect frequencies increases till further
5	24.375	124.375	-76.922	-76.758	4.20,4.21	Defect frequencies increases to much larger values

The comparison of amplitude values for various outer race defect sizes at no load and full load conditions of the motor is shown in Figure 4.22 which indicates that as the bearing outer race single point defect size is increasing the amplitude values at characteristic defect frequencies also increases. However the increase in amplitude values is more prominent at full load condition as compared to at no load conditions.

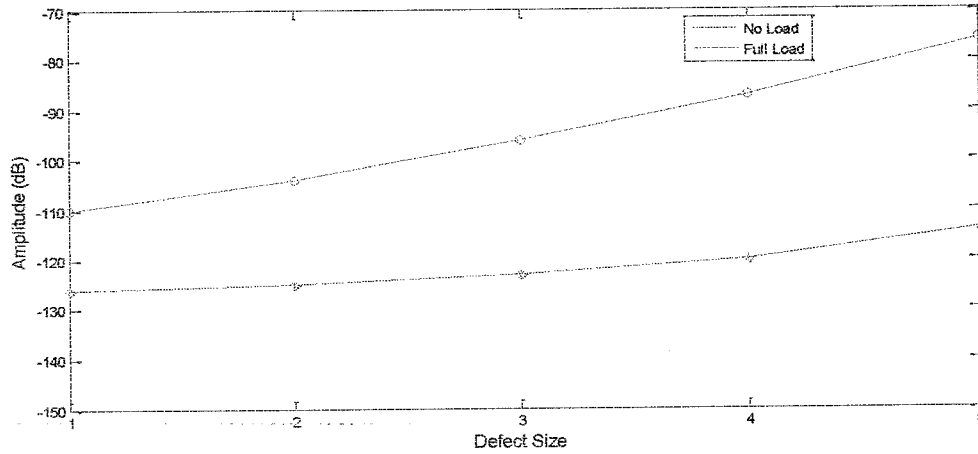


Figure 4.22: Comparison of amplitude values for various outer race defect sizes at no load and full load conditions of the motor

4.2.1.3 Comparison of the Instantaneous Power Analysis with the Stator Current Analysis

The results of the instantaneous power spectrum analysis scheme are compared with the results of stator current analysis scheme [86]. The comparison is shown in Figure 4.23 and Table 4.5. It is observed that for no load conditions of the motor, the difference that occurs in amplitude values from 2mm defect size to 4mm defect size is 3mm for the stator current analysis scheme and 4mm for the instantaneous power analysis scheme. Also for full load conditions of the motor, the change in amplitude values is 4mm for the stator current analysis scheme and 18mm for the instantaneous power analysis scheme. Therefore, the instantaneous power analysis method is more suitable for the diagnosis of the bearing outer race defects.

Table 4.5: Comparison of the instantaneous power analysis with stator current analysis

Performance	Defect Size (mm)	Type of Analysis			
		Stator Current Analysis (dB) [86]		Instantaneous Power Analysis (dB)	
		No Load	Full Load	No Load	Full Load
	2	-73	-73	-125	-104
	4	-70	-69	-121	-86
dB Improvement		3	4	4	18

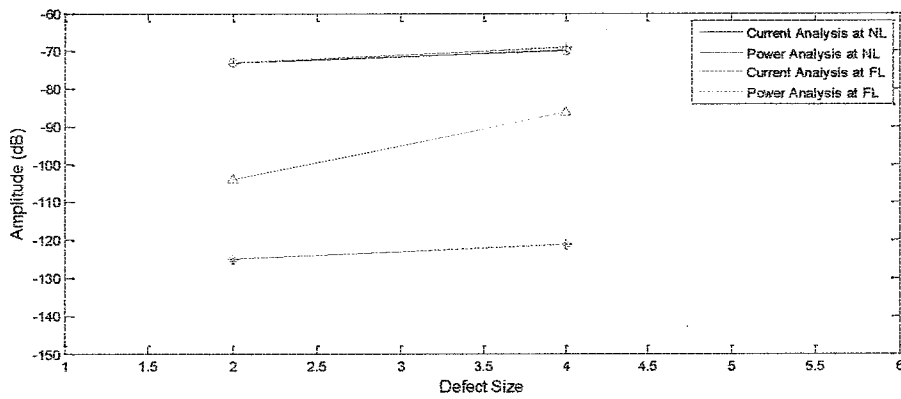


Figure 4.23: Comparison of the instantaneous power analysis with stator current analysis

4.2.2 Bearing Inner Race Defects

The holes of various sizes are induced in the inner race of the bearing to create artificial defects using electric discharge machine (EDM). The defected bearing is shown in Figure 4.24. The bearing inner race characteristic frequencies are shown in Table 4.6 which is calculated using the Equations (4.1) and (4.7) [6,81,83,84].

$$f_{if} = 0.6N_b f_r \quad (4.7)$$

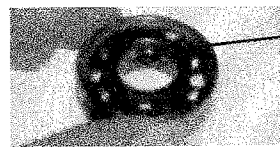
where:

N_b , is the number of balls inside the bearing

f_r , is the rotor frequency in Hz

Table 4.6: Expected inner race defect frequencies under various loading conditions

Motor Speed (rpm)	Load Condition	m=1		m=2	
		LSB(Hz)	USB(Hz)	LSB(Hz)	USB(Hz)
1497	No Load	69.750	169.750	189.50	289.50
1395	Full Load	64	164	178	278



Hole in Inner Race

Figure 4.24: Defect induced in inner race of motor bearing

4.2.2.1 Inner Race Defects Analysis at Various Hole Sizes under no Load condition of the motor

The defected bearing was installed on the shaft-end side of the motor. Five tests were conducted at different inner race hole sizes (1 to 5mm). The frequency spectrum of the healthy and defected instantaneous power spectrum is shown in Figures 4.25 to 4.34. The graph represented in dotted line indicates the healthy motor spectrum and solid line indicates the defected motor spectrum. It is observed from frequency spectrum that the amplitude values are -133.607 dB and -140.348 dB for healthy motor at specific characteristic defect frequencies of 69.75 Hz and 169.75 Hz respectively. For defected motor, it is observed from the frequency spectrums that amplitude values at specific characteristic defect frequencies are not clearly visible because their magnitude is less up-till 3mm defect size. However after 4mm hole size, there is detectable change in amplitude values at specific characteristic defect frequencies. The analysis of the change in amplitude values at characteristic defect frequencies for no load condition is summarized in Table 4.7.

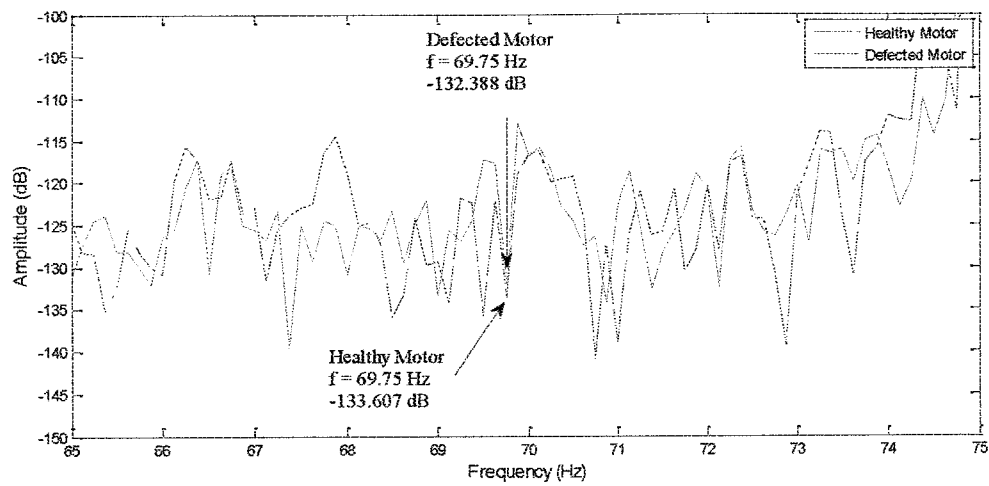


Figure 4.25: Instantaneous power spectrum of the healthy and defected motor under no load condition at 1mm inner race defect at 69.75 Hz

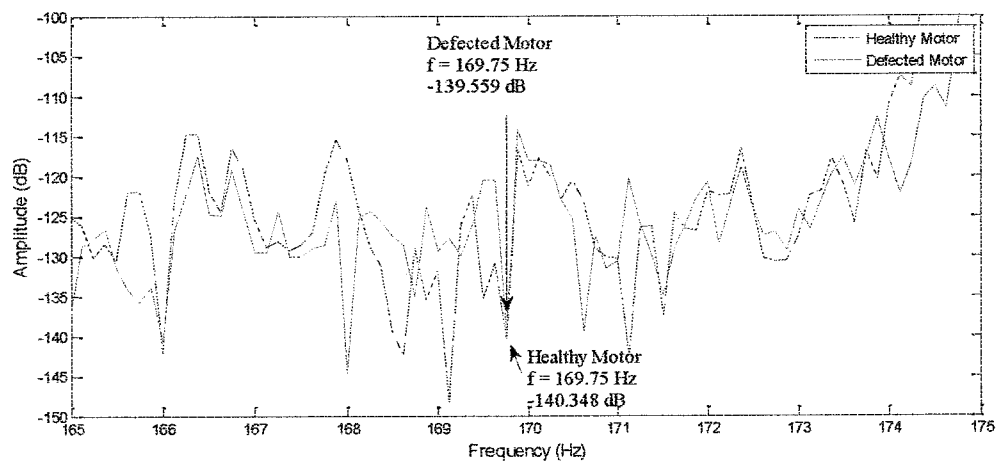


Figure 4.26: Instantaneous power spectrum of the healthy and defected motor under no load condition at 1mm inner race defect at 169.75 Hz

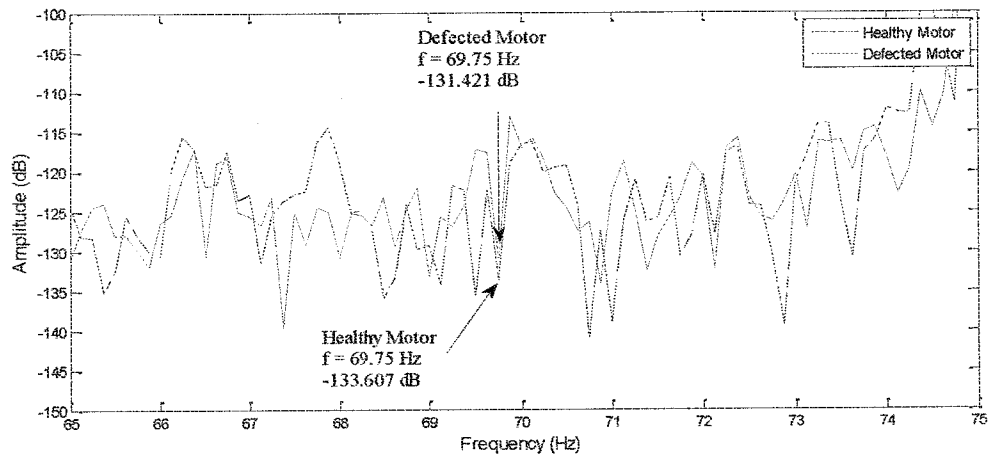


Figure 4.27: Instantaneous power spectrum of the healthy and defected motor under no load condition at 2mm inner race defect at 69.75 Hz

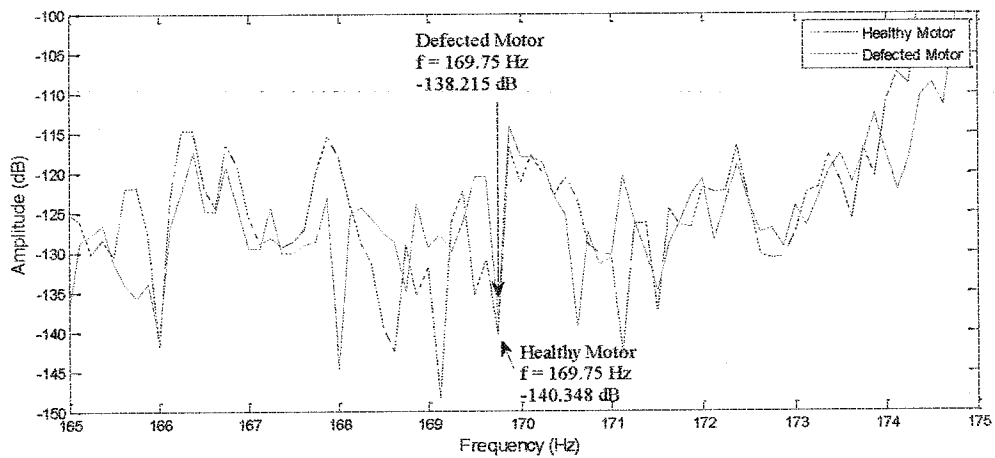


Figure 4.28: Instantaneous power spectrum of the healthy and defected motor under no load condition at 2mm inner race defect at 169.75 Hz

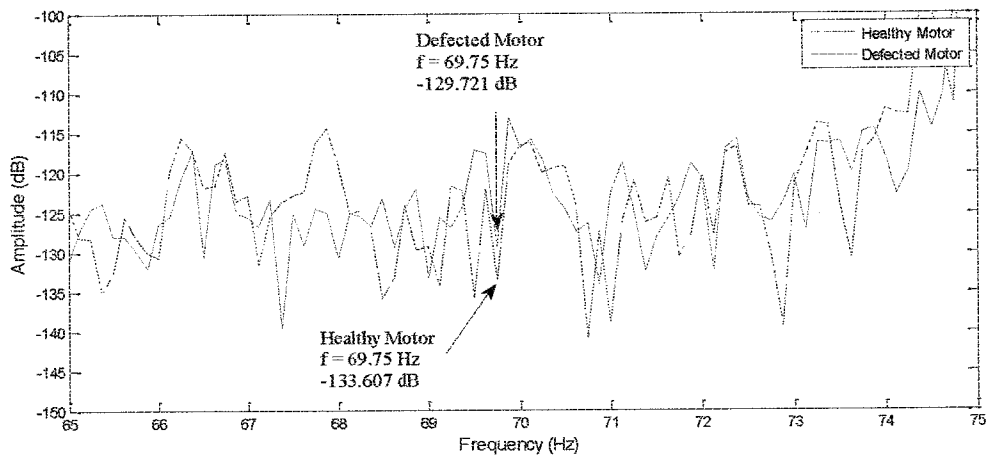


Figure 4.29: Instantaneous power spectrum of the healthy and defected motor under no load condition at 3mm inner race defect at 69.75 Hz

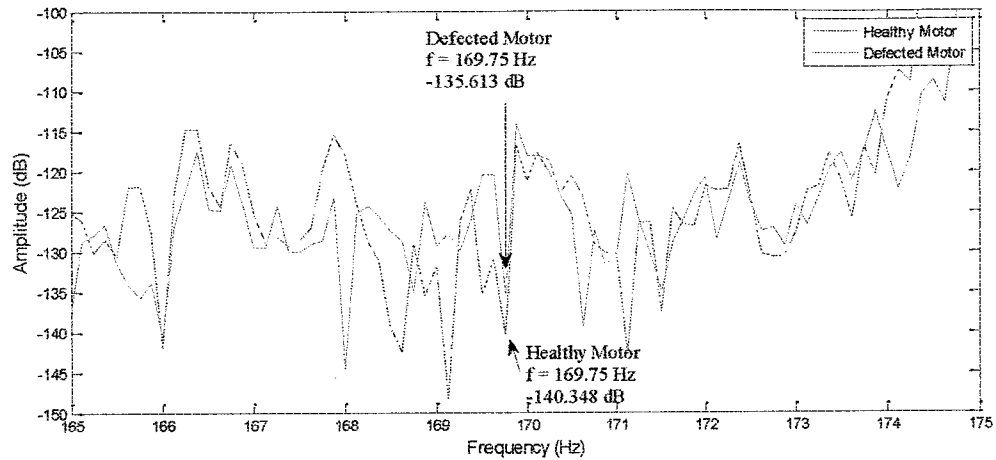


Figure 4.30: Instantaneous power spectrum of the healthy and defected motor under no load condition at 3mm inner race defect at 169.75 Hz

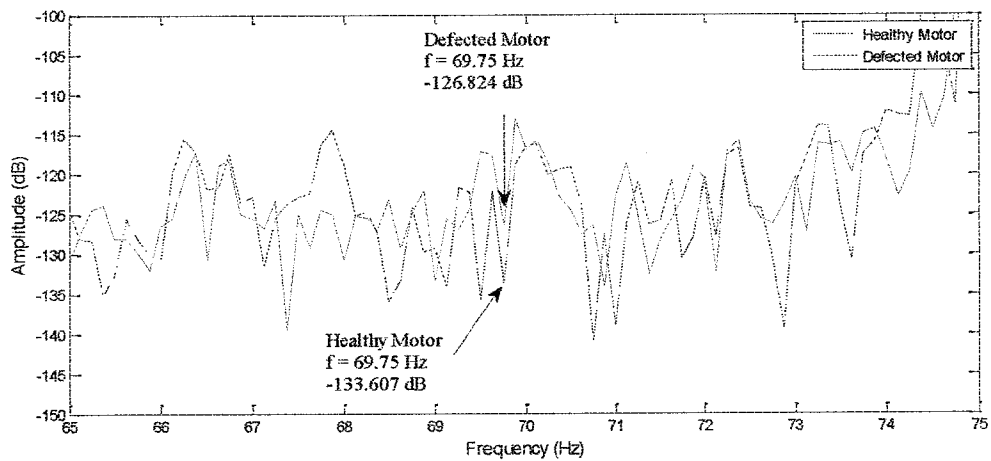


Figure 4.31: Instantaneous power spectrum of the healthy and defected motor under no load condition at 4mm inner race defect at 69.75 Hz

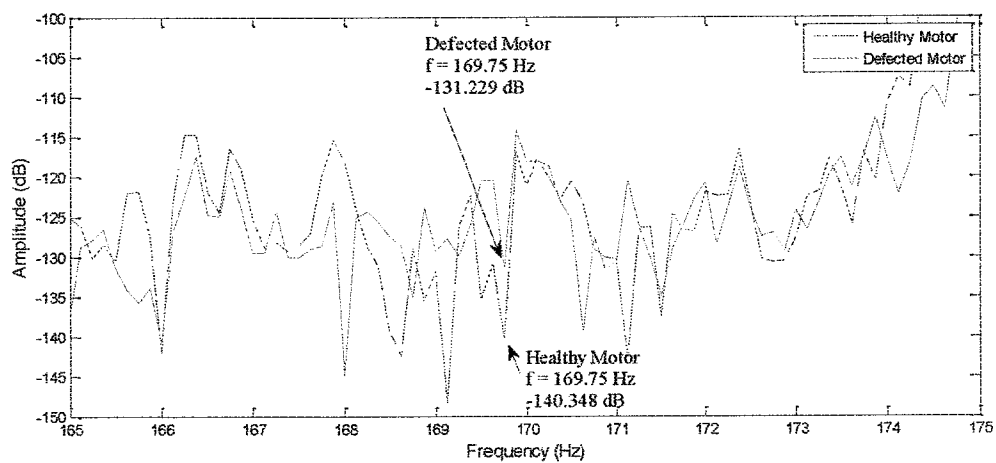


Figure 4.32: Instantaneous power spectrum of the healthy and defected motor under no load condition at 4mm inner race defect at 169.75 Hz

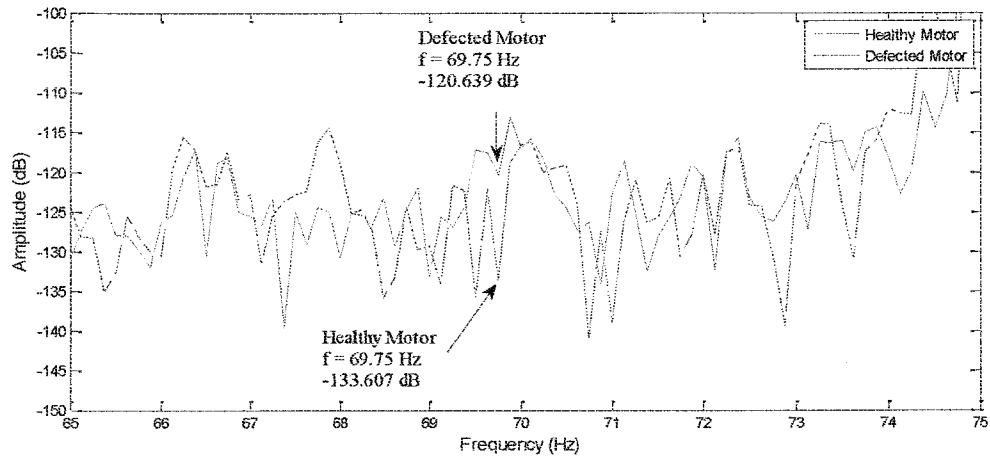


Figure 4.33: Instantaneous power spectrum of the healthy and defected motor under no load condition at 5mm inner race defect at 69.75 Hz

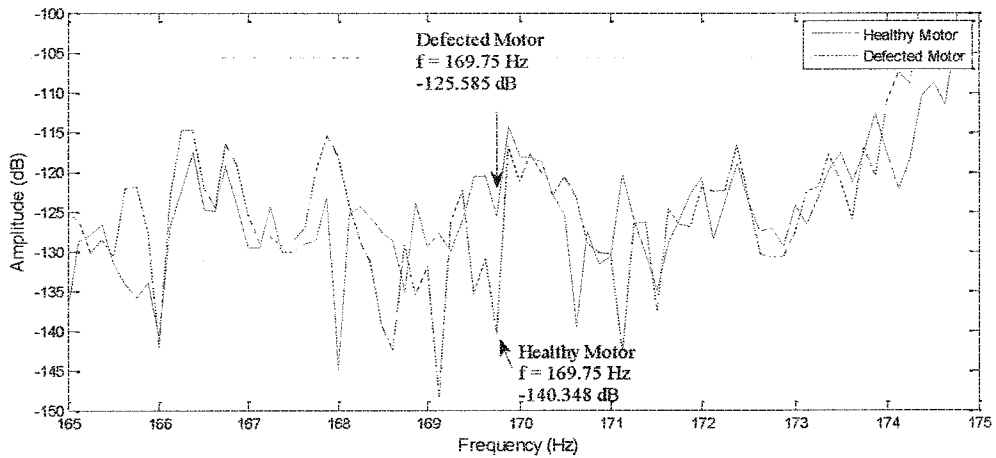


Figure 4.34: Instantaneous power spectrum of the healthy and defected motor under no load condition at 5mm inner race defect at 169.75 Hz

Table 4.7: Amplitude values at inner race defect frequencies at various defect levels
and under no load conditions

Inner Race Defect Size (mm)	Characteristic Inner Race Defect Frequency (Hz)		Amplitude Values(dB)		Reference Figure No.	Remarks
	LSB	USB	LSB	USB		
1	69.750	169.750	-132.388	-139.559	4.25,4.26	Defect frequencies difficult to identify
2	69.750	169.750	-131.388	-138.559	4.27,4.28	Defect frequencies difficult to identify
3	69.750	169.750	-129.388	-135.559	4.29,4.30	Defect frequencies difficult to identify
4	69.750	169.750	-126.388	-131.559	4.31,4.32	Defect frequencies difficult to identify
5	69.750	169.750	-120.388	-125.559	4.33,4.34	Defect frequencies visible

4.2.2.2 Inner Race Defects Analysis at Various Hole Sizes under Full Load condition of the motor

The frequency spectrum of the healthy and defected motor instantaneous power is shown in Figures 4.35 to 4.44. The graph represented in dotted line indicates the healthy motor spectrum and solid line indicates the defected motor spectrum. It is observed from frequency spectrum that the amplitude values are -124.213 dB and -125.811 dB for healthy motor at specific inner race characteristic defect frequencies of 64 Hz and 164 Hz respectively. From the analysis of healthy and defected current spectrums, it is indicated that the presence of fault in inner race of motor bearings appears as an increased in the amplitude values at specific characteristic defect frequencies. It is observed that at full load condition of motor, the amplitude values

have been increased significantly and are clearly visible even at 3mm defect size and the amplitude values increases with the increase of defect size in motor bearing. The analysis of frequency spectrum for various outer race defect sizes is summarized in Table 4.8.

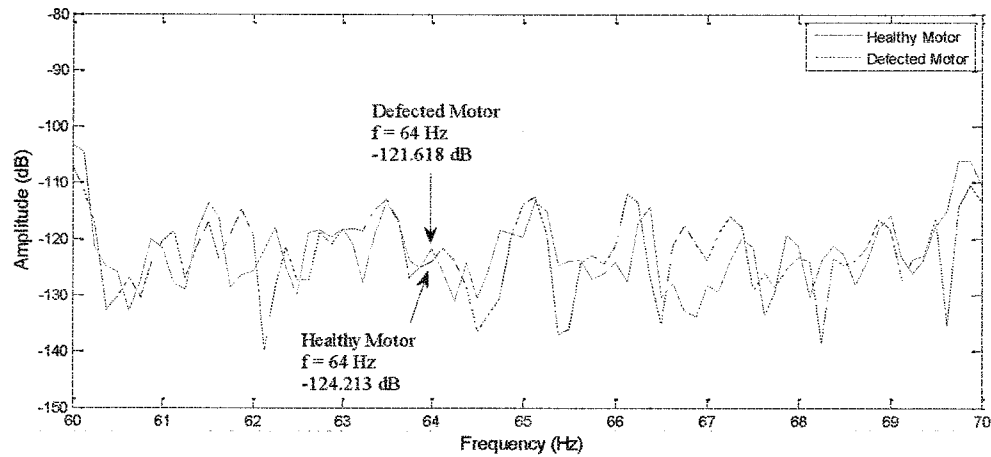


Figure 4.35: Instantaneous power spectrum of the healthy and defected motor under full load condition at 1mm inner race defect at 64 Hz, showing that at the specific defect frequencies the amplitude starts to appear

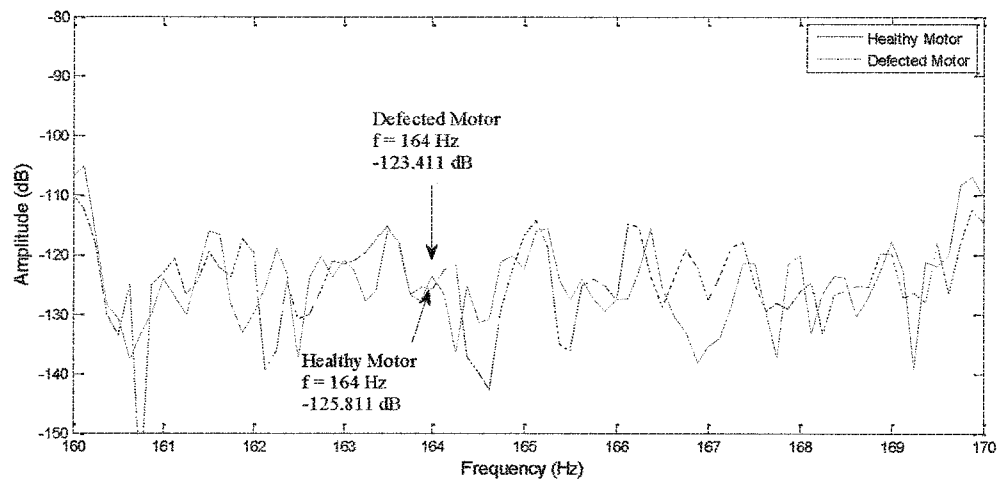


Figure 4.36: Instantaneous power spectrum of the healthy and defected motor under full load condition at 1mm inner race defect at 164 Hz, showing that at the specific defect frequencies the amplitude starts to appear

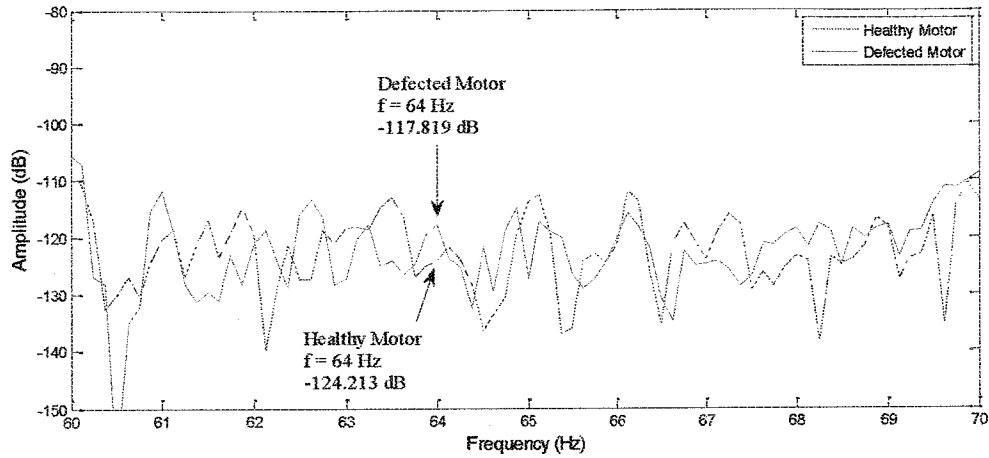


Figure 4.37: Instantaneous power spectrum of the healthy and defected motor under full load condition at 2mm inner race defect at 64 Hz, showing that at the specific defect frequencies the amplitude value increases

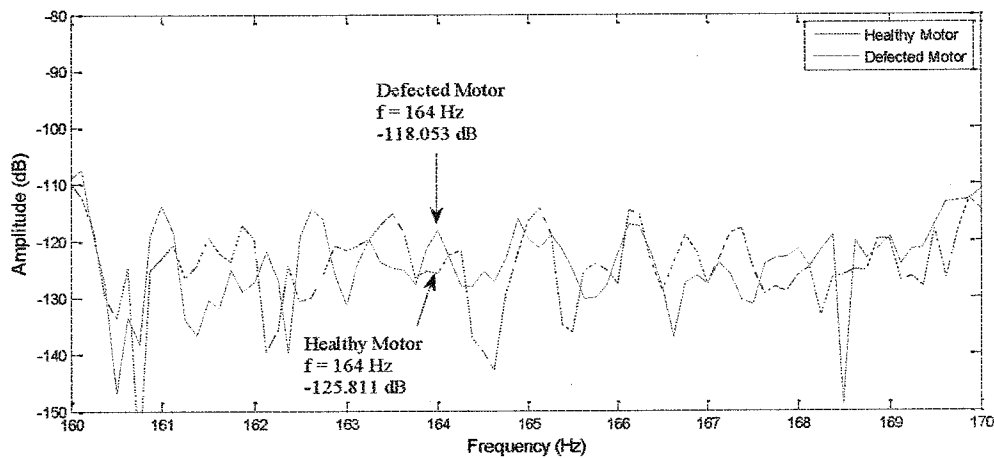


Figure 4.38: Instantaneous power spectrum of the healthy and defected motor under full load condition at 2mm inner race defect at 164 Hz, showing that at the specific defect frequencies the amplitude value increases

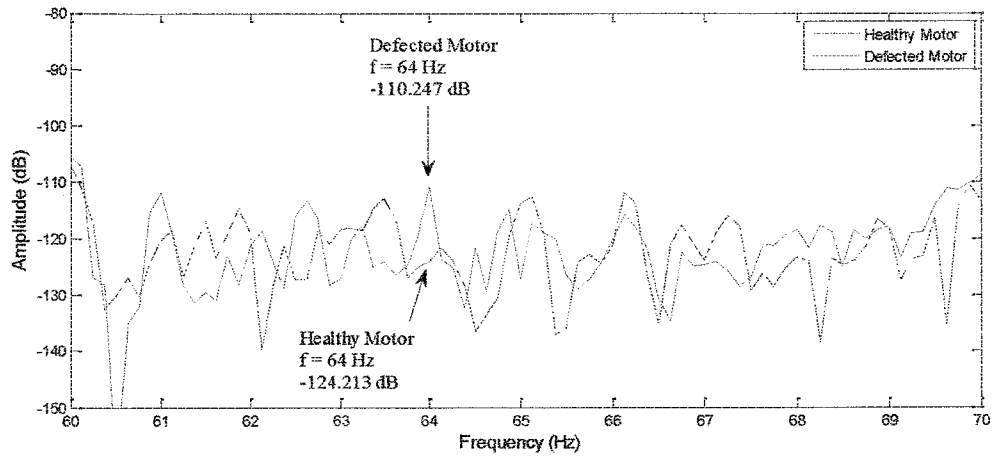


Figure 4.39: Instantaneous power spectrum of the healthy and defected motor under full load condition at 3mm inner race defect at 64 Hz, indicating that at the specific defect frequencies, the amplitude value continue to increase

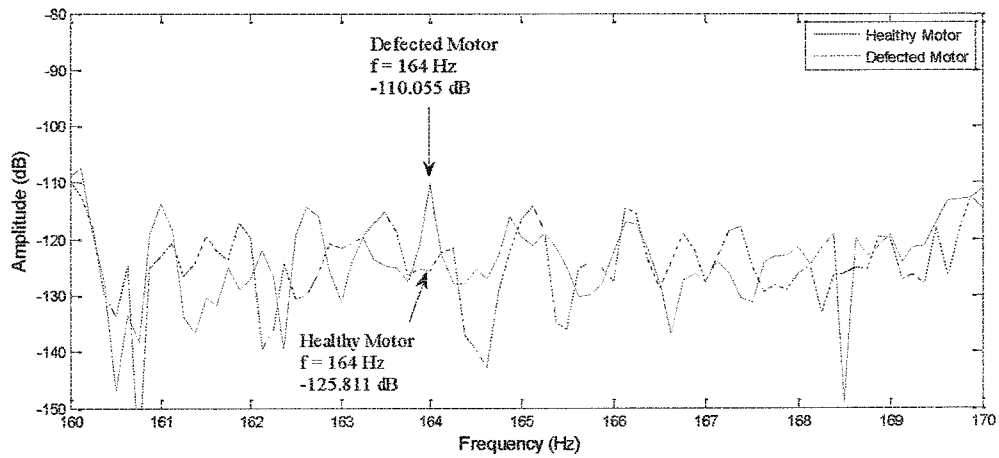


Figure 4.40: Instantaneous power spectrum of the healthy and defected motor under full load condition at 3mm inner race defect at 164 Hz, indicating that at the specific defect frequencies, the amplitude value continue to increase

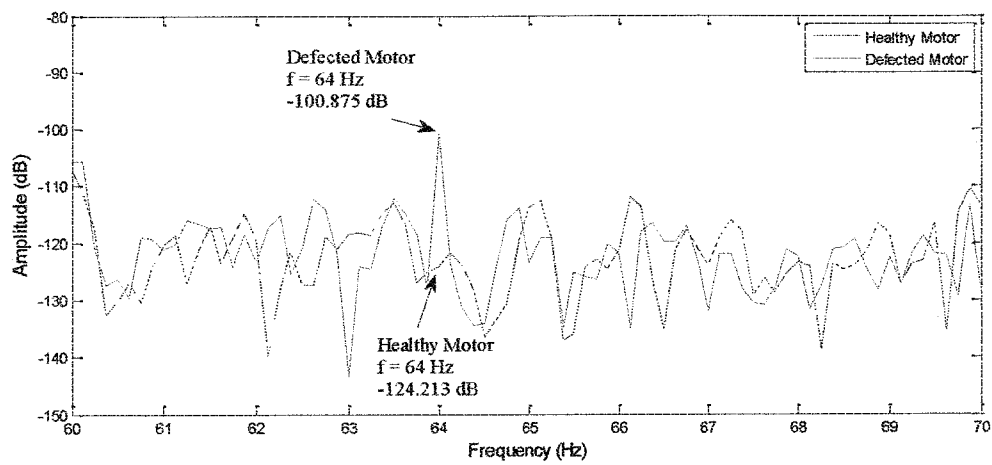


Figure 4.41: Instantaneous power spectrum of the healthy and defected motor under full load condition at 4mm inner race defect at 64 Hz, showing that at the specific defect frequencies the amplitude value increases still further

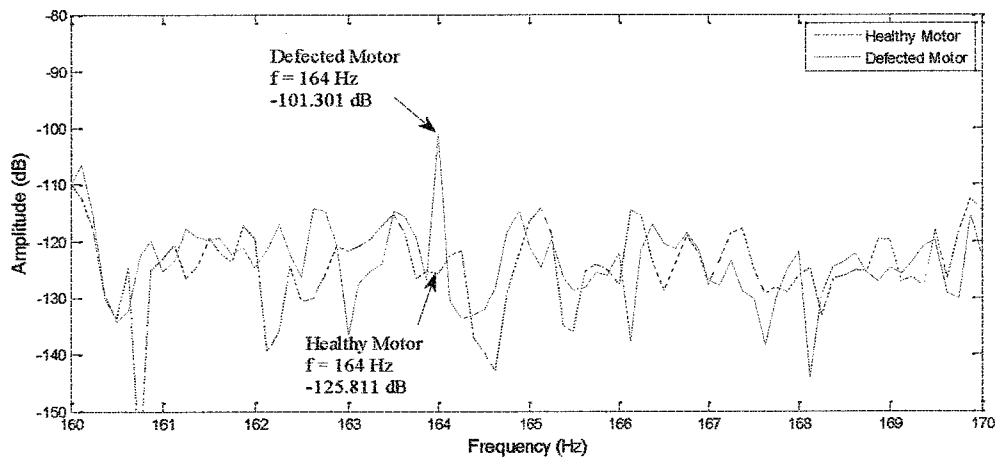


Figure 4.42: Instantaneous power spectrum of the healthy and defected motor under full load condition at 4mm inner race defect at 164 Hz, showing that at the specific defect frequencies the amplitude value increases still further

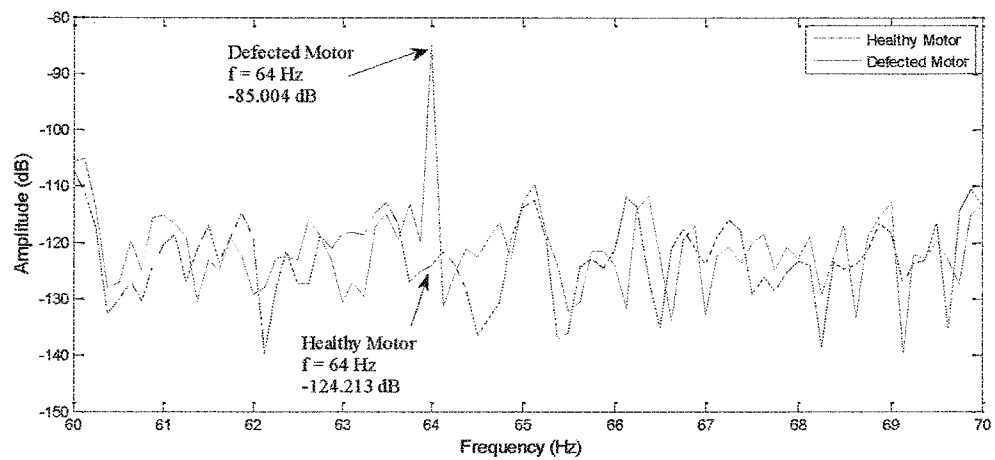


Figure 4.43: Instantaneous power spectrum of the healthy and defected motor under full load condition at 5mm inner race defect at 64 Hz, showing that at the specific defect frequencies the amplitude value increases to much larger values

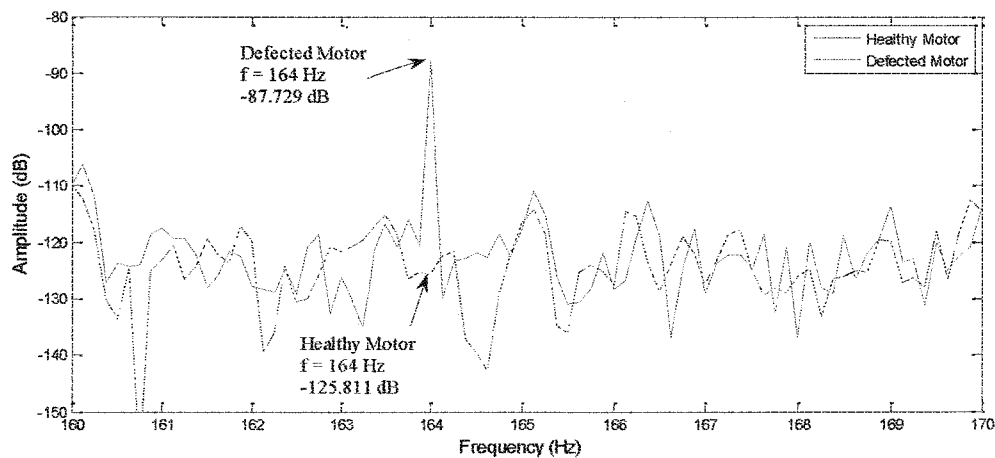


Figure 4.44: Instantaneous power spectrum of the healthy and defected motor under full load condition at 5mm inner race defect at 164 Hz, showing that at the specific defect frequencies the amplitude value increases to much larger values

Table 4.8: Amplitude values at inner race defect frequencies at various defect levels and under full load conditions

Inner Race Defect Size (mm)	Characteristic Inner Race Defect Frequency (Hz)		Amplitude Values(dB)		Reference Figure No.	Remarks
	LSB	USB	LSB	USB		
1	64	164	-121.618	-123.411	3.35,3.36	Defect frequencies starts to appear
2	64	164	-117.819	-118.053	3.37,3.38	Defect frequencies increases
3	64	164	-110.819	-110.053	3.39,3.40	Defect frequencies easily identified
4	64	164	-100.875	-101.301	4.41,4.42	Defect frequencies increases till further
5	64	164	-85.0042	-87.729	4.43,4.44	Defect frequencies increases to much larger values

The comparison of amplitude values for various inner race defect sizes at no load and full load conditions of the motor is shown in Figure 4.45 which indicates that as the bearing outer race single point defect size is increasing the amplitude values at characteristic defect frequencies also increases. However the increase in amplitude values is more prominent at full load condition as compared to at no load conditions.

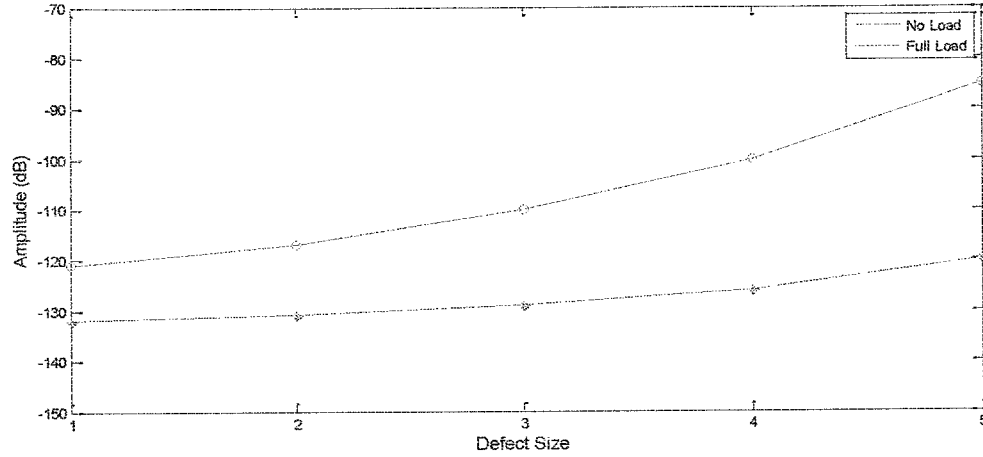


Figure 4.45: Comparison of amplitude values for various inner race defect sizes at no load and full load conditions of the motor

4.2.2.3 Comparison of the Instantaneous Power Analysis with Current Analysis for Bearing Inner race Defects

The results of the instantaneous Power spectrum analysis scheme are compared with the results of the stator current analysis scheme [86]. The comparison is shown in Figure 4.46 and Table 4.9. It is observed that for no load conditions of the motor, the difference that occurs in amplitude values from 2mm defect size to 4mm defect size is 3dB for the stator current analysis scheme and 7dB for the instantaneous power analysis scheme. Also for full load conditions of the motor, the change in amplitude values is 6dB for the stator current analysis scheme and 17dB for the instantaneous power analysis scheme. Therefore, the instantaneous power analysis method is more suitable for the diagnosis of the bearing inner race defects.

Table 4.9: Comparison of the instantaneous power analysis with stator current analysis for bearing inner race defects

Performance	Defect Size (mm)	Type of Analysis			
		Stator Current Analysis (dB)		Instantaneous Power Analysis (dB)	
		No Load	Full Load	No Load	Full Load
	2	-77	-74	-138	-118
	4	-74	-68	-131	-101
dB Improvement		3	6	7	17

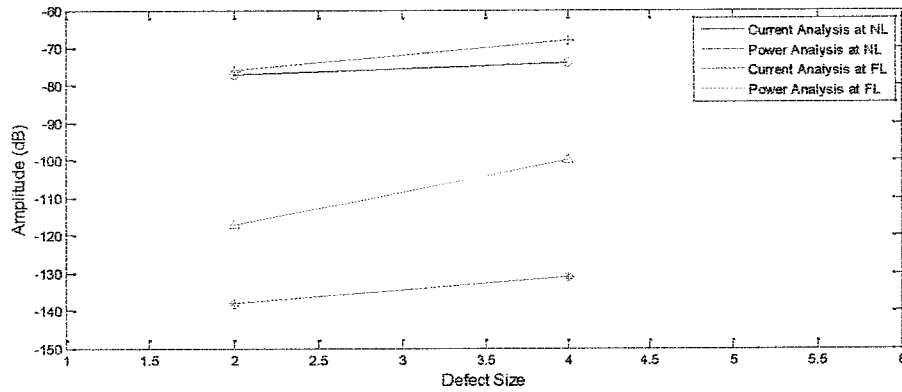


Figure 4.46: Comparison of the Instantaneous power analysis with stator current analysis for bearing inner race defects

4.2.3 Bearing Ball Defects

The balls of bearing are damaged to create artificial defects using electric discharge machine (EDM). The defected bearing is shown in Figure 4.47. The bearing ball defect characteristic frequencies are shown in Table 4.10 which is calculated using the Equations (4.3) and (4.8) [6,81,83,84].

$$f_{db} = \frac{D}{d} f_r \left(1 - \frac{d^2}{D^2} \cos \alpha \right) \quad (4.7)$$

where:

N_b , is the number of balls inside the bearing

f_r , is the rotor frequency in Hz

d , is the ball diameter

D , is the pitch diameter of bearing

α , is the ball contact angle

Table 4.10: Expected ball defect frequencies under various loading conditions

Motor Speed (rpm)	Load Condition	m=1		m=2	
		LSB(Hz)	USB(Hz)	LSB(Hz)	USB(Hz)
1497	No Load	47.875	147.875	145.875	245.875
1395	Full Load	43.25	143.25	136.5	236.5

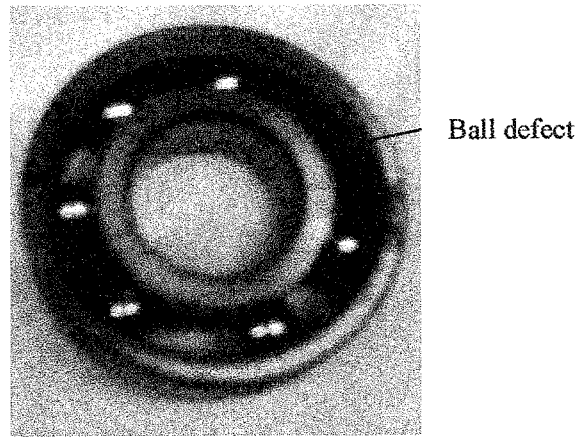


Figure 4.47: Ball defects induced in bearing of motor

4.2.3.1 Bearing Ball Defects under no Load condition of the motor

The bearing with defected balls was installed on the shaft-end side of the motor. Three tests were conducted at different defect levels (1 to 3 balls damaged). The frequency spectrum of the healthy and defected motor instantaneous power is shown in Figures 4.48 to 4.50. The dotted line in graph indicates the healthy motor spectrum and solid line indicates the defected motor spectrum. It is observed from frequency spectrum that the amplitude values are -133.046 dB and -135.968 dB for healthy motor at specific characteristic ball defect frequencies of 145.875 Hz and 147.875 Hz respectively. For a defected motor, it is observed from the frequency spectrums that amplitude values at specific characteristic ball defect frequencies are not clearly visible because their magnitude is less up-till two balls damaged. However, in case for three damaged balls there is a detectable change in amplitude values at specific characteristic ball defect frequencies. The analysis of the change in amplitude values at characteristic ball defect frequencies for no load condition is summarized in Table 4.11.

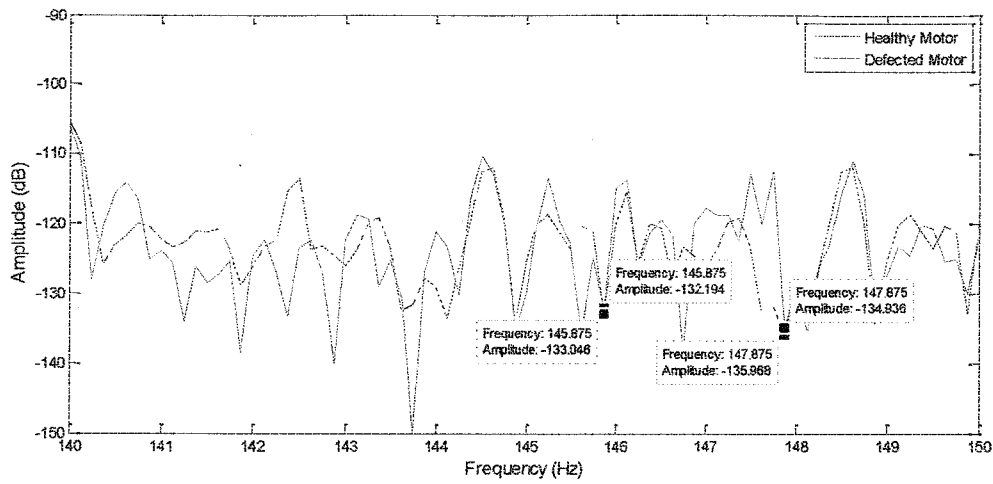


Figure 4.48: Instantaneous power spectrum of the healthy and defected motor under no load condition and at one ball damaged at two different characteristic ball defect frequency of 145.875 Hz and 147.875 Hz

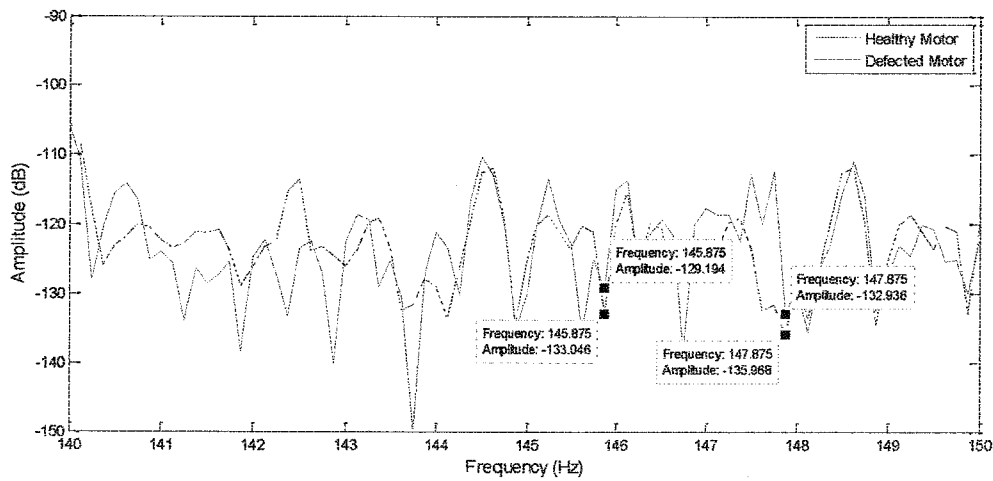


Figure 4.49: Instantaneous power spectrum of the healthy and defected motor under no load condition and at two balls damaged at two different characteristic ball defect frequency of 145.875 Hz and 147.875 Hz

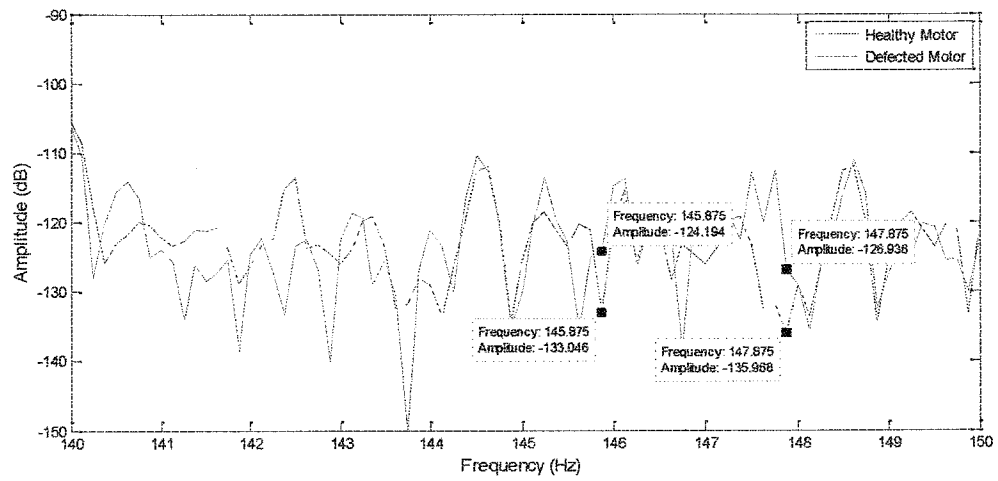


Figure 4.50: Instantaneous power spectrum of the healthy and defected motor under no load condition and at three balls damaged at two different characteristic ball defect frequency of 145.875 Hz and 147.875 Hz

Table 4.11: Amplitude values at bearing ball defect frequencies at various defect levels and under no load conditions

Number of Damaged Balls	Characteristic Ball Defect Frequency (Hz)		Amplitude Values for Defected Motor (dB)		Reference Figure No.	Remarks
	m=1	m=2	m=1	m=2		
1	147.875	145.875	-134.93	-132.94	4.48	Defect frequencies invisible
2	147.875	145.875	-132.93	-129.19	4.49	Defect frequencies invisible
3	147.875	145.875	-126.93	-124.19	4.50	Defect frequencies easily identified

4.2.3.2 Bearing Ball defects under full Load Conditions of the Motor

The frequency spectrum of the healthy and defected motor instantaneous power is shown in Figures 4.51 to 4.53. The dotted line in graph indicates the healthy motor spectrum and solid line indicates the defected motor spectrum. It is observed from frequency spectrum that the amplitude values are -131.8 dB and -127.5 dB for healthy motor at specific ball defect characteristic frequencies of 136.5 Hz and 143.25 Hz respectively. From the analysis of healthy and defected instantaneous power spectrums, it is indicated that the presence of fault in balls of bearing of motor appears as increase in amplitude values at specific ball defect characteristic frequencies. It is observed that at full load condition of motor, the amplitude values have been increased significantly and are clearly visible even at one ball damage and the amplitude values increases with the increase of defect size in motor bearing. The analysis of frequency spectrum for ball defect is summarized in Table 4.12.

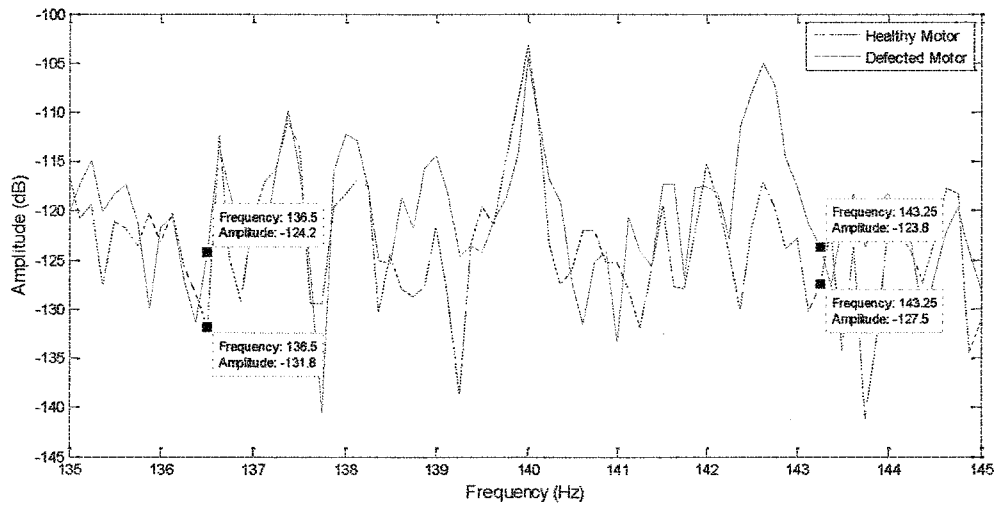


Figure 4.51: Instantaneous power spectrum of the healthy and defected motor under full load condition at one ball damage, showing that at two different characteristic ball defect frequencies of 136.5 Hz and 143.25 Hz the amplitude value starts to appear

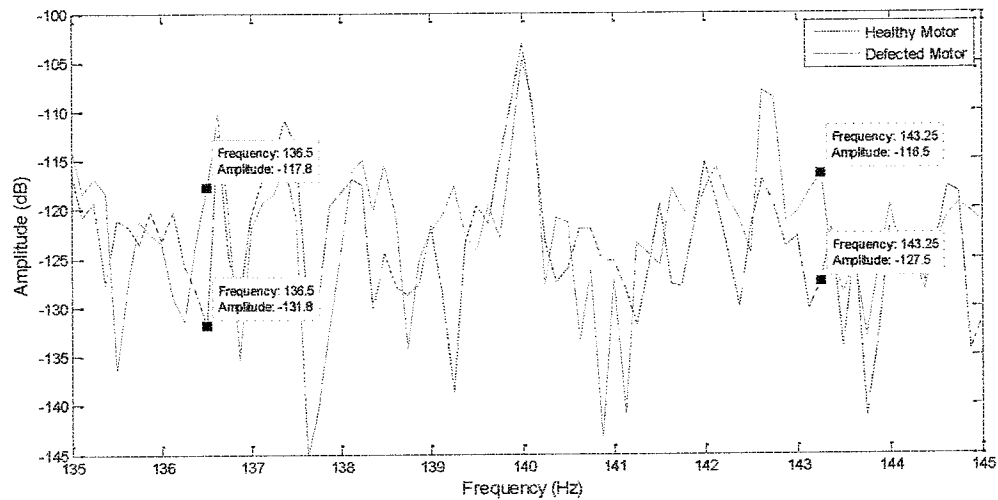


Figure 4.52: Instantaneous power spectrum of the healthy and defected motor under full load condition at two balls damage, showing that at two different characteristic ball defect frequencies of 136.5 Hz and 143.25 Hz the amplitude value increases

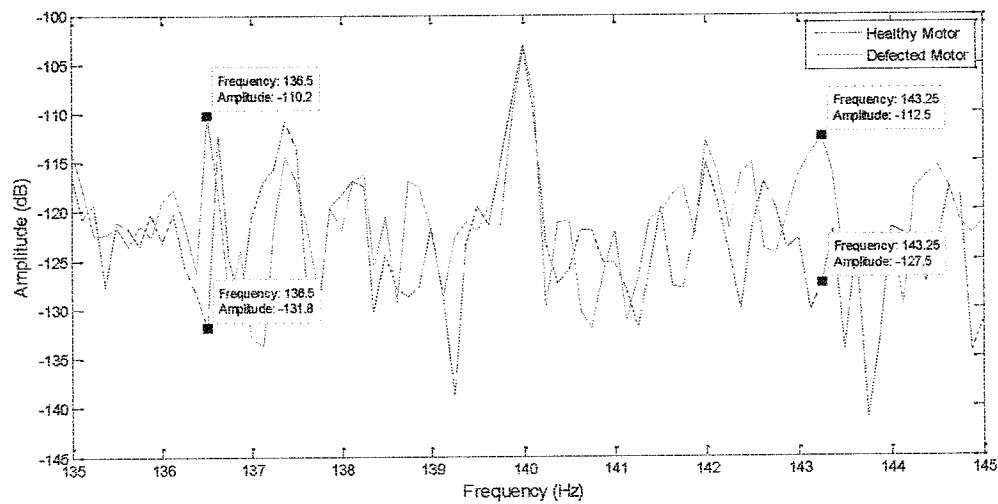


Figure 4.53: Instantaneous power spectrum of the healthy and defected motor under full load condition at three balls damage, showing that at two different characteristic ball defect frequencies of 136.5 Hz and 143.25 Hz the amplitude value increase to much larger value

Table 4.12: Amplitude values at bearing ball defect frequencies at various defect levels and under full load conditions

Number of Damaged Balls	Characteristic Ball Defect Frequency (Hz)		Amplitude Values for Defected Motor (dB)		Reference Figure No.	Remarks
	m=1	m=2	m=1	m=2		
1	143.25	136.5	-123.8	-124.2	4.51	Defect frequencies starts to appear
2	143.25	136.5	-116.5	-117.8	4.52	Defect frequencies visible
3	143.25	136.5	-112.5	-110.2	4.53	Defect frequencies easily identified

The comparison of amplitude values for various bearing ball defect sizes at no load and full load conditions of the motor is shown in Figure 4.54. It is clearly shown that as the bearing ball defect size is increasing the amplitude values at characteristic defect frequencies also increases. However the increase in amplitude values is more prominent at full load condition as compared to at no load conditions.

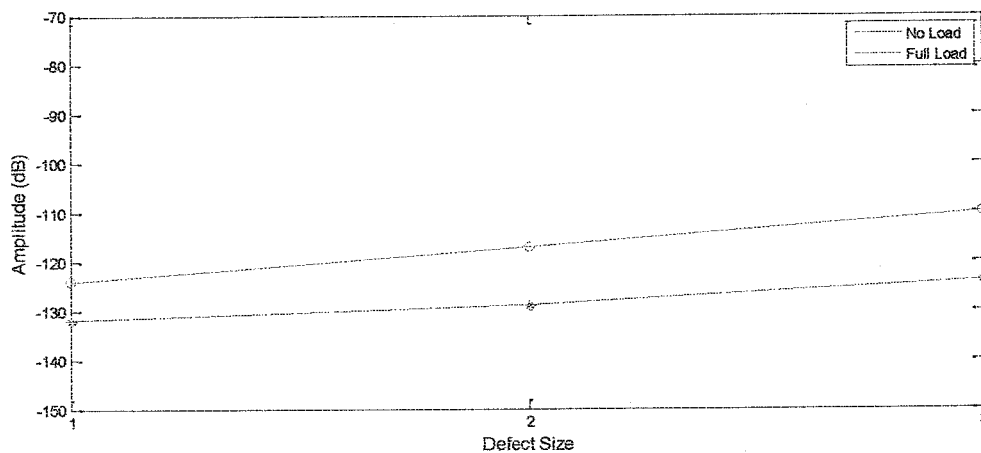


Figure 4.54: Comparison of amplitude values for various ball defect sizes at no load and full load conditions of the motor

4.2.3.3 Comparison of the Instantaneous Power Analysis with Current Analysis for Bearing Ball Defects under Full Load Condition of the Motor

The results of the instantaneous power spectrum analysis scheme are compared with the results of the stator current analysis scheme [85] for the bearing ball defects. The comparison is shown in Figure 4.55 and Table 4.13. It is observed that for full load conditions of the motor, the change in amplitude values from one to three damaged balls is 6dB for the stator current analysis scheme and 17dB for the instantaneous power analysis scheme. Therefore, the instantaneous power analysis method is more suitable for the diagnosis of the bearing ball defects.

Table 4.13: Comparison of the instantaneous power analysis with stator current analysis for bearing ball defects

Performance	Number of Damaged Balls	Type of Analysis	
		Stator Current Analysis (dB) [85]	Instantaneous Power Analysis (dB)
	1	-19.17	-123.8
	3	-14.12	-112.5
dB Improvement		5.05	11.3

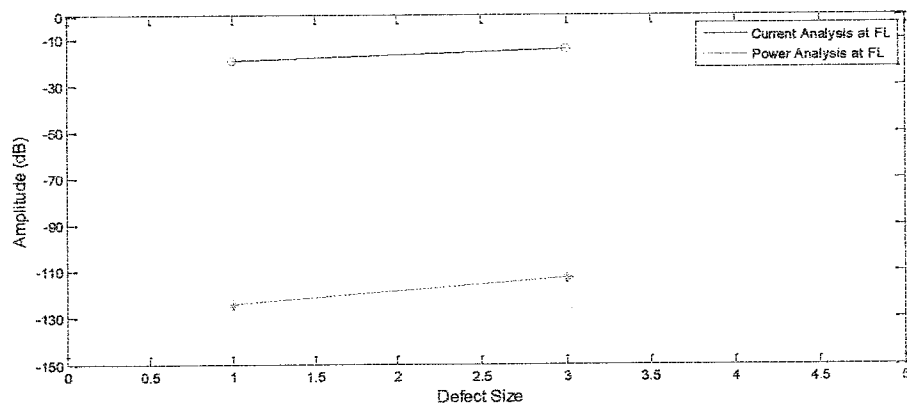


Figure 4.55: Comparison of the instantaneous power analysis with stator current analysis for bearing ball defects

4.2.4 Bearing Cage Defects

The cage of bearing is damaged to create artificial fault. The defected bearing is shown in Figure 4.56. The bearing cage defect characteristic frequencies are shown in Table 4.14 which is calculated using the Equations (4.4) and (4.8) [6,81,83,84].

$$f_c = \frac{f_r}{2} \left(1 - \frac{d}{D} \cos \alpha \right) \quad (4.8)$$

where:

N_b , is the number of balls inside the bearing

f_r , is the rotor frequency in Hz

d , is the ball diameter

D , is the pitch diameter of bearing

α , is the ball contact angle

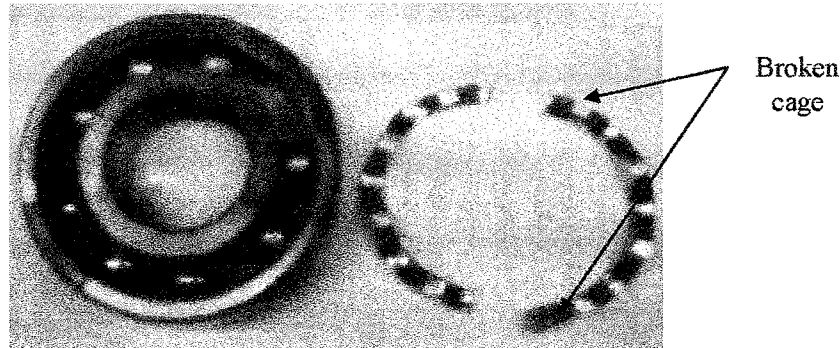


Figure 4.56: Cage defect induced in bearing of motor

Table 4.14: Expected cage defect frequencies under full load on motor

Motor Speed (rpm)	Load Condition	m=1		m=2	
		LSB(Hz)	USB(Hz)	LSB(Hz)	USB(Hz)
1497	No Load	40.5	59.5	31	69
1395	Full Load	41.25	58.875	32.375	67.75

4.2.4.1 Bearing Cage Defects Analysis under no Load conditions of the Motor

The frequency spectrum of the healthy and defected motor instantaneous power are shown in Figures 4.57 to 4.58. The dotted line on the graph represents the healthy motor spectrum while solid line represents the defected motor spectrum. For healthy motor, it is observed in Figures 4.57 and 4.58 that the amplitude values are -131.0661 dB, -122.82 dB, -128.468 and -129.308 which corresponds to the specific characteristic cage defect frequencies of 31 Hz, 40.5 Hz, 59.5 Hz and 69Hz

respectively. While for defected motor, the amplitude values increased to -123.276 dB, -129.426 dB, -119.647 dB and -117.584 dB at the specific characteristic cage defect frequencies of 31 Hz, 40.5 Hz, 59.5 Hz and 69 Hz respectively. From the analysis of healthy and defected instantaneous power spectrums, it is indicated that the presence of fault in cage of motor bearings appears as the increased in amplitude values at specific characteristic defect frequencies. It is observed that at no load condition of motor, the amplitude values have been increased significantly and are clearly visible. The analysis of frequency spectrum for various defect sizes is summarized in Table 4.15.

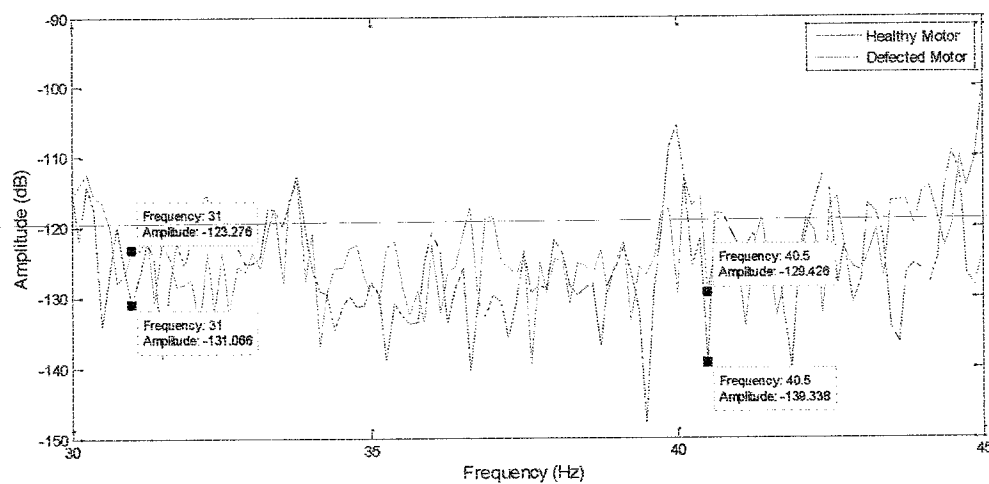


Figure 4.57: Instantaneous power spectrum of healthy and defected motor at no load condition, indicating that presence of cage defect in motor appear as rise in amplitude values at 31 Hz and 40.5 Hz

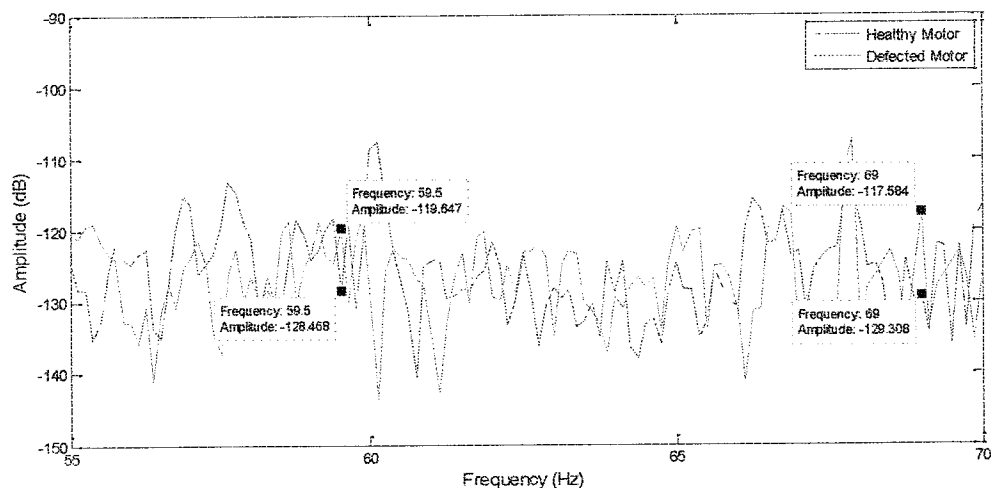


Figure 4.58: Instantaneous power spectrum of healthy and defected motor at no load condition, indicating that presence of cage defect in motor appear as rise in amplitude values at 59.5 Hz and 69 Hz

Table 4.15: Amplitude values at bearing cage defect frequencies under no load conditions

Cage Condition	Characteristic Cage Defect Frequency (Hz)			Amplitude Values (dB)	Remarks
Healthy Cage	m=1	LSB	40.5	-139.338	
		USB	59.5	-128.468	
	m=2	LSB	31	-131.066	
		USB	69	-129.308	
Defected Cage	m=1	LSB	40.5	-129.426	Amplitude at defect frequencies increases to much larger values
		USB	59.5	-119.647	
	m=2	LSB	31	-123.276	
		USB	69	-117.584	

4.2.4.2 Bearing Cage Defects Analysis under Full Load conditions of the Motor

The frequency spectrum of the healthy and defected motor instantaneous power are shown in Figures 4.59 and 4.60. The dotted line in the graph indicates healthy motor spectrum while solid line indicates defected motor spectrum. For the healthy motor, it is observed in Figures 4.59 and 4.60 that the amplitude values are -122.912 dB, -122.825 dB, -124.638 and -126.088 that corresponds to the specific characteristic defect frequencies of 32.75 Hz, 41.25 Hz, 58.875 Hz and 67.75 Hz respectively. While for defected motor, the amplitude values increased to -103.744 dB, -106.837 dB, -105.321 dB and -107.955 dB. From the analysis of healthy and defected instantaneous power spectrums, it is indicated that the presence of fault in the cage of the motor bearings appears as the increased in amplitude values at specific characteristic defect frequencies. It is observed that at full load condition of motor, the amplitude values have been increased significantly and are clearly visible. The analysis of frequency spectrum for various defect sizes is summarized in Table 4.16.

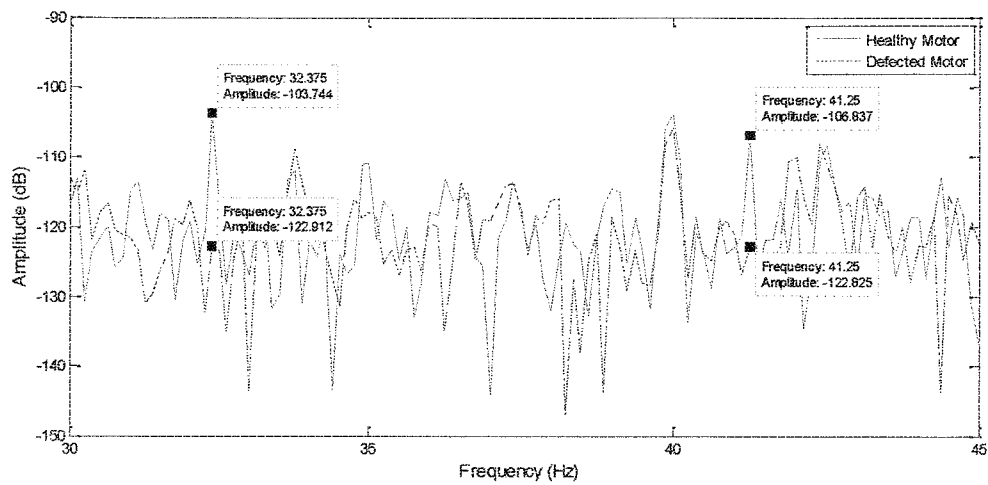


Figure 4.59: Instantaneous power spectrum of healthy and defected motor at full load condition, indicating that presence of cage defect in motor appear as much increase in amplitude values at 32.375 Hz and 41.25 Hz

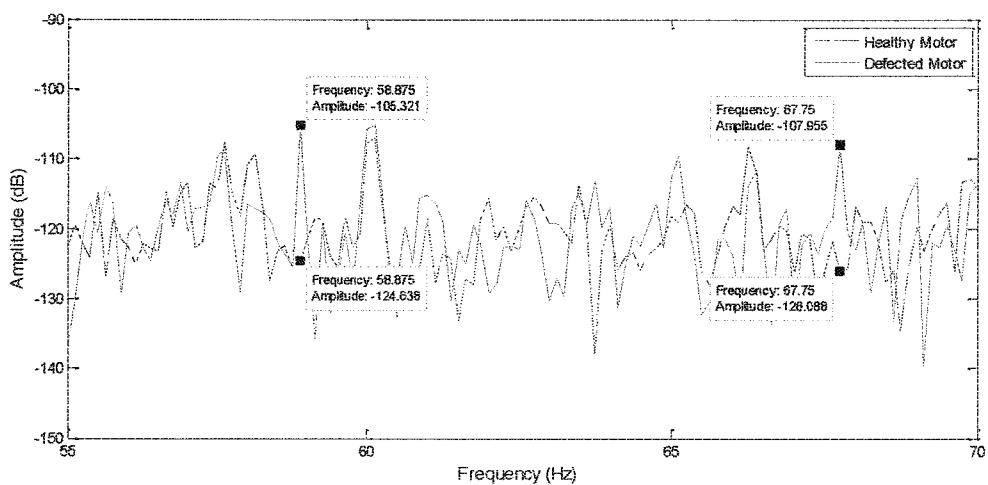


Figure 4.60: Instantaneous power spectrum of healthy and defected motor at full load condition, indicating that presence of cage defect in motor appear as much increase in amplitude values at 58.875 Hz and 67.75 Hz

Table 4.16: Amplitude values at bearing cage defect frequencies under full load conditions

Cage Condition	Characteristic Cage Defect Frequency (Hz)			Amplitude Values (dB)	Remarks
Healthy Cage	m=1	LSB	41.25	-122.825	
		USB	58.875	-124.638	
	m=2	LSB	32.375	-122.91	
		USB	67.75	-126.088	
Defected Cage	m=1	LSB	41.25	-106.83	Amplitude at defect frequencies increases to much larger values
		USB	58.875	-105.32	
	m=2	LSB	32.375	-103.74	
		USB	67.75	-107.95	

4.2.5 Bearing Distributed Defects

In the previous sections bearing localized (single point) defects and their analysis method was discussed. This section focused on the type of defects that are distributed on the whole bearing surface i.e. multiple wholes in outer or inner races or surface roughness in the races of bearing. These types of faults were induced in the test bearing by artificial method. Four experiments were performed for the analysis of distributed faults in the bearing outer and inner surfaces.

4.2.5.1 Distributed Defect in Outer Race of Bearing

In the first experiment, three holes of 3mm size were drilled in the outer race of the bearing. The defected bearing is shown in Figure 4.61. The instantaneous power spectrum of the distributed defect in outer race of bearing is shown in Figures 4.62 and 4.63. From analysis of the instantaneous power spectrum it is clearly shown that there is no amplitude rise for the outer race characteristic defect frequencies of 98.75 Hz and 124.375 Hz. This indicates that mathematical relation as described in Equations (4.6) and (4.8) can only be applied to the bearing localized (single point) defects. It was also observed from the instantaneous power spectrum that the

amplitude peaks were detected at 25.6 Hz and 100.44 Hz as shown in Figures 4.64 and 4.65. Looking at mathematics relations as described by Park's model, it was observed that these peaks values for outer race distributed defect are appearing at $1.35f_{of}$ and $|2f_e - f_{of}|$.

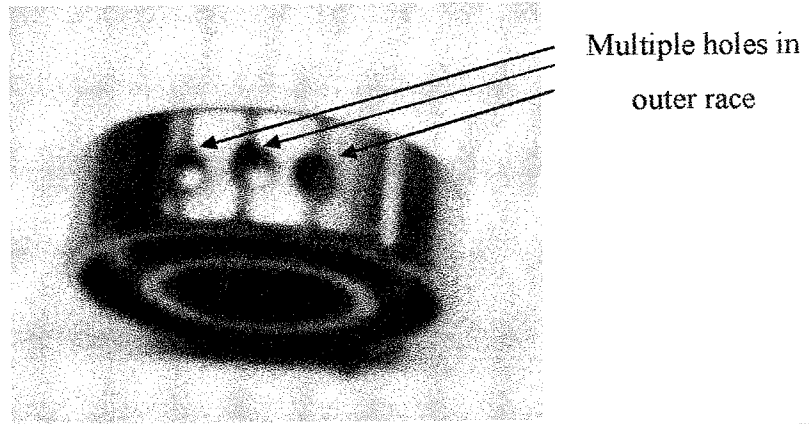


Figure 4.61: Distributed defect in outer surface of bearing

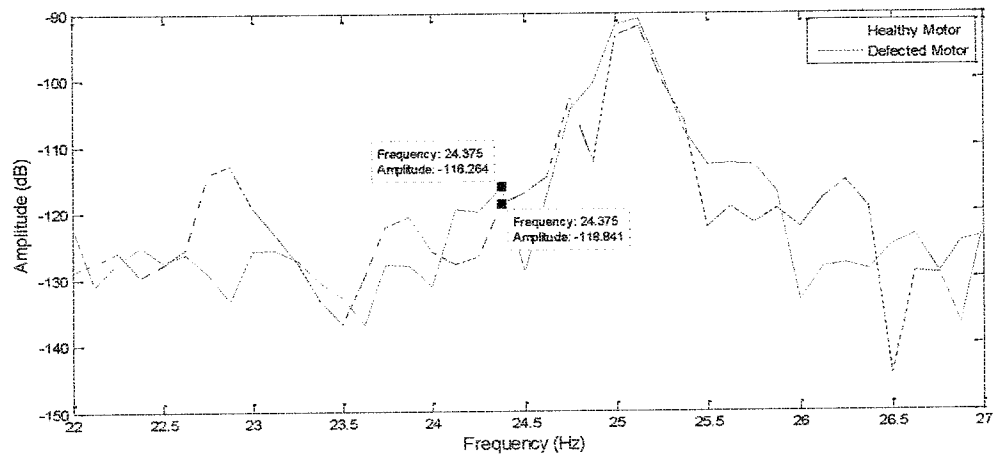


Figure 4.62: Instantaneous power spectrum of the distributed defect in outer race of bearing indicating no change in amplitude at 24.375 Hz

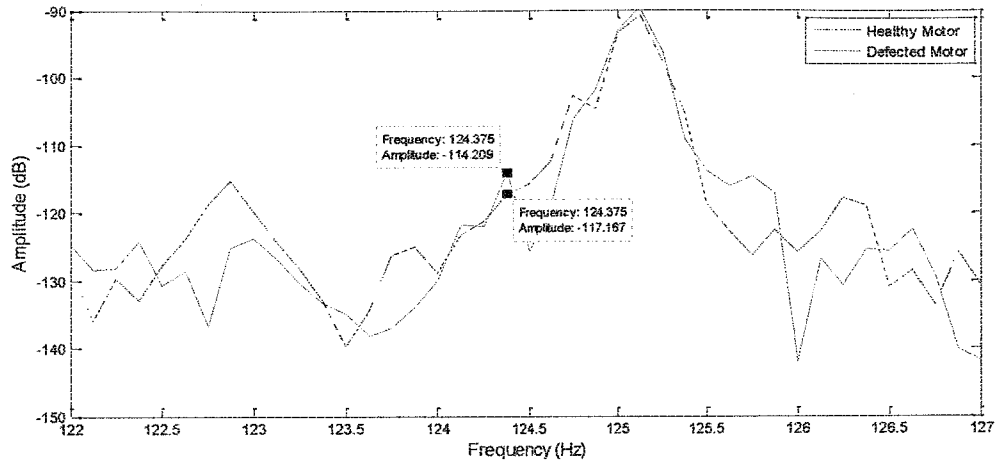


Figure 4.63: Instantaneous power spectrum of the distributed defect in outer race of bearing indicating no change in amplitude value at 124.375 Hz

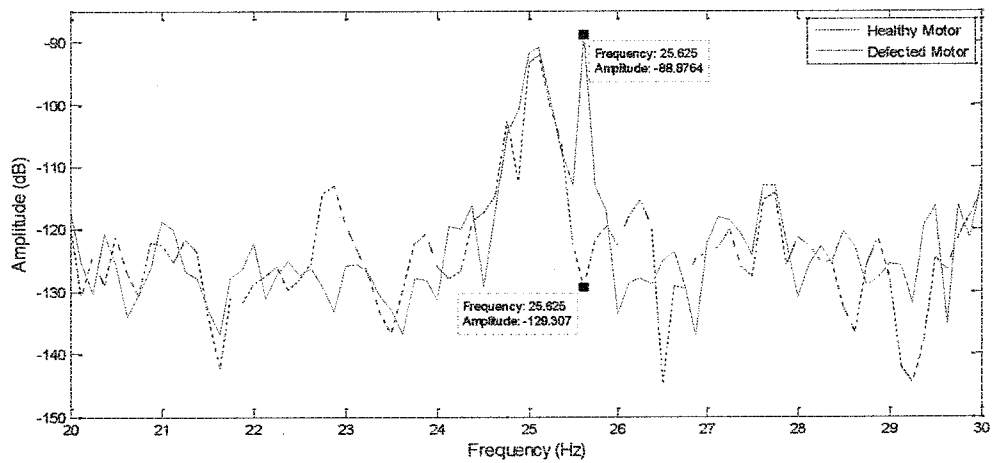


Figure 4.64: Instantaneous power spectrum of the distributed defect in outer race of bearing indicating rise in amplitude value at 25.625 Hz

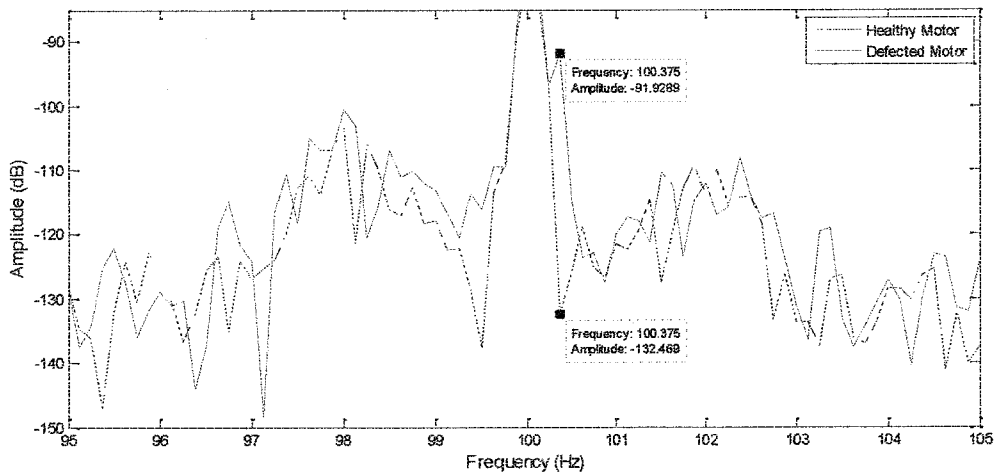


Figure 4.65: Instantaneous power spectrum of the distributed defect in outer race of bearing indicating rise in amplitude value at 100.375 Hz

4.2.5.2 Distributed Defect in Inner Race of Bearing

In order to analyze the distributed faults, three holes of 3mm size were drilled in the inner race of the bearing. The defected bearing is shown in Figure 4.66. The instantaneous power spectrum of the distributed defect in inner race of bearing is shown in Figures 4.67 and 4.68. From analysis of the instantaneous power spectrum it is cleared that no increase in the amplitude for the inner race characteristic defect frequencies of 164 Hz and 178 Hz. This indicates that mathematical relation as described in Equations (4.6) and (4.8) can only be applied to the bearing localized (single point) defects. It was also observed from the instantaneous power spectrum that amplitude peaks were detected at 14 Hz and 153.875 Hz as shown in Figures 4.69 and 4.70. Looking at mathematics relations as described by Park's model, it was observed that these peaks values for inner race distributed defect are appearing at $-1.35f_{if}$ and $|2f_e - f_{if}|$ [91].

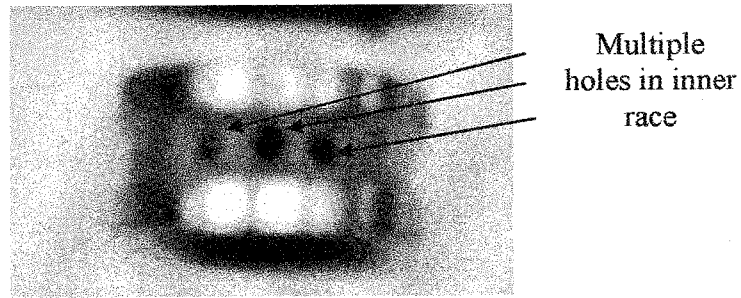


Figure 4.66: Distributed defect in inner race of bearing

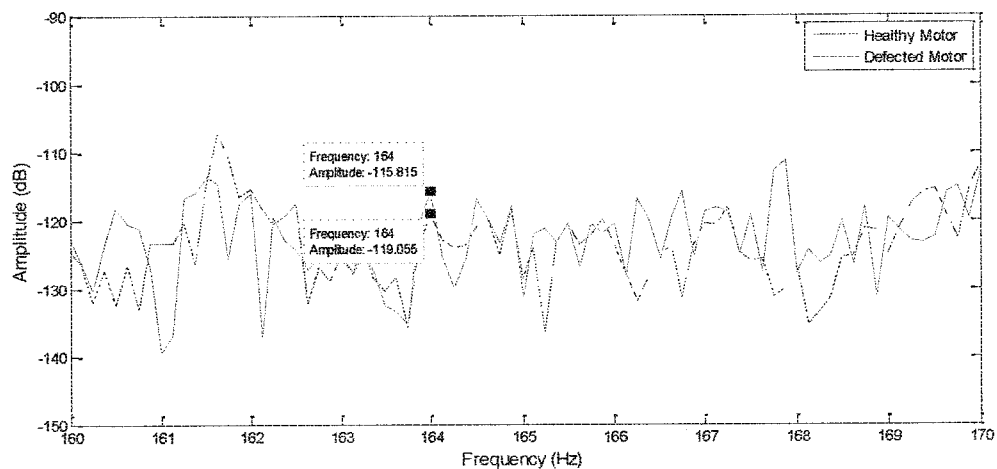


Figure 4.67: Instantaneous power spectrum of the distributed defect in inner race of bearing indicating no change in amplitude at 164 Hz

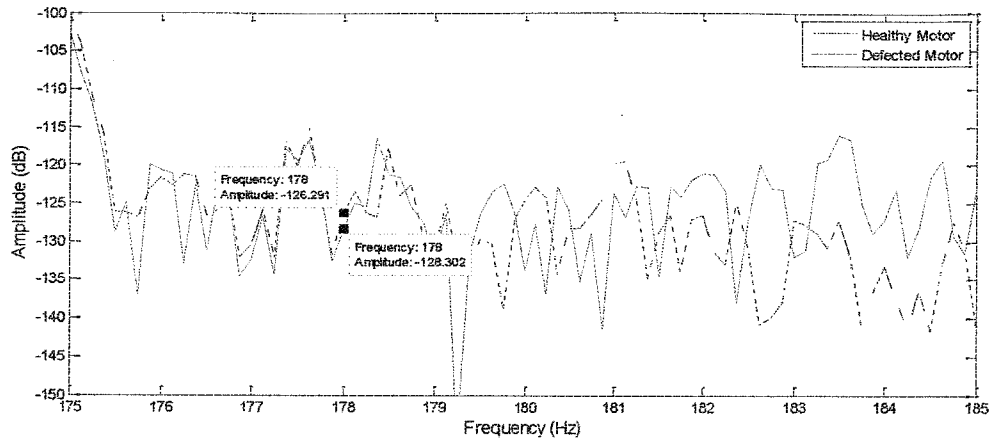


Figure 4.68: Instantaneous power spectrum of the distributed defect in inner race of bearing indicating no change in amplitude value at 178 Hz

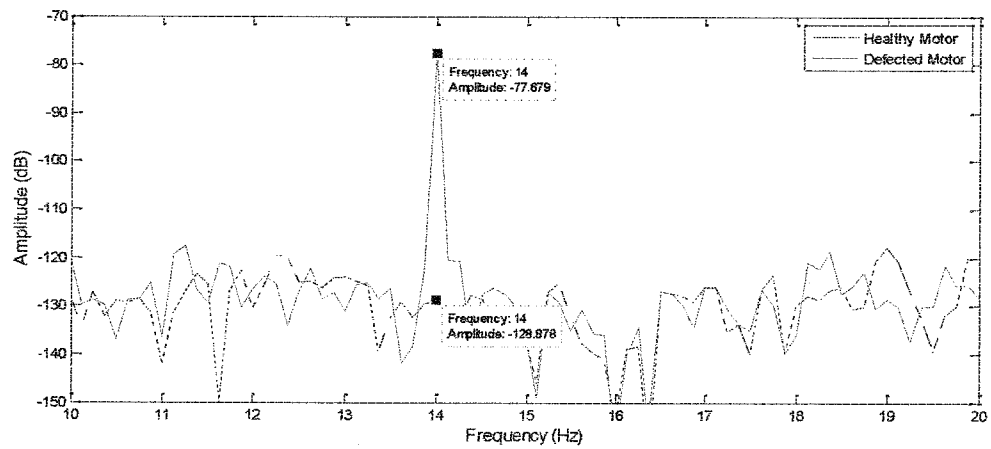


Figure 4.69: Instantaneous power spectrum of the distributed defect in inner race of bearing indicating rise in amplitude value at 14 Hz

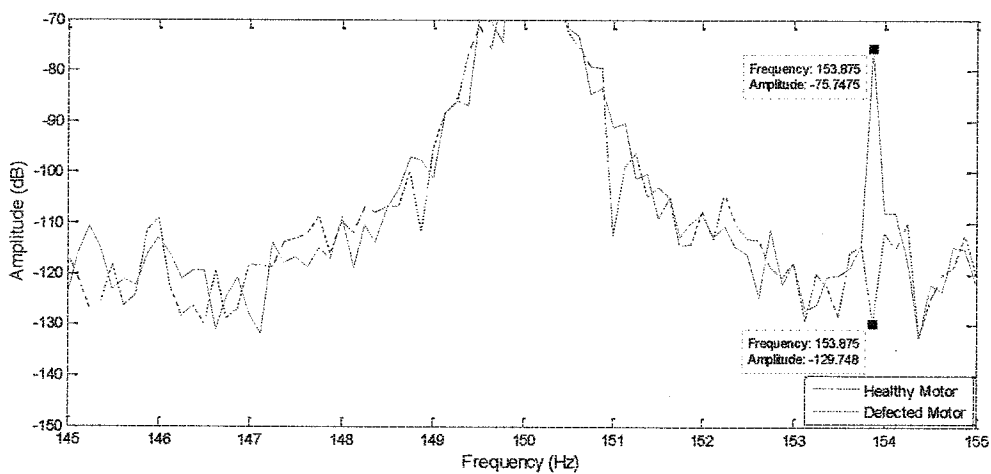


Figure 4.70: Instantaneous power spectrum of the distributed defect in inner race of bearing indicating rise in amplitude value at 153.875 Hz

4.3 A Complete Intelligent Diagnostic CM System

A code was created in LabVIEW using formula node.vi to continuously track the amplitude values at specific characteristic defect frequencies related to motor bearing ball and cage defects. The program routines were designed to track and compare the amplitude values with a base data (healthy motor) and give a 0 volt at the output of the DAQ card if the measured values are equal to base data and a 24 volt if the measured amplitude values are greater than the base data. The status of motor is displayed on the LabVIEW window through green and red signal lights. The green signal light indicates the healthy status and red signal light indicated the defected status of motor. The output of the DAQ card was sent to the input of the programmable logic controller (PLC). The PLC was programmed to produce an alarm if a defect was detected in the bearing and in turn switch the motor off if the defect was higher than a preset value. The LabVIEW front panel window and LabVIEW code of the developed intelligent diagnostic condition monitoring system is shown in Figures 4.71 and 4.72 respectively. The block diagram and the developed experimental test rig of the complete intelligent diagnostic condition monitoring system are shown in Figures 4.73 and 4.74 respectively.

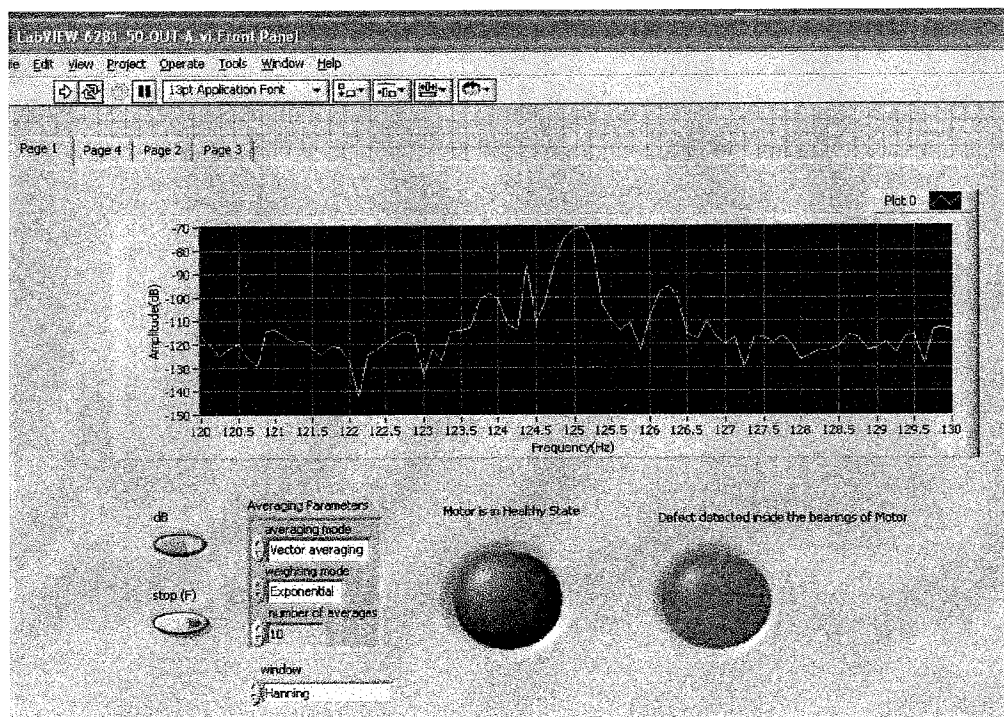


Figure 4.71: LabVIEW front panel

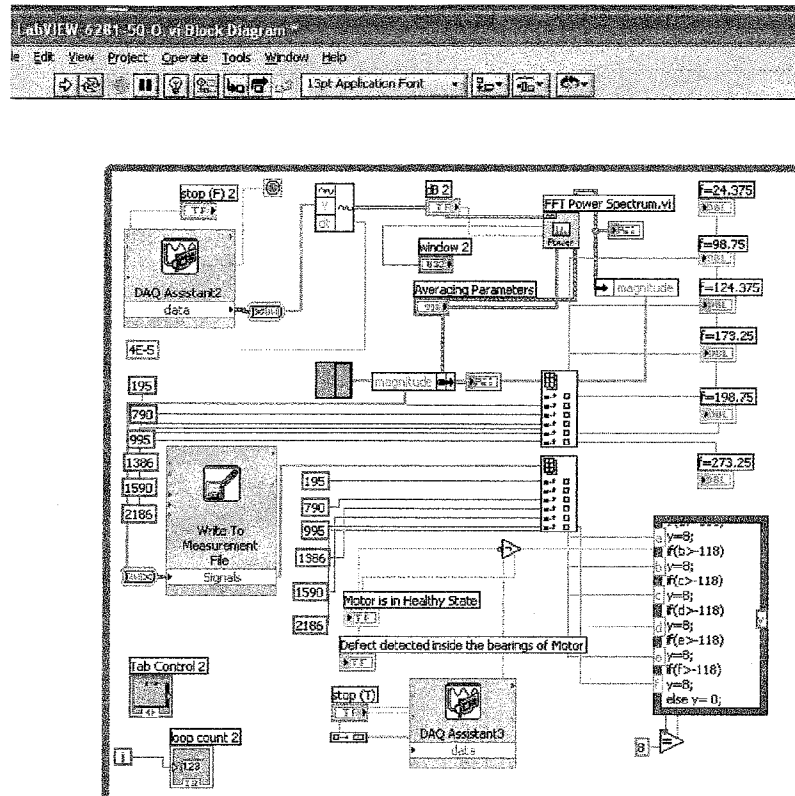


Figure 4.72: LabVIEW block diagram

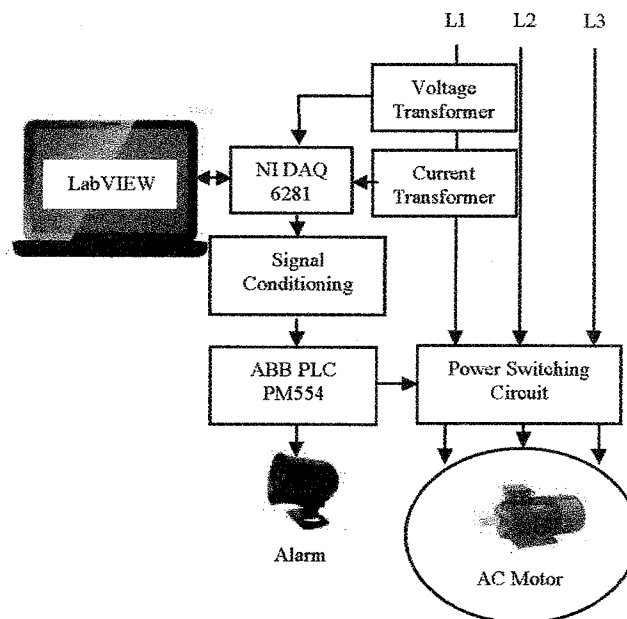


Figure 4.73: Block diagram of the intelligent diagnostic CM system

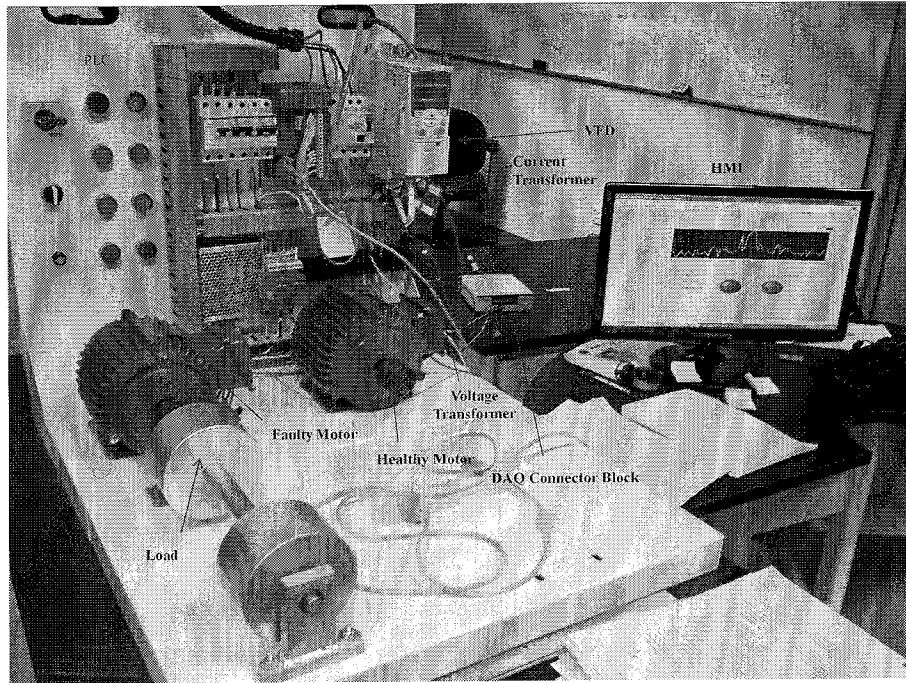


Figure 4.74: The developed experimental test rig

4.4 Summary

This chapter describes the experimental investigation of the motor bearing localized and distributed defects through instantaneous power spectrum analysis. The voltage and current of the motor are used to calculate the instantaneous power which carries more information than the current alone. There are various bearing faults that could occur, and in this work the focus has been to diagnose the bearing localized and distributed faults. The experiments that were conducted on two different fault types related to bearing at un-loaded and loaded conditions revealed the practicality of the approach. The intelligent diagnostic condition monitoring system developed has the capability of real time tracking of different defects inside the bearings of the motors.

CHAPTER 5

CONCLUSIONS AND FUTURE DIRECTIONS

5.1 Conclusions

The main focus of this research is to enhance the fault diagnosis system and to find suitable economical condition monitoring system for induction motors that are being used in several applications especially in severe environment conditions where access to the motor is not easy i.e. nuclear power plants, off-shore stations and etc. As the majority of breakdowns of the motors are due to defects inside the bearings, therefore, diagnostic of various faults of bearings of induction motor is the focus of this research.

An experimental test rig has been developed which comprises of components used in industry for the intelligent diagnosis of motor bearing faults. It consists of a 3 phase AC induction motor, a variable frequency drive, a current and voltage transformer, National Instruments (NI) data acquisition hardware, a programmable logic controller (PLC) PM554, an alarm, and a personal computer with software LabVIEW8.2 and a mechanical load assembly including coupling and bracket.

Present research work investigates two types of bearing faults inside the induction motor. The literature review presents the various kind of existing condition monitoring methods and highlights the need for an economical intelligent fault diagnosis system. The bearing faults are practically implemented and their effects on motor's instantaneous power spectrum are studied. The present research work is structured into following three phases.

- The first phase of this research consists of experimental investigation of localized (single point) faults in the outer race, inner race, rolling elements (balls) and cage of the bearing at no load and full load conditions.

- The second phase of this research work involves the experimental analysis of distributed faults (multiple points) inside the outer and inner race of bearings. The fault frequencies for distributed defects were calculated using extended Parks approximation model. The base line data of the healthy motor is collected during the time of installation and is fed to condition monitoring system.
- In third phase of the research, an intelligent fault diagnosis system is developed. A code was created in LabVIEW to continuously track the amplitude values at specific characteristic defect frequencies related to the motor bearing defects. The program routines were designed to track and compare the amplitude values with a base data (healthy motor) and give a zero volt at the output of the DAQ card if the measured values are equal to base data and a 24 volt if the measured amplitude values are greater than the base data. The status of motor is displayed on the LabVIEW window through green and red signal lights. The green signal light indicates the healthy status and red signal light indicated the defected status of motor. The output of the DAQ card was sent to the input of the programmable logic controller (PLC). The PLC was programmed to produce an alarm if a defect was detected in the bearing and in turn switch the motor off if the defect was higher than preset values. It is observed through experimental results that the change in amplitude values at characteristics defect frequencies is very small for no load conditions. However when the motor is fully loaded, the amplitudes are clearly visible even at small defect size.

In this work, eighteen experiments have been conducted using different types and defect levels of bearing localized and distributed faults at loaded and un-loaded conditions of the motor. It has been foreseen that the results of this research work will enhance the reliability and accuracy of the methods used for the detection and diagnosis of localized and distributed faults at incipient stages related to bearing of the induction motor under loaded and un-loaded conditions by employing the analysis of the instantaneous power spectrum. This research can create the foundation for a more cultivated fault classification method for the distributed faults. The use of instantaneous power as a diagnostic medium for the detection of localized and

distributed faults should provide an enhancement in the field of condition monitoring for the induction motors.

5.2 Contributions

The identification of various bearing faults of the induction motor is the main objective of this research. A laboratory experimental test rig was developed for the experimentation to analyze the defects in different components of the bearing in reliable and accurate manner. The online fault diagnosis system was developed using LabVIEW software.

The contributions of this research are summarized as follows:

- As existing approaches for CM are very dependent on special sensors which are mostly expensive, this work demonstrates the procedures taken in developing a CM system for the motor bearing fault identification, utilizing the commonly available motor stator current and voltage.
- The detailed experimental results comparisons of two bearing fault types based on instantaneous power analysis under localized and distributed defects subjected to un-loaded and loaded conditions of the motor were given. The patterns of the motor instantaneous power spectrum to the different bearing fault types were confirmed through quantitative analysis.
- By integrating the commonly used firmware's (PLC, LabVIEW, current and voltage transformers) available at the site of the production line, a novel intelligent diagnostic condition monitoring system based on the motor instantaneous power analysis has been developed to detect the motor bearing defects at incipient stages. The developed system that posses features like continuous monitoring in real-time as well as providing the information on severity of faults would pave to the development of an automatic decision making.

It is anticipated that the proposed motor protection system in this research will be quicker, more efficient and be more user friendly than other available methods.

5.3 Directions for Future Work

Based on the findings, there are further problems to be consider both in the development of the technique and the experimental design. These include:

- Multiple bearing fault analysis.

Even though the two techniques as proposed i.e., the stator current spectral analysis and the instantaneous power spectrum analysis can monitor the conditions of induction motors from various scenarios, however these are not sufficient for most applications because outcomes of the analysis are based on the assumptions that each fault occurs independently. The extension on the approach as proposed in this work, to understand how each approach reacts to a combination of several faults (e.g stator, rotor, eccentricity, bearings and etc) would be required.

- Development of new approach for fault analysis.

The development of other fault analysis technique for example, using the vector analysis viewpoint such as the Park's vector approach to provide insights and better analysis and identification of faults, would need to be explored

REFERENCES

- [1] W. T. Thomson and M. Fenger, "Current Signature Analysis to Detect Induction Motor Faults," *IEEE Industry Applications Magazine*, pp. 26-34, July/August 2001.
- [2] Ahmed, R. Supangat, J. Grieger, J. N. Ertugrul, and W.L Soong, "A Baseline Study for On-Line Condition Monitoring of Induction Machines," *Australian Universities Power Engineering Conference*, Brisbane, Australia 2004.
- [3] M.L. Sin, W.L. Soong and N. Ertugrul, "Induction Machine On-Line Condition monitoring and Fault diagnosis- A Survey," *AUPEC*, Christchurch, NewZealand, 2003.
- [4] H. A. Toliyat and Alexander G. Parlos, "Condition Monitoring and Fault Diagnosis of Electrical Machines—A review," *IEEE-IAS Annual Meeting*, vol. 1, Phoenix, AZ, pp. 197–204, 1999.
- [5] B. S. Payne, B. Liang and A. D. Ball, "Modern Condition Monitoring Techniques for Electric Machines," *Proceedings of the 1st International Conference on the Integration of Dynamics, Monitoring and Control (DYMAC 99)*, Manchester, UK, pp. 325-330, September 1999.
- [6] M.E.H. Benbouzid, "A Review of Induction motors Signature Analysis as a Medium for Faults Detection," *IEEE Transaction on Industry Electronics*, Vol. 47, No. 5, Oct., pp 984 – 993, 2000.
- [7] S.F. Farag and M.K. Jhaveri, "Intelligent Microprocessors-Based Devices Provide Advanced Motor Protection, Flexible Control, and Communication in Paper Mills," *IEEE Transaction on Industry Applications*, Vol.33, No.3, May 1997.
- [8] D. M. T. Siyambalapitiya "Reliability Improvement and Economic Benefits of On-Line Monitoring System for Large Induction Machines," *IEEE Transactions on Industry Applications*, vol. 26, pp. 1018–1025, July/Aug. 1990.
- [9] F. J. Discenzo "Motor Diagnostics: Technological Drivers Leading to 21st Century Predictive Diagnostics," *International Conference on Maintenance and Reliability*, vol. 1, Knoxville, TN, pp. 30.01-30.12, 1997.

- [10] P. C. Krause, "Analysis of Electric Machinery," New York: McGraw-Hill, 1986.
- [11] P. C. Sen, "Principles of Electric Machines and Power Electronics," John Wiley and Sons, 1989.
- [12] J. Robinson, C. D. Whelan, and N. K. Haggerty, "Trends in Advanced Motor Protection and Monitoring," *IEEE Transactions on Industry Applications*, Vol. 40, No. 3, pp. 853- 860, 2004.
- [13] M. Pineda, R. Puche and M. Riera, "Motor Condition Monitoring of Induction Motor with Programmable Logic Controller and Industrial Network," *IEEE Proceedings on Power Electronics*, September 2011.
- [14] IAS Motor Reliability Working Group, "Report of large motor reliability survey of industrial and commercial installations—Part I," *IEEE Transactions on Industry Applications*, vol. IA-21, pp. 853–864, July/Aug. 1985.
- [15] IAS Motor Reliability Working Group, "Report of large motor reliability survey of industrial and commercial installations—Part II," *IEEE Transactions on Industry Applications*, vol. IA-21, pp. 865–872, July/Aug. 1985.
- [16] IAS Motor Reliability Working Group, "Report of large motor reliability survey of industrial and commercial installations—Part III," *IEEE Transactions on Industry Applications*, vol. IA-23, pp. 153–158, Jan. /Feb. 1987.
- [17] EPRI Publication EL-2678, "Improved motors for Utility applications," Vol. 5, October 2005.
- [18] Peter Vas, "Parameter Estimation, Condition Monitoring, and Diagnosis of Electrical Machines," Clarendon Press Oxford, 1993.
- [19] P.J. Tavner and J. Penman, "Condition Monitoring of Electrical Machines," Hertfordshire, England: Research Studies Press Ltd, ISBN: 0863800610, 1987.
- [20] S. Nandi and H. A. Toliyat, "Condition Monitoring and Fault Diagnosis of Electrical Machines – A Review," *34th Annual Meeting of the IEEE Industry Applications*, pp. 197-204, 1999.
- [21] Randy R. Schoen, Thomas G. Habetler, Farrukh Kamran and Robert G. Bartheld, "Motor Bearing Damage Detection using Stator Current

- Monitoring,” *IEEE Transactions on Industry Applications*, Vol. 31, No 6, pp. 1274-1279, 1995.
- [22] Eschmann P, Hasbargen L, Weigand K, “Ball and Roller Bearings: Their Theory, Design, and Application,” (London: K G Heyden), 1958.
- [23] D. G.Dorrell, W. T. Thomson, and S.Roach, “Analysis of Air-Gap Flux, Current, and Vibration Signals as Function of a Combination of Static and Dynamic Eccentricity in 3-Phase Induction Motors,” *IEEE Transactions on Industry Applications*, Vol. 33, Jan./Feb., pp. 24-34, 1997.
- [24] S.Wu, T. W. S.Chow, “Induction Machine Fault Detection using SOM-Based RBF Neural Networks,” *IEEE Transactions on Industrial Electronics*, Vol. 51, No. 1, February, pp. 183-194, 2004.
- [25] M. Bradford, “Unbalanced Magnetic Pull in a 6-Pole Induction Motor,” *IEEE Proceedings*, Vol. 115, No. 11, pp. 1619-1627, 1968.
- [26] G. Dalpiaz and U. Meneghetti, “Monitoring Fatigue Cracks in Gears,” *NDT & E International*, Vol. 24, No. 6, pp.303-306, 1991.
- [27] J. Sottile and J. L. Kohler, “An On-Line Method to Detect Incipient Failure of Turn Insulation in Random-Wound Motors,” *IEEE Transactions on Energy Conversion*, vol. 8, no. 4, pp. 762-768, December, 1993.
- [28] S. B. Lee, R. M. Tallam, and T. G. Habetler, “A Robust, on-Line Turn-Fault Detection Technique For Induction Machines Based on Monitoring the Sequence Component Impedance Matrix,” *IEEE Transactions on Power Electronics*, Vol. 18, No. 3, pp. 865- 872, May, 2003.
- [29] T. A. Lipo, “Introduction of AC machine design,” *Wisconsin Power Electronics Research Center*, 2nd edition, 2004.
- [30] S. F. Farag, R. G. Bartheld, and W. E. May, “Electronically Enhanced Low Voltage Motor Protection and Control,” *IEEE Transactions on Industry Applications*, Vol. 29, No. 1, pp. 45-51, Jan./Feb., 1994.
- [31] S. B. Lee and T. G. Habetler, “An Online Stator Winding Resistance Estimation Technique for Temperature Monitoring of Line-Connected Induction Machines,” *IEEE Transactions on Industry Applications*, Vol. 39, No. 3, pp. 685-694, May/June, 2003.
- [32] A. H. Bonnet and G. C. Soukup, “Cause and Analysis of Stator and Rotor Failures in Three- Phase Squirrel Case Induction Motors,” *IEEE Transactions Industry Application*, Vol., 28, No.4, pp. 921-937, July/August, 1992.

- [33] W. L. Roux, R. G. Harley, and T. G. Habetler, "Detecting Rotor Faults in Permanent Magnet Synchronous Machines," *SDEMPED'03*, pp. 198-203, Atlanta, GA, USA, August, 2003.
- [34] J. R. Stack, T. G. Habetler, and R. G. Harley, "Bearing Fault Detection via Autoregressive Stator Current Modeling," *IEEE Transactions Industry Applications*, Vol. 40, No. 3, pp. 740-747, May/June, 2004.
- [35] M. A. Cash, "Detection of Turn Faults Arising from Insulation Failure in the Stator Windings of AC Machines," Ph.D Thesis, Georgia Institute of Technology, USA, 1998.
- [36] D. G. Dorrell, A. C Smith, "Calculation and Measurements of Unbalance Magnetic Pull in Cage Induction Motors with Eccentric Rotors, Part 2: Experimental Investigation," *IEEE Proceedings Electric Power Applications*, Vol. 143, No. 3, May, pp. 202-210, 1996.
- [37] A. Belahcen, A. Arkkio, A. Klinge, P. Linjama, J. Voutilainen, "Radial Forces Calculation in A Synchronous Generator for Noise Analysis," *Proceeding of the Third Chinese International Conference on Electrical Machines*, Xi'an, China, pp. 199-122, August 1999.
- [38] Li B. Chow, M. Y. Tipsuwan Y. Hung, "Neural-Network-Based Motor Rolling Bearing Fault Diagnosis," *IEEE Transactions on Industrial Electronics*, Vol. 47, No. 5, October, pp. 1060-1069, 2000.
- [39] L. B. Jack, A. K. Nandi, "Genetic Algorithm for Feature Selection in Machine Condition Monitoring with Vibration Signals," *IEE Proceedings Vision, Image and Signal Processing*, Vol. 147, June, pp. 205-212, 2000.
- [40] W. R. Finley, M. M. Hodowanec, W. G. Holter, "An Analytical Approach to Solving Motor Vibration Problems," *IEEE Transactions on Industry Applications*, Vol. 36, No.5, September/October, pp. 1467-1480, 2000.
- [41] Mohammad A.A. Elmaleeh, N.Saad and N.Ahmad, "On-line Fault Detection & Diagnosis of Rotating Machines using Acoustic Emission Monitoring Techniques," *IEEE International Conference on Intelligent and Advanced Systems*, 2007.
- [42] S. Bagnoli and R. Capitani, "Comparison of Accelerometer and Acoustic Emission Signals as Diagnostic Tool in Assessing Bearing," *Proceedings of 2nd International Conference on Condition Monitoring*, May 1998.

-
- [43] P. H. Mellor, D. Roberts, and D. R. Turner, "Lumped Parameter Thermal Model for Electrical Machines of TEFC Design," *IEEE Proceedings on Electric Power Application*, Vol. 138, pp. 205-218, 1991.
- [44] O. I. Okoro, "Steady and Transient States Thermal Analysis of a 7.5-kw Squirrel-Cage Induction Machine at Rated-Load Operation," *IEEE Transactions on Energy Conversion*, Vol. 20, No. 4, pp. 730-736, December, 2005.
- [45] Z. Gao, T. G. Habetler, and R. G. Harley, "An Online Adaptive Stator Winding Temperature Estimator Based on a Hybrid Thermal Model for Induction Machines," *IEEE IEMDC'05*, pp. 754-761, San Antonio, Texas, USA, May, 2005.
- [46] J. F. Moreno, F. P. Hidalgo, and M. D. Martinez, "Realization of Tests to Determine the Parameters of the Thermal Model of an Induction Machine," *IEEE Proceedings on Electric Power Application*, Vol. 148, No. 5, pp.393-397, September, 2001.
- [47] P. Milanfar and J. H. Lang, "Monitoring the Thermal Condition of Permanent-Magnet Synchronous Motors," *IEEE Transactions on Aerospace and Electronic Systems*, Vol. 32, No. 4, pp. 1421-1429, October, 1996.
- [48] A. J. Ellison and S. J. Yang, "Effects of Rotor Eccentricity on Acoustic Noise from Induction Machines," *Proceedings of IEE*, 118, (1), pp. 174-184, 1971.
- [49] Tavner, J. Pennman, "Condition Monitoring of Electrical Machines," *Letchworth, England: Research Studies Press Ltd.* 1987.
- [50] Wei Zhou and Thomas G. Habetler, "Bearing Condition Monitoring Methods for Electric Machines," *IEEE Transaction on Diagnosis for Electric Machines, Power Electronics and Drives*, 2007.
- [51] Randy R. Schoen, Thomas G. Habetler, Farrukh Kamran and Robert G. Bartheld, "Motor Bearing Damage Detection using Stator Current Monitoring," *IEEE Transactions on Industry Applications*, Vol. 31, No 6, pp. 1274-1279, 1995.
- [52] Randy R. Schoen, Brian K. Lin, Thomas G. Habetler, Jay H. Schlag, and Samir Farag, "An Unsupervised, On-Line System for Induction Motor Fault Detection using Stator Current Monitoring," *IEEE Transactions on Industry Applications*, Vol. 31, No. 6, pp. 1280-1286, 1995.

- [53] Randy R. Schoen, and Thomas G. Habetler, "Evaluation and Implementation of a System to Eliminate Arbitrary Load Effects in Current-Based Monitoring of Induction Machines," *IEEE Transactions on Industry Applications*, Vol. 33, No. 6, pp. 1571-1577, 1997.
- [54] John S. Hsu, "Monitoring of Defects in Induction Motors through Air-Gap Torque Observation," *IEEE Transactions on Industry Applications*, Vol. 31, No. 5, pp.1016- 1021, 1995.
- [55] Hamid A. Toliyat, Mohammed S. Arefeen, and Alexander G. Parlos, "A Method for Dynamic Simulation of Air-Gap Eccentricity in Induction Machines," *IEEE Transactions on Industry Applications*, Vol. 32, No. 4, pp.910-918, 1996.
- [56] M. E. H. Benbouzid , H. Nejjari, R. Beguenane, and M. Vieira, "Induction Motor Asymmetrical Faults Detection using Advanced Signal Processing Techniques," *IEEE Transactions on Energy Conversion*, Vol. 14, No. 2, pp.147-152, June 1999.
- [57] M. E. H. Benbouzidi, M. Viera, and C. Theys, "Induction Motors Faults Detection and Localization using Stator Current Advanced Signal Processing Techniques," *IEEE Transactions on Power Electronics*, Vol. 14, No. 1, pp14-22, Jan. 1999.
- [58] W. T. Thomson, D. Rankin, and D. G. Dorrell, "On-line Current Monitoring to Diagnose Airgap Eccentricity-an Industrial Case History of a Large High-Voltage Three-Phase Induction Motors," *Electric Machines and Drives Conference Record*, pp.MA2/4.1- MA2/4.3, 1997.
- [59] Le. Roux, R. G. Harley, and T. G. Habetler, "Rotor Fault Analysis of a Permanent Magnet Synchronous Machine," *International Conference on Electric Machines*, Bruges, Belgium, 2002.
- [60] Birsen Yazıcı, and Gerald B. Kliman, "An Adaptive Statistical Time-Frequency Method for Detection of Broken Bars and Bearing Faults in Motors using Stator Current," *IEEE Transactions on Industry Applications*, Vol. 35, No. 2, pp.442-452, 1999.
- [61] Jafar Milimonfared, Homayoun Meshgin Kelk, Subhasis Nandi, Artin Der Minassians and Hamid A. Toliyat, "A Novel Approach for Broken-Rotor-Bar Detection in Cage Induction Motors," *IEEE Transactions on Industry Applications*, Vol. 35, No. 5, pp.1000-1006, 1999.

- [62] Alberto Bellini, Fiorenzo Filippetti, Giovanni Franceschini, and Carla Tassoni, "Closed- Loop Control Impact on the Diagnosis of Induction Motors Faults," *IEEE Transactions on Industry Applications*, Vol. 36, No. 5, pp. 1318-1329, 2000.
- [63] M. E. H. Benbouzid, "A Review of Induction Motors Signature Analysis as a Medium for Faults Detection," *IEEE Transactions on Industrial Electronics*, Vol. 47, October, No.5, pp. 984-993, 2000.
- [64] G. M. Joksimovic and J. Penman, "The Detection of Inter-Turn Short Circuits in the Stator Winding of Operating Motors," *IEEE Transactions on Industrial Electronics*, Vol.47, No. 5, October, pp. 1078-1084, 2000.
- [65] M. Haji and H. A. Toliyat, "Pattern Recognition – a Technique for Induction Machines Rotor Broken Bar Detection," *IEEE Transactions on Energy Conversion*, Vol. 16, No. 4, pp. 312–317, 2001.
- [66] M. Arkan, D. K. Perovic and P. Unsworth, "Online Stator Fault Diagnosis in Induction Motors," *IEE Proceedings Electric Power Applications*, Vol. 148, No. 6, November, pp. 537-547, 2001.
- [67] R. M. Tallam, T. G. Habetler, and Ronald G. Harley, "Stator Winding Turn-Fault Detection for Closed-Loop Induction Motor Drives," *IEEE Industry Applications Society Annual Meeting*, pp.1553-1557, 2002.
- [68] A. Miltic and M. Cettolo " Frequency Converter Influence on Induction Motor Rotor Faults Detection using Motor Current Signature Analysis- Experimental Research," *Symposium on Diagnostic for electric machines, Power Electronics and Derives*, Atlanta, GA, USA, 24-26 march, pp. 124-128, August 2003.
- [69] R. R. Obaid and T. G. Habetler, "Current-Based Algorithm for Mechanical Fault Detection in Induction Motors with Arbitrary Load Conditions," *IEEE Industry Applications Society Annual Meeting*, pp. 1347-1351, 2003
- [70] M.E.H. Benbouzid and G.B. Kliman, "What Stator Current Processing Based Technique to use for Induction Motor Rotor Faults Diagnosis?," *IEEE Transactions on Energy Conversion*, Vol.18, pp. 238-244, June 2003.
- [71] L. Szabó, K.Á. Bíró, J.B. Dobai, "On the Rotor Bar Faults Detection in Induction Machines," *Proceedings of the International Scientific Conference MicroCAD*, Miskolc (Hungary), Section J (Electrotehnics and Electronics), pp. 81-86, 2003.

- [72] Jason R. Stack, Thomas G. Habetler, Ronald G. Harley, "Fault Classification and Fault Signature Production for Rolling Element Bearings," *IEEE Transactions on Industry Applications*, Vol. 40, No. 3, pp.735-739, 2004.
- [73] Jason R. Stack, Thomas G. Habetler, Ronald G. Harley, "Bearing Fault Detection via Stator Current Modeling," *IEEE Transactions on Industry Applications*, Vol. 40, No. 3, pp.740-747, 2004.
- [74] M. A. Sérgio Cruz and A. J. Marques Cardoso, "Diagnosis of Stator Inter-Turn Short Circuits in DTC Induction Motor Drives," *IEEE Transactions on Industry Applications*, Vol. 40, No. 5, pp.1249-1360, 2004.
- [75] Humberto Henao, Claudia Martis, and Gérard-André Capolino, "An Equivalent Internal Circuit of the Induction Machine for Advanced Spectral Analysis," *IEEE Transactions on Industry Applications*, Vol. 40, No. 3, pp.726-734, 2004.
- [76] Lyubomir, V.Dimitrov, and V.J.Chobanov, "Diagnosis of Rotor Faults of Induction Motors, Operated in Non-Rated Condition," *27th International Spring Seminar on Electronics Technology*, 2004 IEEE, No. 0-7803-8422-9/04, pp.110-113, 2004.
- [77] J.H. Jung, J.J. Lee and B.H. Kwon, "Online Diagnosis of Induction Motor using MCSA," *IEEE Transactions on Industrial Electronics*, Vol. 53, No. 6, pp. 1842-1852, Dec. 2008.
- [78] L. Szabó, F. Tóth, E. Kovács, G. Fekete, "An Overview on Induction Machine's Diagnosis Methods," *Journal of Computer Science and Control Systems*, Oradea, 2008, pp. 229-234. ISSN: 1844-6043.
- [79] L. Frosini and E. Bassi, "Stator Current and Motor Efficiency as Indicators for Different Types of Bearing Faults in Induction Motors," *IEEE Transactions on Industrial Electronics*, Vol. 57, No. 1, pp. 244 – 251, 2010.
- [80] J. Faiz, , B.M. Ebrahimi, B. Akin and H.A. Toliyat, "Dynamic Analysis of Mixed Eccentricity Signatures at Various Operating Points and Scrutiny of Related Indices for Induction Motors," *Electric Power Applications*, IET, Vol.4 , No.1, pp. 1 – 16, 2010.
- [81] S. Nandi, Hamid A. Toliyat, Xiaodong Li, "Condition Monitoring and Fault Diagnosis of Electrical Motors - A Review," *IEEE Transaction on Energy Conversion*, Vol. 20, No. 4, December 2005.

-
- [82] Wei, Zhou, Thomas G. Habetler and Ronald G. Harley, "Bearing Condition Monitoring Methods for Electric Machines: A General Review," *IEEE International Symposium on Diagnostics for Electric Machines, Power Electronics and Drives*, 2007.
- [83] N. Tandon, G.S. Yadava and K.M. Ramakrishna, "A Comparison of Some Condition Monitoring Techniques for the Detection of Defect in Induction Motor Ball Bearings," *Mechanical System and Signal Processing*, pp. 244-256, 2007.
- [84] Martin Blodt, Pierre Granjon, Bertrand Raison and Gilles Rostaing, "Models for Bearing Damage Detection in Induction Motors using Stator Current Monitoring," *IEEE Transaction on Industrial Electronics*, Vol. 55, No. 4, April 2008.
- [85] Jose Ignacio Terra, Marcelo Castelli and Juan Pablo Fossati, "Fault Detection and Remote Monitoring System for Induction Motors using MCSA Technique," *IEEE Transaction on Transmission and Distribution*, Vol. 11, No. 2, October 2008.
- [86] Neelam Mehala, "Condition Monitoring and Fault Diagnosis of Induction Motor using Motor Current Signature Analysis," Ph.D Thesis, National Institute of Technology Kurukshetra, India, 2010.
- [87] Intesar Ahmad, "Investigation of Single and Multiple Faults Under Varying Load Conditions Using Multile Sensor Types to Improve Condition Monitoring of Induction Machines," Ph.D Thesis, Univeristy of Adelaide, Australia, 2007.
- [88] Ramzan Bayindir, Ibrahim Sfa and Ilhami Colak, "Fault Detection and Protection of Induction Motors using Sensors," *IEEE Transaction on Energy Concersion*, Vol. 23, No. 3, September 2008.
- [89] Maria G. Ioannides, "Design and Implementation of PLC-Based Monitoring Control System for Induction Motor," *IEEE Transaction on Energy Concersion*, Vol. 19, No. 3, September 2004.
- [90] Robert H. Bishop, "Learning with LabVIEW 8," Pearson/Prentic Hall, 2007.
- [91] Jafar Zarei and Javad Poshtan, "An Advanced Parks Vector Approach for Bearing Fault Detection," *IEEE International Conference on Indutrial Technology*, pp. 1472-1479, 2006.

LIST OF PUBLICATIONS

1. Muhammad Irfan, Nordin Saad, Rosdiazli Ibrahim and Vijanth S. Asirvadam, "An Intelligent Diagnostic Condition Monitoring System AC Motors via Instantaneous Power Analysis," *International Review of Electrical Engineering*, Vol.8, No. 2, pp. 664-672, April 2013.
2. Muhammad Irfan, Nordin Saad, Rosdiazli Ibrahim and Vijanth S. Asirvadam, "Development of an Intelligent Condition Monitoring System for AC Induction Motors using PLC," *IEEE Business Engineering and Industrial Applications Colloquium*, pp. 758-763, Langkawi, Malaysia, April 2013.
3. Muhammad Irfan, Nordin Saad, Rosdiazli Ibrahim and Vijanth S. Asirvadam, "AC Motor Fault Diagnosis at Incipient Stages using Programmable Logic Controller," *IEEE Conference on Sustainable Utilization and Development in Engineering and Technology*, pp.25-30, Cyberjaya, Malaysia, May 2013.
4. Muhammad Irfan, Nordin Saad, Rosdiazli Ibrahim and Vijanth S. Asirvadam, "An Intelligent Diagnostic System for Condition Monitoring of AC Motors," *The 8th IEEE Conference on Industrial Electronics and Applications*, Melbourne, Australia, June 2013.
5. Muhammad Irfan, Nordin Saad, Rosdiazli Ibrahim and Vijanth S. Asirvadam, "Investigation of Bearing Faults in Induction Motors via Instantaneous Power Analysis," *Annual Post Graduate Conference*, Tronoh, Malaysia, June 2013 (submitted for review).

